Active and potentially active volcanoes of the Central Volcanic Zone of the Andes (CVZA)

Reyes Hardy, Maria-Paz; Di Maio, Luigia Sara; Dominguez, Lucia; Frischknecht, Corine; Biasse, Sébastien; Guimarães, Leticia; Nieto-Torres, Amiel; Elissondo, Manuela; Pedreros, Gabriela; Aguilar, Rigoberto; Amigo, Álvaro; García, Sebastián; Forte, Pablo; Bonadonna, Costanza

This publication URL: https://archive-ouverte.unige.ch/unige:172413
Publication DOI: 10.13097/archive-ouverte/unige:172413

ACTIVE AND POTENTIALLY ACTIVE VOLCANOES OF THE CENTRAL VOLCANIC ZONE OF THE ANDES (CVZA)

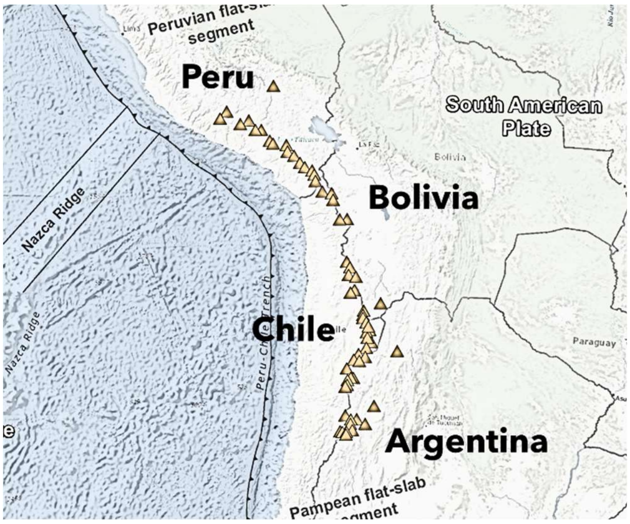

Edited by:

María-Paz Reyes-Hardy[1], Luigia Sara Di Maio[1], Lucia Dominguez[1], Corine Frischknecht[1], Sébastien Biass[1], Leticia Freitas Guimarães[2], Amiel Nieto-Torres[3], Manuela Elissondo[4], Gabriela Pedreros[5], Rigoberto Aguilar [6], Álvaro Amigo[5], Sebastián García[4], Pablo Forte[7], Costanza Bonadonna[1].

[1] Department of Earth Sciences, University of Geneva, 1205 Geneva, Switzerland; [2] Departamento de Geologia, Instituto de Geociências, Universidade Federal da Bahia; [3] Millennium Institute on Volcanic Risk Research - Ckelar Volcanoes, Avenida Angamos 0610, Antofagasta, Chile; [4] Servicio Geológico Minero Argentino, SEGEMAR, Argentina; [5] Servicio Nacional de Geología y Minería, Red Nacional de Vigilancia Volcánica, Temuco, Chile; [6] Instituto Geológico Minero y Metalúrgico, Observatorio Vulcanológico del INGEMMET, Arequipa, Perú;[7] Observatorio Argentino de Vigilancia Volcánica (OAVV), SEGEMAR, CONICET, Argentina.

Statement: The authors declare that this is a non-peer reviewed report as part of the study "Volcanic risk ranking and regional mapping of the Central Volcanic Zone of the Andes".

Abstract

The Central Volcanic Zone of the Andes (CVZA) extends from southern Peru, through the altiplano of Bolivia, to Puna de Atacama of northern Chile and Argentina, between latitudes 14-28°S of the Andean cordillera, with altitudes raising up to more than 4,000 m above sea level. There is a large number of volcanoes in this area, the identification of the active ones is difficult though, particularly due to the lack of geochronological evidence and/or preserved historical records of eruptions. In this report we have considered the criteria of the geological services of three out of the four countries comprising the CVZA, and we have therefore included active and potentially active volcanoes, i.e., all volcanoes that have had at least one eruption in the last 11,700 years; or the volcanoes that, in the absence of data or eruption occurrence in that period, show visible signs of activity such as degassing, seismicity or ground deformation. In this way, 62 active and potentially active volcanoes have been identified for the CVZA, and a brief description of their physical characteristics, eruptive frequency and types of hazards is provided.

Resumen

La Zona Volcánica Central de los Andes (ZVCA) se extiende desde el sur del Perú, a través del altiplano de Bolivia, hasta la Puna de Atacama del norte de Chile y Argentina, entre las latitudes 14-28°S de la cordillera de los Andes, con altitudes que se elevan hasta más de 4.000 m sobre el nivel del mar. Existe una gran cantidad de volcanes en esta área, aunque la identificación de aquellos activos es difícil, particularmente debido a la falta de evidencia geocronológica y/o registros históricos conservados de sus erupciones. En este estudio hemos considerado el criterio de los servicios geológicos de tres de los cuatro países que componen la ZVCA, y, por consiguiente, se han incluido los volcanes activos y potencialmente activos, es decir, todos aquellos volcanes que han tenido al menos una erupción en los últimos 11,700 años o que, en ausencia de datos u ocurrencia de erupciones en ese periodo, presentan signos visibles de actividad como desgasificación, sismicidad o deformación del suelo. De esta manera, se han identificado 62 volcanes activos y potencialmente activos para la ZVCA, sobre los cuales una breve descripción a cerca de sus características físicas, frecuencia eruptiva y tipos de peligros es presentada en este informe.

Table of contents

1 Volcanoes of the Central volcanic zone of the Andes

After an extensive compilation of information on the volcanoes of the CVZA, in collaboration with SEGEMAR, SERNAGEOMIN, and INGEMMET, including a comprehensive analysis of 7 catalogs (i.e., De Silva and Francis, 1991; GVP, 2013; Elissondo et al., 2016b; Macedo et al., 2016; SERNAGEOMIN, 2020a, b; Aguilera et al., 2022), we found that the most comprehensive list of volcanoes of the CVZA comprises a total of 62 active and potentially active volcanic centers as listed in Table 1.

Table 1. Comparison table of the CVZA volcanoes compilations (De Silva and Francis, 1991; GVP, 2013; Macedo et al., 2016; SERNAGEOMIN, 2020a, b; Elissondo et al., 2016; Aguilera et al., 2022). Volcano names with black letters correspond to Holocene and blue letters correspond to Pleistocene volcanoes according to the Global Volcanism Program database (GVP, 2013). Selected volcanic centers are highlighted in green. Eruptive centers with white background were not included**.** *Ampato: it is part of the Ampato-Sabancaya volcanic complex. Notice that the last column lists the volcanoes identified in this work (in black bold).

N°	Volcanoes of the Central Andes[1)]	Global Volcanism Program[2)]	INGEMMET/IGP[(3)]	SERNAGEOMIN[(4)]	SEGEMAR[(5)]	Advances in scientific understanding of the CVZA[(6)]	This work
1		Quimsachata	Quimsachata				**Quimsachata**
2		Auquihuato, Cerro	Auquihuato, Cerro			Cerro Auquihuato	**Cerro Auquihuato**
3		Sara Sara	Sara Sara			Sara Sara	**Sara Sara**
4	Coropuna	Coropuna	Coropuna			Coropuna	**Coropuna**
5		Andahua-Orcopampa	Andahua-Orcopampa			Andagua	**Andahua-Orcopampa**
6		Huambo	Huambo			Huambo	**Huambo**
7	Sabancaya	Sabancaya	Sabancaya			Sabancaya *Ampato	**Sabancaya**
8	Chachani, Nevado	Chachani, Nevado	Chachani, Nevado			Chachani	**Chachani**
9		Nicholson, Cerro					
10	Misti, El	Misti, El	Misti, El			Misti	**El Misti**
11	Ubinas	Ubinas	Ubinas			Ubinas	**Ubinas**
12	Huaynaputina	Huaynaputina	Huaynaputina			Huaynaputina	**Huaynaputina**
13		Ticsani	Ticsani			Ticsani	**Ticsani**
14	Tutupaca	Tutupaca	Tutupaca			Tutupaca	**Tutupaca**
15	Yucamane	Yucamane	Yucamane			Yucamane	**Yucamane**

16	Casiri, Nevados	Casiri, Nevados	Casiri, Nevados			Casiri	**Casiri**
17		Purupuruni, Cerros	Purupuruni			Purupuruni	**Purupuruni**
18	Tacora	Tacora		Tacora		Tacora	**Tacora**
19		Taapaca		Taapaca		Taapaca	**Taapaca**
20	Parinacota	Parinacota		Parinacota		Parinacota	**Parinacota**
21	Guallatiri	Guallatiri		Guallatiri		Guallatiri	**Guallatiri**
22	Arintica	Arintica					
23	Tambo Quemado	Tambo Quemado					
24	Isluga	Isluga		Isluga		Isluga	**Isluga**
25	Tata Sabaya	Tata Sabaya				Tata Sabaya	**Tata Sabaya**
26		Jayu Khota, Laguna					
27		Jatun Mundo Quri Warani					
28	Irruputuncu	Irruputuncu		Irruputuncu		Irruputuncu	**Irruputuncu**
29	Pampa Luxsar	Pampa Luxsar					
30	Olca-Paruma	Olca-Paruma		Olca-Paruma		Olca-Paruma	**Olca-Paruma**
31	Aucanquilcha	Aucanquilcha		Aucanquilcha		Aucanquilcha	**Aucanquilcha**
32	Ollagüe	Ollagüe		Ollagüe		Ollagüe	**Ollagüe**
33	Azufre, Cerro del	Azufre, Cerro del		Apacheta-Aguilucho		Apacheta	**Cerro del Azufre (Apacheta-Aguilucho)**
34	San Pedro-San Pablo	San Pedro-San Pablo		San Pedro		San Pedro	**San Pedro**
35	Putana	Putana		Putana		Putana	**Putana**
36	Sairecabur	Sairecabur		Escalante-Sairecabur		Escalante-Sairecabur	**Escalante-Sairecabur**
37	Licancabur	Licancabur		Licancabur		Licancabur	**Licancabur**
38	Guayaques	Guayaques					
39	Colachi	Colachi		Colachi		Colachi	**Colachi**
40	Acamarachi	Acamarachi		Acamarachi		Acamarachi	**Acamarachi (Pili)**
41	Overo, Cerro	Overo, Cerro					
42	Chiliques	Chiliques		Chiliques		Chiliques	**Chiliques**
43	Aguas Calientes						

44	Lascar	Lascar		Lascar		Lascar	**Lascar**
45	Cordon de Puntas Negras	Cordon de Puntas Negras		Puntas Negras		Cordon de Puntas Negras	**Puntas Negras**
46	Punta Negra						
47		Miniques					
48	Tucle, Cerro	Tujle, Cerro					
49		Caichinque		Caichinque		Caichinque	**Caichinque**
50		Tilocalar					
51	Negrillar, El	Negrillar, El					
52	Pular	Pular		Pular-Pajonales		Pular Pajonales	**Pular Pajonales**
53	Negrillar, La	Negrillar, La					
54	Socompa	Socompa		Socompa	Socompa	Socompa	**Socompa**
55	Llullaillaco	Llullaillaco		Llullaillaco	Llullaillaco	Llullaillaco	**Llullaillaco**
56	Escorial	Corrida de Cori Volcanic Field			Escorial	Cerro Escorial	**Escorial (Corrida de Cori)**
57	Lastarria	Lastarria		Lastarria	Lastarria	Lastarria	**Lastarria**
58	Cordon del Azufre	Cordon del Azufre		Cordón del Azufre	Cordón del Azufre	Cordon del Azufre	**Cordón del Azufre**
59	Bayo Gorbea, Cerro	Bayo Gorbea, Cerro		Bayo, Cerro	Bayo, Cerro	Cerro Bayo	**Cerro Bayo**
60	Nevada, Sierra	Nevada, Sierra		Nevada, Sierra	Nevada, Sierra	Sierra Nevada	**Sierra Nevada**
61	Falso Azufre	Falso Azufre			Falso Azufre	Falso Azufre	**Falso Azufre**
62		Incahuasi, Nevado de		Incahuasi, Nevado de	Incahuasi, Nevado de	Nevado de Incahuasi	**Nevado de Incahuasi**
63	Ojos del Salado, Nevados	Ojos del Salado, Nevados		Ojos del Salado, Nevados	Ojos del Salado	Nevados Ojos del Salado	**Nevados Ojos del Salado**
64		Solo, El			El Solo	El Solo	**El Solo**
65	Tuzgle	Tuzgle			Tuzgle	Tuzgle	**Tuzgle**
66		Aracar			Aracar	Aracar	**Aracar**
67		Unnamed			Sin Nombre	Unnamed	**Sin nombre (Unnamed)**
68		Antofagasta Volcanic Field			CV Antofagasta	Antofagasta Volcanic Field (Alumbrera)	**Antofagasta de la Sierra (Antofagasta volcanic field**
69	Condor, El	Condor, El			Cóndor, El	El Cóndor	**Cerro El Cóndor**

70	Peinado	Peinado			Peinado	Peinado	**Peinado**
71	Blanco, Cerro	Blanco, Cerro			Blanco, Cerro	Cerro Blanco	**Cerro Blanco**
72	Tipas	Tipas			Tipas	Tipas	**Cerro Tipas (Walker Penk)**
73	Lquilla Chico						
74	Nuevo Mundo						
75	Chascon (Bolivia)	Chascon, Cerro					
76	Chao						
77	Chillahuita						
78	Tocopuri						
79	Chascon de Purico (Chile)	Purico Complex		Purico Complex		Purico	**Chascón-Purico Complex**
80	La Poruña						
81	Andagua						
82	Antofalla						
83	Frailes Plateau						
84	Kari Kari						
85	Altiplano Puna Volcanic Complex						
86	Pastos Grandes						
87	Panizos						
88	La Pacana caldera						
89	Cerro Guacha						
90	Cerro Purico						
91	Aguas Calientes						
92	Cerro Galan	Galan, Cerro					
93	Cerro Bonete						
94		Tres Cruces		Nevado Tres Cruces		Nevado Tres Cruces	**Nevado Tres Cruces**
95				Alitar		Alitar	**Alitar**
96					Salar de Arizaro	Arizaro Volcanic Field	**Arizaro volcanic field**
97		Uturuncu				Uturuncu	**Uturuncu**

(1) De Silva and Francis (1991); (2) GVP (2013); (3) Macedo et al. (2016); (4) SERNAGEOMIN (2020a, b); (5) Elissondo et al. (2016); (6) Aguilera et al. (2022).

Most of these volcanoes are Holocene, but some Pleistocene volcanic centers, showing fresh volcanic morphology and/or signs of unrest, are also included. There are 55 Holocene and 7 Pleistocene volcanic centers (Figure 1), from which a total of 19 volcanic centers are located in borders (i.e., Parinacota, Irruputuncu, Olca-Paruma, Ollagüe, Putana, Escalante-Sairecabur, Licancabur, Socompa, Llullaillaco, Escorial (Corrida de Cori), Lastarria, Cordón del Azufre, Cerro Bayo, Sierra Nevada, Falso Azufre, Nevados de Incahuasi, Nevados Tres Cruces, El Solo and Ojos del Salado) (Figure 2).

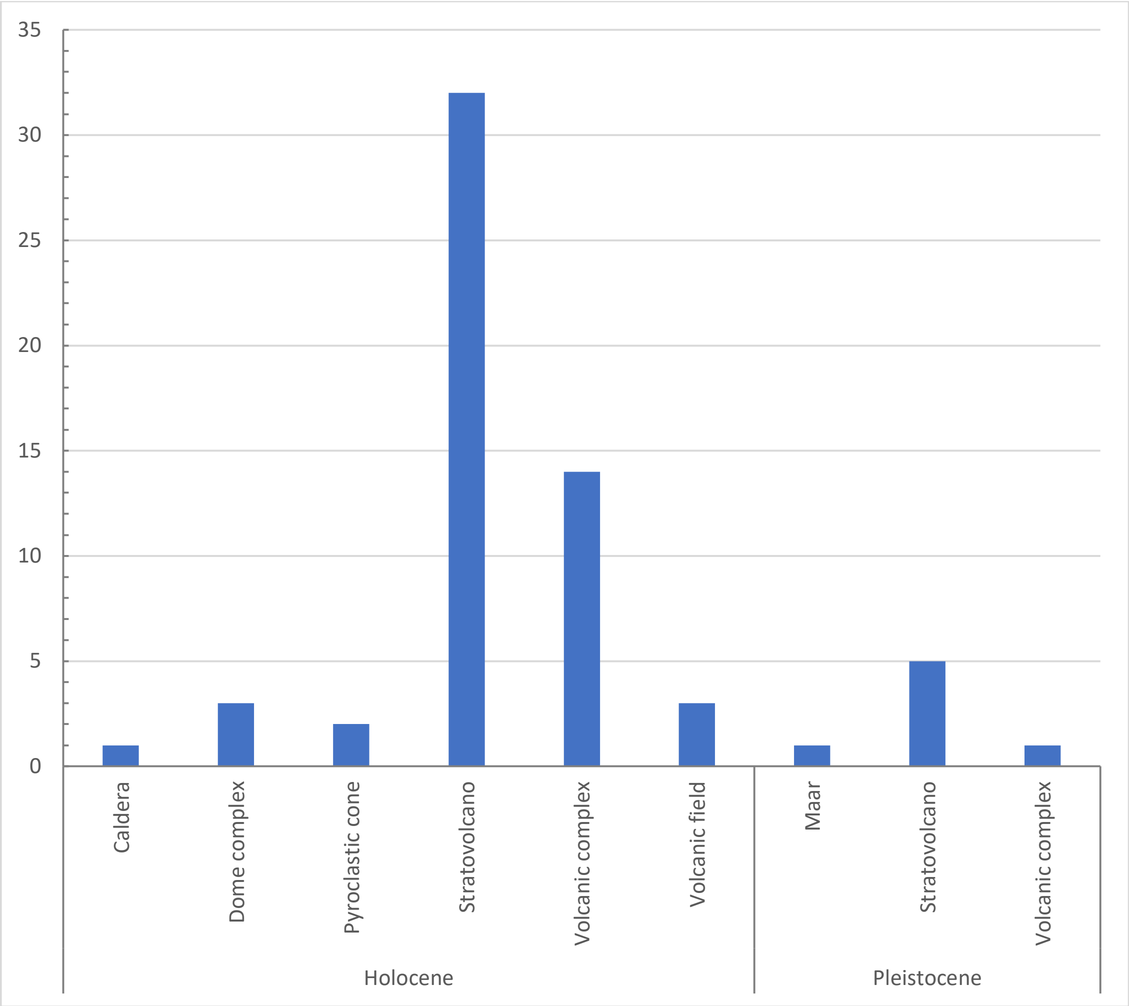

Figure 1. Volcano types of the CVZA. 37 are stratovolcanoes, 15 are volcanic complex, 3 are volcanic fields, 2 are pyroclastic cones, 3 are dome complex, 1 is a maar and 1 a caldera.

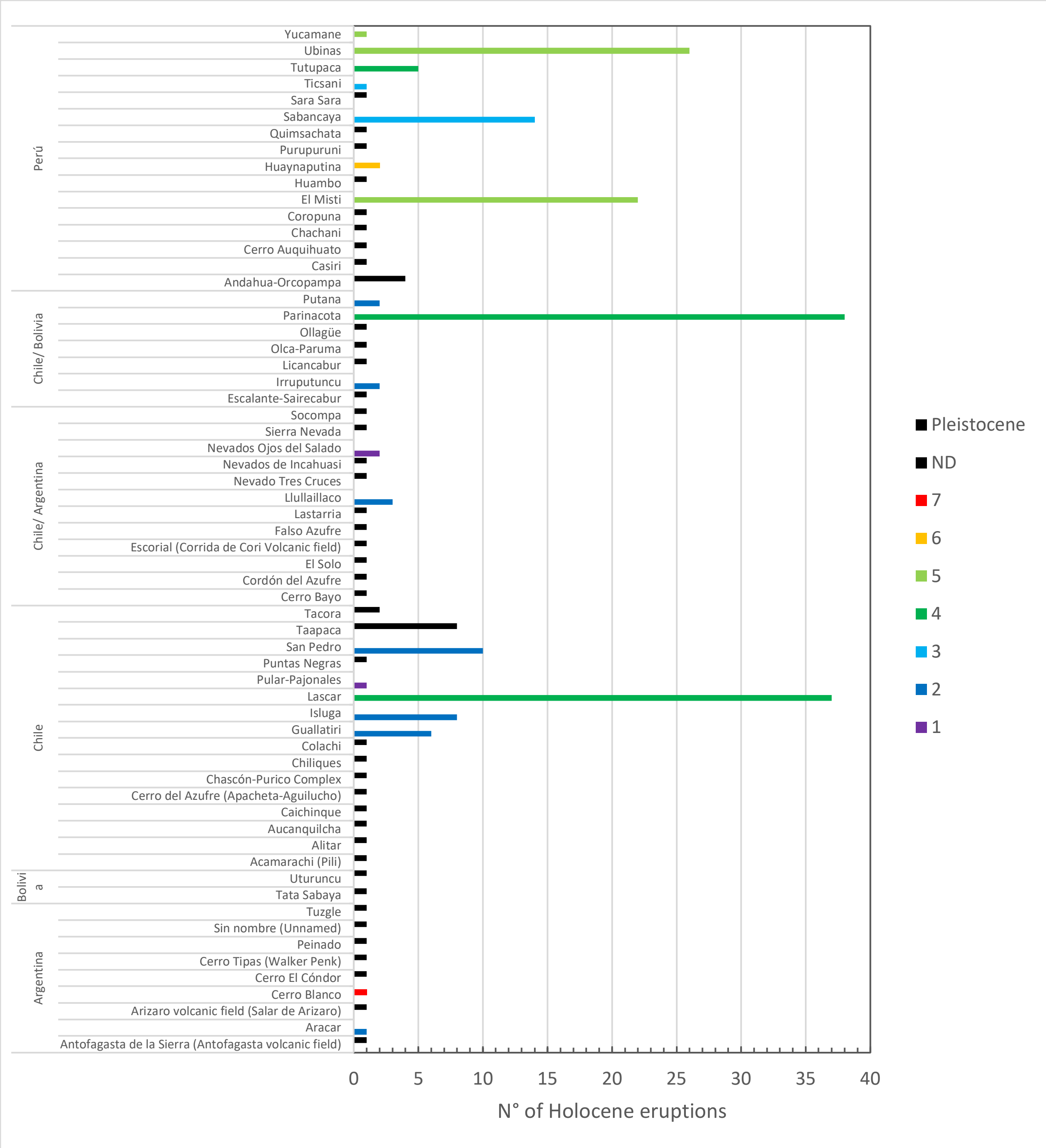

Figure 2. Volcanoes of the CVZA per country versus their number of eruptions and maximum VEI during the Holocene. Notice that Pleistocene volcanoes or volcanoes with unknown VEI (ND) and unknown number of Holocene eruptions, have been represented with a N° of Holocene eruptions equal to 1 for visualization.

The following sections present a brief description of each one of the 62 volcanoes, describing three main aspects: 1) physical characteristics, 2) eruption frequency and, 3) hazard types.

1.1 Quimsachata

Physical characteristics

Quimsachata is a 3848 m high lava dome of Holocene age (González-Ferrán, 1995), located ~120 km S of the Cusco city, Peru (Domingues et al., 1988). It has two sources of emission: an andesitic scoria cone, surrounded by a layer of lavas along the Vilcanota River; and a rhyolitic lava dome, Oroscocha (Macedo et al., 2016). Its main edifice has an estimated volume of ~ 33 km^3 (Fídel et al., 1997).

It is a very scarcely investigated volcano, some geological (Marocco and Garcia, 1974; González-Ferrán, 1995), petrographic (Domingues et al., 1988), surface deformation (Morales Rivera et al., 2016), and volcanic hazards works (Fídel et al., 1997; Macedo et al., 2016; Aguilar et al., 2021; Machacca et al., 2021; Aguilera et al., 2022) have been carried out.

Eruption frequency

Its rhyolitic lava dome, Oroscocha produced a thin lava flow, dated to 6400 years (Macedo et al., 2016). The Global Volcanism Program recognizes 1 Holocene eruptive period with no maximum VEI registered and it is not monitored.

Hazard types

According to Macedo et al. (2016) it has not flank collapse potential nor characteristics which could represent primary lahar sources. No deformation was detected at Quimsachata during a regional ALOS survey of Central Andes Volcanoes (Morales Rivera et al., 2016). There are not records of observed seismic unrest, nor fumarolic and/or magmatic degassing (Macedo et al., 2016).

The Quimsachata volcano is one of the easternmost witnesses of quaternary effusive magmatism in this area (Marocco and Garcia, 1974). Thus, the most characteristic volcanic process, which would be the most likely to occur in the event of an eruption, is extrusion of lavas.

1.2 Cerro Auquihuato

Physical characteristics

Cerro Auquihuato is a 4980 m high cinder cone of Pleistocene - Holocene age, located ~ 30 km NE of the Sara Sara volcano and East of the Ocoña River in the Ayacucho Region, Peru (Macedo et al., 2016). It has a lava flow of ~ 13 km long, of less than 1 km width, an average N-S direction (Martínez and Cervantes, 2003); and it has an estimated volume of ~ 5 km^3 (Fídel et al., 1997).

It is a very scarcely investigated volcano, some geological (Fídel et al., 1997; Martínez and Cervantes, 2003), surface deformation (Morales Rivera et al., 2016), and volcanic hazards works (Macedo et al., 2016; Aguilar et al., 2021; Machacca et al., 2021; Aguilera et al., 2022) have been carried out.

Eruption frequency

The Global Volcanism Program is not aware of any Holocene eruptions from Cerro Auquihuato. However, satellite images show a young pahoehoe lava flow suggesting possible Holocene activity (Macedo et al., 2016). It is monitored by CENVUL (Centro vulcanológico del Instituto Geofísico del Perú), with 1 permanent seismic station, and 1 inclinometer (IGP, 2021).

Hazard types

According to Macedo et al. (2016) it has not flank collapse potential nor characteristics which could represent primary lahar sources. Remarkable deformation was detected (up to 1.8 cm / year and ~ 7 km SE of the volcano) during a regional InSAR survey, attributed to pressurization of a magmatic source, although it could also be of hydrothermal origin (Morales Rivera et al., 2016). There are not records of observed seismic unrest, nor fumarolic and/or magmatic degassing (Macedo et al., 2016).

The most characteristic volcanic process of Cerro Auquihuato, which would be the most likely to occur in the event of an eruption, is extrusion of lavas (Martínez and Cervantes, 2003).

1.3 Sara Sara

Physical characteristics

Sara Sara is a 5522 m high stratovolcano of Pleistocene age, located ~12 km SW of Pausa town in the Ayacucho Region of Perú (Rivera et al., 2020a). It is the northernmost major volcanic center of Perú, its volcanic products cover an area of 21-47 km^2 and the main edifice has an estimated volume of 20-25 km^3 (Grosse et al., 2014; Rivera et al., 2020).

There are few works related to the geological-vulcanological study of the Sara Sara volcano; those that exist are mainly based on field geological reconnaissance (Olchauski, 1980; Pecho, 1983; Martínez and Cervantes, 2003; Grosse et al., 2014) and volcanic hazards (Morche and Núñez, 1998; Cueva, 2016; Cueva et al., 2018; Rivera et al., 2018, 2020; Aguilar et al., 2021; Machacca et al., 2021; Aguilera et al., 2022).

Eruption frequency

The Global Volcanism Program is not aware of any Holocene eruptions from Sara Sara. However, pristine lava flows on the upper slopes of the volcano and ash layers in peat deposits at its base suggest a very young, probably Holocene age (GVP, 2013). It is monitored by CENVUL (Centro vulcanológico del Instituto Geofísico del Perú), with 2 permanent seismic stations, 1 scientific camera and 1 inclinometer (IGP, 2021).

Hazard types

It suffered a partial sector collapse of its eastern flank, directed 12 km towards the NE (more than 200 m thick) and 7 km to the north there are avalanche deposits where Quilcata locality has settled (Rivera et al., 2020). Satellite images of the Sara Sara show that the area covered by ice and snow in wintertime is of ~ 0.01 km^3, with an average of 2 m of thickness (Rivera et al., 2020) which could represent a primary lahar source for Sara Sara volcano. No ground deformation was detected at Sara Sara during a regional ALOS survey (Morales Rivera et al., 2016), and there are no records of observed seismic unrest nor fumarolic or magmatic degassing.

According to the geological and volcanological hazard assessment of Rivera et al. (2020) the five main volcanic processes of Sara Sara volcano, which would be the most likely to occur in the event of an eruption, are tephra fallout, pyroclastic density currents, lahars, debris avalanches, and lava flows.

1.4 Andahua-Orcopampa

Physical characteristics

Andahua-Orcopampa is a 4713 m high volcanic field of Holocene age, located ~ 20 km ENE of Nevados de Coropuna in the Arequipa Region, Peru (GVP, 2013). It has been originated by a monogenetic volcanism on a graben-type valley, slightly oblique to the Andean direction, and controlled by faults oriented NNO-

SSE (Mariño and Zavala, 2010). It contains more than 15 cones concentrated in an area of approximately 240 km^2 (Delacour et al., 2007); and its total erupted volume is about 15 km^3 (Ruprecht and Wörner, 2007).

Several geological (Mariño and Zavala, 2010), petrographic (Venturelli et al., 1978; Delacour et al., 2002; Ruprecht and Wörner, 2007; Sørensen and Holm, 2008), surface deformation (Morales Rivera et al., 2016), geochronological (Kaneoka and Guevara, 1984; Eash and Sandor, 1995), geological evolution (Delacour et al., 2007; Gałaś, 2011), and volcanic hazards works (Macedo et al., 2016; Aguilar et al., 2021; Machacca et al., 2021; Aguilera et al., 2022) have been carried out.

Eruption frequency

Scoria cones represent the youngest episode of the Andahua Group activity (Gałaś, 2011), burned twigs from Ticsho cone were dated to 4,050 years BP (Cabrera and Thouret, 2000). The Global Volcanism Program recognizes 4 Holocene eruptive periods with no maximum VEI registered (GVP, 2013) and it is not monitored.

Hazard types

According to Macedo et al. (2016) it has not flank collapse potential nor characteristics which could represent primary lahar sources. There are not records of ground deformation, no observed seismic unrest because they are monogenetic volcanoes, and it shows fumaroles and gases (Macedo et al., 2016).

There are so many proofs of quite recent activity of the numerous centres that future eruptions may be expected (Gałaś, 2011). Following Macedo et al. (2016), the main volcanic processes of Andahua-Orcopampa volcanic field, which would be the most likely to occur in the event of an eruption, are tephra fallout (ashfall, lapilli and bombs), as well as lava flows. A potential reactivation would cause damage to both homes and farmland in the areas of Andahua, Ayo, Orcopampa, and Chachas (Macedo et al., 2016).

1.5 Coropuna

Physical characteristics

Nevado Coropuna is a 6377 m high stratovolcano of Neogene age (Venturelli et al., 1978; Forget et al., 2008), located ~150 km NW of Arequipa city and ~110 km away from the Pacific Ocean (Venturelli et al., 1978; Úbeda et al., 2018). It is the highest and largest volcanic center of Perú, its volcanic products cover an area of 224-350 km^2 and the main edifice has an estimated volume of 270 km^3 (De Silva and Francis, 1991; González-Ferrán, 1995; Grosse et al., 2014).

Several geological (De Silva and Francis, 1991; González-Ferrán, 1995; Grosse et al., 2014), petrographic (Frangipane, 1976; Venturelli et al., 1978), geochemical (Weibel et al., 1978), glaciological (Lamadon, 1999; Forget et al., 2008; Úbeda et al., 2012 , 2015, 2018), geochronological (Juvigne et al., 2002), and volcanic hazard studies (Olchauski and Dávila, 1994; Fídel et al., 1997; Núñez and Valenzuela, 2001; Macedo et al., 2016; Aguilar et al., 2021; Machacca et al., 2021; Aguilera et al., 2022) have been carried out.

Eruption frequency

Bromley et al. (2019) reported ages of 12.5 to 1.6 ka for its last lava flows. The Global Volcanism Program is not aware of any Holocene eruptions from Coropuna and the age of its latest eruption is not known, but according IGP (Instituto Geofísico del Perú) the last eruption was ~ 700 years ago. Macedo et al. (2016) indicate possible eruptive activity at the beginning of the Holocene due to the observation of pumice deposits. Solfataric activity has been reported and several young Holocene lava flows descend the NE, SE, and W flanks (GVP, 2013). It is monitored by CENVUL (Centro vulcanológico del Instituto Geofísico del Perú), with 5 permanent seismic stations, 1 scientific camera and 2 inclinometers (IGP, 2021).

Hazard types

It suffered a partial sector collapse of its SW flank and formed a landslide deposit as well as a horseshoe-shaped valley that was later filled by glaciers (Forget et al., 2008). Currently it has a glacial system of ~40 km^2 (Úbeda et al., 2015) which could represent a primary lahar source. No ground deformation was recorded by the COBE and COVI GPS stations at Coropuna until 2019 (Apaza et al., 2019). There are no records of observed seismic unrest. During a monitoring campaign in 2018, a ~ 50 m high column of water vapor was seen rising from the N flank (Ramos, 2019). Six hot springs have been located in the area with temperatures ranging from 18 to 51 °C (Núñez and Valenzuela, 2001). Monitoring does not show significant changes (Apaza et al., 2019).

According to the preliminary volcanic hazard map of Coropuna (Núñez and Valenzuela, 2001) the most characteristic volcanic processes, which would be the most likely to occur in the event of an eruption are lava flows, lahars, ballistics, pyroclastic flows, ash and pumice flows, side explosions, domes destruction and shock waves.

1.6 Huambo

Physical characteristics

Huambo is a 4554 m high volcanic field of Holocene age, located SSE of the Andahua-Orcocampo volcanic field, and W of Sabancaya volcano, in the Arequipa Region, Peru (Macedo et al., 2016). It is divided into two segments, the northern part forms a large lava flow field and a cinder cone "Cerro Keyocc", and the southern part contains other cinder cones and lava flows (Delacour et al., 2007).

It is a very scarcely investigated volcanic field, some petrographic (Mamani et al., 2010), geological evolution (Delacour et al., 2007), and volcanic hazards works (Rivera and Zavala, 2015; Macedo et al., 2016; Aguilar et al., 2021; Machacca et al., 2021; Aguilera et al., 2022) have been carried out.

Eruption frequency

The northern part contains a single vent, the Cerro Keyocc cinder cone, which produced an extensive lava field dated at about 2,650 years ago (Delacour et al., 2007). The Global Volcanism Program recognizes 1 Holocene eruptive period with no maximum VEI registered (GVP, 2013), and it is not monitored.

Hazard types

According to Macedo et al. (2016) it has not flank collapse potential nor characteristics which could represent primary lahar sources. There are not records of ground deformation, no observed seismic unrest, nor fumarolic and/or magmatic degassing (Macedo et al., 2016).

Following Macedo et al. (2016), as in Andahua-Orcopampa volcanic field the main volcanic processes of Huambo volcanic field, which would be the most likely to occur in the event of an eruption, are tephra fallout (ashfall, lapilli and bombs), as well as lava flows. A potential reactivation would cause damage to both homes and farmland in the areas of Andahua, Ayo, Orcopampa, and Chachas (Macedo et al., 2016).

1.7 Sabancaya

Physical characteristics

Sabancaya is a 5960 m high stratovolcano of Holocene age (Macedo et al., 2016), located ~75 km NW of Arequipa city, Perú (Boixart et al., 2020). It is the youngest and most recently active of the three volcanoes of the Ampato-Sabancaya Volcanic Complex (Rivera et al., 2016). Its volcanic products cover an area of 43-70 km^2 and the main edifice has an estimated volume of 6-10 km^3 (De Silva and Francis, 1991; Rivera et al., 2016; Grosse et al., 2014, 2018).

Several geological (De Silva and Francis, 1991; González-Ferrán, 1995; Grosse et al., 2014, 2018), petrographic (Gerbe and Thouret, 2004), fluid geochemistry (Moussallam et al., 2017; Ilanko et al., 2019), surface deformation (Pritchard and Simons, 2002, 2004), geological evolution (Bulmer et al., 1999), geochronological (Thouret et al., 2002; Juvigné et al., 2008), seismological (Jay et al., 2015; Boixart et al., 2020; MacQueen et al., 2020) and volcanic hazards works (Mariño et al., 2012; Rivera et al., 2016; Aguilar et al., 2021; Machacca et al., 2021; Aguilera et al., 2022) have been carried out.

Eruption frequency

The Global Volcanism Program recognizes 14 Holocene eruptive periods with a maximum registered VEI of 3 (GVP, 2013). There are no records of a partial sector collapse of its flanks. It has a glacier of 0.15 km^3 (Macedo et al., 2016) and snow and ice are deposited on it during rainy seasons (Dec-Apr), which remains until Jun-Jul, with thickness of ~2 m (Rivera et al., 2016). There are records of ground deformation (Pritchard and Simons, 2002; Jay et al., 2015) and it is monitored by CENVUL with 7 permanent seismic stations, 2 GPS stations, 1 multigas station and 4 scientific cameras (IGP, 2021); and OVI through DOAS gas scanners, GPS and seismic stations, inclinometer, video and thermal surveillance cameras, ash gauges and hot springs (OVI, 2021).

Hazard types

It had frequent signs of unrest since 2013 (Samaniego et al., 2016) and during most of 2016, maintained a level of seismic and fumarolic unrest similar to levels recorded in 2014 and 2015, with almost constant water-vapor and SO_2 plumes rising from the crater. An explosion on 27-08-2016 produced new areas of fumarolic activity on its N flank. Hybrid seismic events related to the movement of magma, and SO_2 emissions, increased noticeably during sept-oct 2016. An explosive eruption with numerous ash plumes began on 6-11-2016. Continuous ash emissions with plume heights exceeding 10 km altitude were recorded several times through Feb-2017. Thermal anomalies were first measured in satellite data in early Nov, along with numerous significant SO_2 plumes (GVP, 2017).

The current eruptive period began in Nov 2016 and has recently been characterized by lava dome growth, daily explosions, ash plumes, ashfall, SO_2 plumes, and ongoing thermal anomalies (BGVN, 2021). The most recent IGP bulletin (5-11, 04-2021) reports that its eruptive activity remains at moderate levels, with the average occurrence of 100 daily volcanic explosions and the observation of columns of ash and gases up to 2 km high over the summit (IGP/CENVUL, 2021).

1.8 Chachani

Physical characteristics

Chachani is a 6057 m high volcanic complex of Late Pleistocene-Holocene age (García et al., 1997), located ~20 km N of Arequipa city in Perú (De Silva and Francis, 1991). It is a group of lava domes, a stratovolcano complex, and a flank shield volcano (GVP, 2013). Its volcanic products cover an area of 313-360 km^2 and the main edifice has an estimated volume of 156-190 km^3 (De Silva and Francis, 1990, 1991; Grosse et al., 2014).

Several geological (De Silva and Francis, 1990, 1991; González-Ferrán, 1995; Grosse et al., 2014), surface deformation (Morales Rivera et al., 2016), geological evolution (García et al., 1997; Aguilar et al., 2016; 2022b), glaciological (Palacios et al., 2009; Andrés et al., 2011; Úbeda et al., 2015), geochronological (Paquereau et al., 2005, 2006; Paquereau-Lebti et al., 2008), seismological (Centeno et al., 2013) and volcanic hazards works (Degg and Chester, 2005; Macedo et al., 2016; Aguilar et al., 2021; Machacca et al., 2021; Aguilera et al., 2022) have been carried out.

Eruption frequency

The Global Volcanism Program is not aware of any Holocene eruptions from Chachani and no current or recent eruptive activity has been recorded or detected (Paquereau et al., 2006). The last volcancillo dome has probably more than 20 ka (ages reported in Aguilar et al. (2022)). Despite the lack of reliable records of its eruptive activity in the last 10,000 years, lava flows (Pampa de Palacio) and the presence of hot springs on the SW and W slopes suggest possible Holocene activity (González-Ferrán, 1995). It is monitored by CENVUL, with 1 permanent seismic station and 1 inclinometer (IGP, 2021), and represents a significant hazard potential, particularly because of its height and proximity to Arequipa.

Hazard types

There are no records of a partial sector collapse of its flanks and there are no glaciers conserved at the present day (Úbeda et al., 2015), however, permafrost and rock glaciers still exist (Andrés et al., 2011). No deformation was detected at Nevado Chachani during a regional ALOS survey (Morales Rivera et al., 2016). Frequent seismic activity occurs on its SW flank maybe related to either geothermal or tectonic phenomena (Centeno et al., 2013); there are records of solfataras in the summit region (Gałaś et al., 2014) and hot springs at Socosani and Yura which suggest hydrothermal activity (Degg and Chester, 2005).

The most characteristic volcanic processes of Chachani, which would be the most likely to occur in the event of an eruption, are lava flows, tephra fallout, lahars; and eventually, if the eruption is of greater magnitude, pyroclastic flows may occur (Macedo et al., 2016).

1.9 El Misti

Physical characteristics

El Misti is a 5822 m high stratovolcano of Holocene age, located above Arequipa, ~17 km NE of the city center, which is built up on its lowermost western slopes (approximately 3500 m lower than the volcano summit). Its volcanic products cover an area of ~ 89 km^2 and the main edifice has an estimated volume of 70-83 km^3 (De Silva and Francis, 1990, 1991; Thouret et al., 2001; Grosse et al., 2014, 2018).

Several geological (De Silva and Francis, 1990, 1991; González-Ferrán, 1995; Tort and Finizola, 2005; Grosse et al., 2014, 2018; Bernard et al., 2017), petrographic (Ruprecht and Wörner, 2007; Tepley et al., 2013; Rivera et al., 2017), fluid geochemistry (Birnie and Hall, 1974; Chávez Chávez, 1992; Finizola et al., 2004; Moussallam et al., 2017), surface deformation (Pritchard and Simons, 2004; Gonzales, 2009), geological evolution (Thouret et al., 2001; Paquereau et al., 2006), glaciological (Andrés et al., 2011), geochronological (Ayala-Arenas et al., 2019), seismological (Pacheco and Sykes, 1992) and volcanic hazards works (Legros, 2001; Delaite et al., 2005; Mariño et al., 2008; Cobeñas et al., 2012; Sandri et al., 2014; Pallares et al., 2015; Charbonnier et al., 2020; Aguilar et al., 2021; Machacca et al., 2021; Aguilera et al., 2022) have been carried out.

Eruption frequency

The GVP recognizes 22 Holocene eruptive periods with a maximum VEI registered of 4 (GVP, 2013). It is monitored by CENVUL, with 6 permanent seismic stations, 2 scientific camera and 1 GNSS station (IGP, 2021); and OVI through GPS and seismic stations, video cameras and hot springs surveillance (OVI, 2021).

Hazard types

Although there is no trace of a partial sector collapse in the recent history of Misti, the steepness of the present slopes (~30°), the height of the cone, and its location on the faulted edge of the Altiplano are favorable factors for a slope failure (Legros, 2001). Currently it has no glaciers or any glacial or periglacial landforms (Andrés et al., 2011). Data from the past 110 years reveal 12 tectonic unrest episodes, two unrest episodes due to increased degassing, but no magmatic unrest (Sandri et al., 2014). No ground deformation was detected at El Misti during InSAR surveys of the edifice between 1992 and 2002 (Pritchard and Simons, 2004) nor between 2006 and 2009 (Gonzales, 2009). The current fumarolic activity has persisted since at least 1787 (Thouret et al., 2001). A persistent thermal anomaly of ~+6 K has been identified at the summit in ASTER thermal infrared images from 2000 to 2010 (Moussallam et al., 2017 and references therein).

According to the volcanic hazard map of Mariño et al. (2008) and the geological survey carried out in Legros (2001) the four primary volcanic processes of El Misti volcano, which would be the most likely to occur in the event of an eruption, are ash and pumice fallout, pyroclastic flows, lahars, and debris avalanches.

1.10 Ubinas

Physical characteristics

Ubinas is a 5672 m high stratovolcano of Holocene age (Thouret et al., 2005), located ~ 70 km E of Arequipa city in the Moquegua Region, Perú (Del Carpio and Torres, 2020). It has a truncated appearance due to a large summit crater; its volcanic products cover an area of 58-65 km^2 and the main edifice has an estimated volume of 22-56 km^3 (De Silva and Francis, 1990; Thouret et al., 2005; Rivera et al., 2010; Grosse et al., 2014, 2018).

Several geological (Bullard, 1962; De Silva and Francis, 1990, 1991; González-Ferrán, 1995; Thouret et al., 2005; Rivera et al., 2010; Grosse et al., 2014, 2018), petrographic (Rivera et al., 2014; Samaniego et al., 2020), fluid geochemistry (Cruz et al., 2009, 2019), thermal anomalies (Coppola et al., 2015), geological evolution (Thouret et al., 2005; Lavallée et al., 2009), seismological (Del Carpio and Torres, 2020) and volcanic hazards works (Mariño et al., 2006; Rivera et al., 2008, 2010, 2011; Mariño et al., 2017; Del Carpio and Tavera, 2019; Aguilar et al., 2021; Machacca et al., 2021; Aguilera et al., 2022) have been carried out.

Eruption frequency

Ubinas is considered the most active volcano of Peru, with an average of seven eruptions (VEI 2–3) per century (Thouret et al., 2005; Rivera et al., 2014; Coppola et al., 2015). The Global Volcanism Program recognizes 26 Holocene eruptive periods with maximum VEI registered of 5. It is monitored by both CENVUL and OVI, with 6 permanent seismic stations, 2 scientific camera, 2 GNSS station and 3 inclinometers (IGP, 2021); and DOAS gas scanners, MultiGAS meter, GPS and seismic stations, inclinometer, video surveillance cameras, ash gauges and hot springs (OVI, 2021).

Hazard types

The geological setting, the presence of older sector collapse, recent flank failure episodes, and the extent of the hydrothermal system downslope towards the south increase the probability of sector collapse (Gonzales et al., 2014). During Dec-Apr, the upper part of the volcano is covered by a thin layer of snow (Mariño et al., 2006) which could represent a primary lahar source as well as rainfall, as occurred in Jan-Feb 2016 (Mariño et al., 2017). There are records of observed seismic unrest from 2006 to the present (Del Carpio and Torres, 2020) and 23 reported historical periods of unrest, most of them fumarolic or strong degassing episodes, between 1550-1996 (Rivera et al., 2010 and references therein). Throughout June (2019), SO_2 emissions climbed to over 4,000 t/d, proximal VT swarms began to occur beneath the volcanic edifice, and deformation measurements indicated a pressurization of the system. This ramp-up in activity culminated with an explosive eruption on 19 July 2019 (Apaza et al., 2021).

According to the volcanic hazard map of Mariño et al. (2006) the most characteristic volcanic processes of Ubinas volcano, which would be the most likely to occur in the event of an eruption, are tephra fallout, pyroclastic flows, south flank collapse and emplacement of debris avalanche flows and lahar flows.

1.11 Huaynaputina

Physical characteristics

Huaynaputina is a 4850 m high stratovolcano of Holocene age, located ~75 km SE of Arequipa city in the Moquegua Region (De Silva and Francis, 1990; González-Ferrán, 1995). It does not have the typical stratovolcano shape, only an extensive plateau is observed (4500 m.a.s.l.) that presents three openings or craters adjoining the edges of a deep valley (Macedo et al., 2016).

Several geological (Bullard, 1962; De Silva and Francis, 1990, 1991; González-Ferrán, 1995; Cueva et al., 2018), petrographic (Costa et al., 2003; Dietterich and de Silva, 2010), fluid geochemistry (Cruz et al., 2019), surface deformation (Morales Rivera et al., 2016), structural (Lavallée et al., 2006, 2009), geological evolution (Thouret et al., 1996, 1997, 1999; Adams et al., 2001), geochronological (Juvigné et al., 2008; Fei and Zhou, 2009), seismological (Antayhua et al., 2011, 2013; Centeno and Rivera, 2020) and volcanic hazards works (De Silva and Zielinski, 1998; Degg and Chester, 2005; Verosub and Lippman, 2008; Macedo et al., 2016; Fei et al., 2016; Slawinska and Robock, 2018; Prival et al., 2020; Aguilar et al., 2021; Machacca et al., 2021; Aguilera et al., 2022) have been carried out.

Eruption frequency

Is a relatively inconspicuous volcano that was the source of the largest historical eruption of South America in 1600 CE (GVP, 2013). The Global Volcanism Program recognizes 2 Holocene eruptive periods with maximum VEI registered of 6 and it is monitored by CENVUL, with 3 permanent seismic stations and 1 inclinometer (IGP, 2021).

Hazard types

It suffered a partial sector collapse of its E flank and directed towards the Río Tambo Canyon (Lavallée et al., 2009; Prival et al., 2020). Currently there are not primary sources for lahars, however they can occur, especially the post-eruptive type although sin-eruptive lahars can also be triggered, as was the case of the Tambo River in 1600 (Cueva et al., 2018). No ground deformation was detected at Huaynaputina during a regional ALOS survey of CVZ (Morales Rivera et al., 2016). Seismic activity from Huaynaputina alerted the local population and led to a volcanological investigation from May-Oct 2010. No seismic activity was recorded around the amphitheater and appeared to be associated mainly with the faults and lineaments in the region (Antayhua et al., 2011). In the summit area, the existence of a hydrothermal system is evidenced with fumarolic gases located inside the crater ranging from 51.8 to 78.7 °C (Antayhua et al., 2013). Likewise, there are hot springs located 10 to 14 km SE from the crater, which arise in the valley of the Tambo river with temperatures between 22.6 - 61.3 °C; and 20 to 22 km to the W with temperatures between 44.1 - 81 °C (Cruz et al., 2019).

According to the geological maps of the sectors of Calicanto and Chimpapampa and the geological survey carried out in Cueva et al. (2018) the most characteristic volcanic processes of Huaynaputina volcano, which would be the most likely to occur in the event of an eruption, are tephra fallout, pyroclastic density currents, lava flows and lahars.

1.12 Ticsani

Physical characteristics

Ticsani is a 5408 m high Stratovolcano (GVP, 2013; Macedo et al., 2016; Aguilera et al., 2022) of Holocene age, located ~ 59 km NW of the Moquegua city, in the Moquegua Region of Peru (Apaza et al., 2015). It is made up of a complex of domes, three of which are located inside a horseshoe-shaped avalanche caldera (Cruz, 2020); the "gray Ticsani" pumice fall deposit is the most voluminous tephra fallout from Ticsani, its 1-cm isopach covers an area of about 806 km^2, and the "old Ticsani" debris avalanche deposits has an estimated volume of ~ 12 km^3 (Mariño and Thouret, 2003).

Several geological (González-Ferrán, 1995; Thouret et al., 2002; Mariño and Thouret, 2003), fluid geochemistry (Byrdina et al., 2013; Apaza et al., 2015), surface deformation (González-Ferrán, 1995; Jay et al., 2013; Morales Rivera et al., 2016), seismological (Holtkamp et al., 2011; Cruz, 2020) and volcanic hazards works (Macedo et al., 2016; Cruz et al., 2018; Prival et al., 2020; Aguilar et al., 2021; Machacca et al., 2021; Aguilera et al., 2022) have been carried out.

Eruption frequency

According to Cruz (2020), Ticsani is an active volcano that has had at least three subplinian and phreatomagmatic eruptions in the last 10,000 years. The Global Volcanism Program recognizes 1 Holocene eruptive period (GVP, 2013), and a maximum VEI of 2-3 (Cruz, 2020). It is monitored by both CENVUL and OVI, with 5 permanent seismic stations, 1 scientific camera, and 1 inclinometer (IGP, 2021); and 3 seismic stations, 1 video surveillance camera, 2 GNSS station, and hot springs gauges (OVI, 2021).

Hazard types

It suffered a partial sector collapse (Cruz, 2020). This debris avalanche reached the confluence of the Tambo and Omate rivers (~ 44 km), turned into a lahar and moved along the Tambo River to the Pacific Ocean, covering more than 150 km (Mariño and Thouret, 2003). Currently, lahars could be generated from the voluminous deposits of debris avalanches (Mariño and Thouret, 2003). No deformation was detected during a regional ALOS survey (Morales Rivera et al., 2016), but deformation measurements carried out in 2005 identified two deformation zones (Jay et al., 2013; Gonzáles et al., 2006). Unrest is reported in 2018 (Prival et al., 2020). There are records of an earthquake swarm in 2005 (Holtkamp et al., 2011). Two fumaroles are located near the summit (Byrdina et al., 2013), and an important hydrothermal activity is observed in the area (Cruz et al., 2018) with 5-10 hot springs that sprout in its surroundings (Apaza et al., 2015).

According to Macedo et al. (2016) a potential reactivation would pose risk to the surrounding villages and numerous hamlets, located to the W and SW within a 12 km radius of the volcano, where more than 5,000 people live. The most characteristic volcanic processes, which would be the most likely to occur in the event of an eruption, are tephra fallout, lahars, and eventually pyroclastic flows and lava flows.

1.13 Tutupaca

Physical characteristics

Tutupaca is a 5801 m high stratovolcano of Holocene age, located ~60 km E of Moquegua city and 105 km N of Tacna city in Perú (Centeno and Rivera, 2020). Its volcanic products cover an area of ~ 60 km^2 and the main edifice has an estimated volume of ~ 13 km^3 (De Silva and Francis, 1990; Grosse et al., 2014).

Several geological (Bullard, 1962; De Silva and Francis, 1990, 1991; González-Ferrán, 1995; Grosse et al., 2014; Valderrama et al., 2016, 2018), petrographic (Manrique et al., 2020), fluid geochemistry (Apaza et al., 2015), surface deformation (Morales Rivera et al., 2016), geological evolution (Manrique, 2013; Valderrama et al., 2014, 2015; Samaniego et al., 2015; Mariño et al., 2019; 2021), seismological (Centeno and Rivera, 2020) and volcanic hazards works (Fidel and Zavala, 2001; Mariño et al., 2019; Aguilar et al., 2021; Machacca et al., 2021; Aguilera et al., 2022) have been carried out.

Eruption frequency

Eastern Tutupaca (5815 m above sea level) is the youngest edifice, constructed on top of the hydro thermally altered basal Tutupaca edifice (Mariño et al., 2019). It is composed of at least seven coalescent domes of dacitic composition that are not affected by Pleistocene glaciations, suggesting a Holocene age (Manrique et al., 2020). The Global Volcanism Program recognizes 5 Holocene eruptive periods with a maximum VEI registered of 4 (GVP, 2013), and it is monitored by CENVUL, with 3 permanent seismic stations and 1 inclinometer (IGP, 2021).

Hazard types

It suffered a partial sector collapse of its N flank, directed towards the NE (De Silva and Francis, 1990; Samaniego et al., 2015; Valderrama et al., 2016) and currently the conditions of height, humidity, precipitation and snow cover in the Tutupaca are similar to the Ampato-Sabancaya, Ubinas and Misti volcanoes (Mariño et al., 2019), which could represent primary lahar sources. No ground deformation was detected at Tutupaca during a regional ALOS survey of Central Andes Volcanoes (Morales Rivera et al., 2016). There are no records of observed seismic unrest, however, the presence of fumaroles located in the Tutupaca Este building, which present temperatures of up to 58.8 ºC (Mariño et al., 2019) and 2 hot springs in its surroundings make it a potentially active volcano (Apaza et al., 2015).

According to the geological and volcanic hazard map (Mariño et al., 2019) the most characteristic volcanic processes of Tutupaca volcano, which would be the most likely to occur in the event of an eruption, are lava flows, pyroclastic flows, tephra fallout, debris avalanche and lahars.

1.14 Yucamane

Physical characteristics

Yucamane is a 5495 m high stratovolcano of Holocene age, located ~11 km NE of Candarave town in the Tacna Region, Perú (Rivera and Mariño, 2004). Its volcanic products cover an area of 45-77 km^2 and the main edifice has an estimated volume of 21-26 km^3 (De Silva and Francis, 1990; Grosse et al., 2014; Rivera et al., 2018).

Several geological (Jaén, 1965; De Silva and Francis, 1990, 1991; González-Ferrán, 1995; Grosse et al., 2014), petrographic (Morche and De la Cruz, 1994), fluid geochemistry (INGEMMET and ELECTROPERÚ, 1994; Cotrina et al., 2009; Cruz et al., 2010), surface deformation (Morales Rivera et al., 2016), geological evolution (De la Cruz and De la Cruz, 2001), geochronological (Vela et al., 2014; Rivera et al., 2019, 2020), and volcanic hazards works (Fídel et al., 1997; Fídel and Huamaní, 2001; Rivera and Mariño, 2004; Rivera et al., 2018; Aguilar et al., 2021; Machacca et al., 2021; Aguilera et al., 2022) have been carried out.

Eruption frequency

The Global Volcanism Program recognizes 1 Holocene eruptive period with maximum VEI registered of 5 (GVP, 2013) and it is monitored by CENVUL, with 3 permanent seismic stations, 1 scientific camera and 2 inclinometers (IGP, 2021).

Hazard types

It suffered a partial sector collapse generating debris-avalanche deposits that extends more than 12 km to the S, SE, and E (Rivera et al., 2018). During Jan, Feb, Mar and Jun, a large part of Yucamane is practically covered with ice and snow; and during Dec-Apr, there are abundant rains that consequently generate or accelerate landslides which represents primary lahar sources (Rivera et al., 2018). No deformation was detected at Yucamane during a regional ALOS survey of Central Andes Volcanoes (Morales Rivera et al., 2016). There are no records of observed seismic unrest but fumarolic and magmatic degassing (Fídel and Huamaní, 2001; Cruz et al., 2010). Fumaroles have been located in its crater, as well as hot springs, with temperatures between 20-86 °C (Fídel and Huamaní, 2001). Stable isotopes δ18O and δD relationship proves that the thermal waters are coming up from a mixing of meteoric and magmatic waters (Cruz et al., 2010).

According to the geological maps and surveys carried out in the Tarata Quadrangle (Jaén, 1965; De la Cruz and De la Cruz, 2001) and volcanic hazard maps of Yucamane volcano (Fídel and Huamaní, 2001; Rivera and Mariño, 2004; Rivera et al., 2018) the most characteristic volcanic processes, which would be the most likely to occur in the event of an eruption, are tephra fallout, pyroclastic flows, lahars, debris avalanche and lava flows.

1.15 Purupuruni

Physical characteristics

Purpuruni is a 5315 m high dome complex of probable Holocene age, located ~ 48 km NW of the Chilean border in the Tacna Region, Peru (Bromley et al., 2019). It consists of a set of dacitic domes, a sequence of pyroclastic density currents, and its volcanic products cover an area of 20 km^2 (Vargas et al., 2012).

It is very scarcely investigated, some geological (Mendivil, 1965), fluid geochemistry (Vargas et al., 2012), surface deformation (Morales Rivera et al., 2016), seismological (Velarde et al., 2020), geochronological (Bromley et al., 2019) and volcanic hazards works (Macedo et al., 2016; Aguilar et al., 2021; Machacca et al., 2021; Aguilera et al., 2022) have been carried out.

Eruption frequency

The Global Volcanism Program is not aware of any Holocene eruptions from Purupuruni, it is in the list of Pleistocene volcanoes (GVP, 2013). However, a lava dome aged at 5.3 ka was reported in Bromley et al. (2019). It is not monitored but considered as one of the 16 active or potentially active volcanoes in Peru, with a low level of hazard (Macedo et al., 2016).

Hazard types

According to Macedo et al. (2016) it has not flank collapse potential nor characteristics which could represent primary lahar sources. No deformation was detected at Purupuruni during a regional ALOS survey of Central Andes Volcanoes (Morales Rivera et al., 2016). There are not records of observed seismic unrest, nor fumarolic and/or magmatic degassing (Macedo et al., 2016). However, between April to July 2020, many earthquakes were recorded with epicenters distributed between the Domes of the Purupuruni volcano due to the temporary reactivation of the Pacollo fault (Velarde et al., 2020), which according to Velarde et al. (2020), would have generated pressure and altered the internal fluids present in the hot springs located south of the crater of the volcano.

Following Vargas et al. (2012), the main volcanic processes of Purupuruni, which would be the most likely to occur in the event of an eruption, are lava domes, pyroclastic density currents and lava flows.

1.16 Casiri

Physical characteristics

Casiri is a 5650 m high stratovolcano of Holocene age, is ~25 km from the Tacora volcano located in Chilean territory, right on the border with Peru (Macedo et al., 2016). Its volcanic products cover an area of ~ 20 km^2 and the main edifice has an estimated volume of 3-7 km^3 (De Silva and Francis, 1990; Grosse et al., 2014).

There are few geological (Mendivil, 1965; Fídel et al., 1997b; De Silva and Francis, 1990, 1991; Monge and Cervantes, 2000), fluid geochemistry (Cruz et al., 2020), surface deformation (Morales Rivera et al., 2016), geochronological (Bromley et al., 2019), and volcanic hazards works (Macedo et al., 2016; Aguilar et al., 2021; Machacca et al., 2021; Aguilera et al., 2022) that have been carried out.

Eruption frequency

There are no reports of historic or current activity (De Silva and Francis, 1990, 1991) and the Global Volcanism Program is not aware of any Holocene eruptions from Casiri (GVP, 2013). However, due to evidence of postglacial activity found in two lava flows from the youngest cone, the volcano is considered to be potentially active (De Silva and Francis, 1990, 1991) and it is monitored by CENVUL, with 2 permanent seismic stations, and 1 inclinometer (IGP, 2021).

Hazard types

The vent itself has been breached to the south, probably due to dome collapse flows, as indicated by a thick apron of pyroclastic deposits on the slopes below (Bromley et al., 2019) and currently there are not characteristics which could represent primary lahar sources. No deformation was detected at Nevados Casiri during a regional ALOS survey of Central Andes Volcanoes (Morales Rivera et al., 2016). There are no records of observed seismic unrest and volcanic manifestations are sulfur deposits, solfataras and thermal springs (Mendivil, 1965). The heat source for the Casiri- Kallapuma geothermal zone is attributed to the Casiri-Paucarani volcanic complex, whose magmatic activity could be less than 1 Ma (Cruz et al., 2020).

There is no more information or reports of historical activity at Casiri, but according to the volcanic risk assessment report in south of Peru (Macedo et al., 2016), the most characteristic volcanic processes which would be the most likely to occur in the event of an eruption, are pyroclastic flows, extrusion of domes, and lava flows.

1.17 Tacora

Physical characteristics

Tacora is a 5980 m high stratovolcano of Holocene age, located ~100 km NE of Arica city in the Arica y Parinacota Region, close to the Peruvian border (GVP, 2013). It is the northernmost volcano of Chile; its volcanic products cover an area of ~ 30 km^2 and the main edifice has an estimated volume of 9-27 km^3 (Grosse et al., 2014; Aravena et al., 2015).

Several geological (Casertano, 1963; González-Ferrán, 1995; De Silva and Francis, 1991; Contreras, 2013; Grosse et al., 2014; Aravena et al., 2015), petrographic (Douglas, 1914; Montecinos, 1970), fluid geochemistry (Aguilera, 2008; Capaccioni et al., 2011), glaciological (Barcaza et al., 2017), surface deformation (Morales Rivera et al., 2016), geochronological (García et al., 2012), geological evolution (Salas et al., 1966; Wörner et al., 2000), seismological (Clavero et al., 2006; Pavez et al., 2019) and volcanic hazards works (Hantke, 1939; Lara et al., 2011; Amigo et al., 2012; Barrientos, 2013; ONEMI Arica y Parinacota, 2018; SERNAGEOMIN, 2020a, b; Amigo, 2021; Aguilera et al., 2022) have been carried out.

Eruption frequency

Hot springs on the eastern side of the edifice and young lava flows on the southern flank apparently overlying glacial valleys suggest possible Holocene activity (González-Ferrán, 1995). The Global Volcanism Program recognizes 2 Holocene eruptive periods with no maximum VEI registered. It is not monitored, and it is in the 42nd place of the last version of the Chilean volcanic risk ranking (SERNAGEOMIN, 2020a, b).

Hazard types

It suffered a partial sector collapse directed towards the south (Clavero et al., 2006) and currently the caldera is covered by glaciers above ~5500 m and has active rock glaciers (Capaccioni et al., 2011; Barcaza et al., 2017) which does not represents a primary lahar source for Tacora volcano (Lara et al., 2011). No ground deformation was detected at Tacora during a regional ALOS survey of Central Andes Volcanoes (Morales Rivera et al., 2016). There are records of observed seismic unrest (Clavero et al., 2006; Pavez et al., 2019) and fumarolic and magmatic degassing (Lara et al., 2011; Capaccioni et al., 2011; Contreras, 2013).

According to the geological map of the Visviri - Villa Industrial charts (García et al., 2012), the volcanic hazard map "Peligros volcánicos de la zona norte de Chile" (Amigo et al., 2012) and the geological survey carried out in Barrientos (2013) the most characteristic volcanic processes of Tacora volcano, which would be the most likely to occur in the event of an eruption, are minor tephra fallout, pyroclastic flows, extrusion of domes, volcanic avalanches, lahars and extrusion of blocky lavas.

1.18 Taapaca

Physical characteristics

Taapaca is a 5860 m high volcanic complex of Holocene age, located at the NE of the small town of Putre, the principal settlement of the northern Chilean Altiplano (GVP, 2013). Its volcanic products cover an area of 90-250 km^2 and the main edifice has an estimated minimum volume of 26-38 km^3 (Clavero et al., 2004; Aravena et al., 2015; Grosse et al., 2014, 2018; SERNAGEOMIN, 2021).

Several geological (González-Ferrán, 1995; Kohlbach and Lohnert, 1999; García et al., 2004; Aravena et al., 2015; Grosse et al., 2014, 2018), petrographic (Douglas, 1914), fluid geochemistry (Inostroza et al., 2020), geological evolution (Salas et al., 1966; Muñoz and Sepulveda, 1992; Muñoz and Charrier, 1996; Garcia et al., 1999; Wörner et al., 2000; Garcia, 2001), and volcanic hazards works (Amigo et al., 2012;

Clavero et al., 2004; Clavero and Sparks, 2005; Clavero, 2007; Lara et al., 2011; ONEMI Arica y Parinacota, 2018; SERNAGEOMIN, 2021; Amigo, 2021; Aguilera et al., 2022) have been carried out.

Eruption frequency

Taapaca had previously been considered an extinct volcanic complex (Salas et al., 1966). However, the presence of numerous hot and sulphurous hot springs are indicating the existence of an important hydrothermal activity, associated with the still active volcanic heat source (González-Ferrán, 1995). New data indicate that Taapaca Volcanic complex is a dormant volcano, with a potential for future eruptions (Clavero et al., 2004). The Global Volcanism Program recognizes 8 Holocene eruptive periods with no maximum VEI registered. It is monitored by OVDAS (Observatorio Vulcanológico de los Andes del Sur, SERNAGEOMIN, 2021), and it is in the 37th place of the last version of the Chilean volcanic risk ranking (SERNAGEOMIN, 2020a, b).

Hazard types

At least three major edifice collapse events have produced debris-avalanche deposits, the youngest of which underlies Putre. It thus represents a significant volcanic hazard to the town of Putre located at the base of the volcano and built on Taapaca volcanic avalanche deposits (Wörner et al., 2000). It does not have a primary lahar source or registered seismic unrest, but it has records of ground deformation and fumarolic and magmatic degassing (Lara et al., 2011).

According to SERNAGEOMIN (2021) a potential reactivation would be linked to the location of dacitic domes and the subsequent generation of pyroclastic density currents that would affect the southwest flank of the volcano (Amigo et al., 2012).

1.19 Parinacota

Physical characteristics

Parinacota is a 6336 m high stratovolcano of Holocene age, located at the southernmost part of the Nevados de Payachata volcanic group along the Chile-Bolivia border (GVP, 2013). Its volcanic products cover an area of 31-180 km^2 and the main edifice has an estimated minimum volume of 11-56 km^3 (Aravena et al., 2015; Grosse et al., 2014, 2018; SERNAGEOMIN, 2021).

Several geological (Francis and Self, 1987; De Silva and Francis, 1991; Clavero et al., 2002; 2004; Stern et al., 2007; Aravena et al., 2015; Grosse et al., 2014, 2018), petrographic (Davidson et al., 1990; Entenmann, 1994), fluid geochemistry (Inostroza et al., 2020), geochronological (Hora et al., 2007; Sáez et al., 2007; Guédron et al., 2019) geological evolution (Katsui and González, 1968; Francis and Wells, 1988; Wörner et al., 1988; Bourdon et al., 2000; Wörner et al., 2000), and volcanic hazard works (Lara et al., 2011; Amigo et al., 2012; Clavero et al., 2012; Bertín and Amigo, 2013; ONEMI Arica y Parinacota, 2018; Amigo, 2021; SERNAGEOMIN, 2021; Aguilera et al., 2022; Bertin et al., 2022) have been carried out.

Eruption frequency

Although no historical eruptions are known from Parinacota according to GVP (2023), Helium surface-exposure dates have been obtained, giving ages between 1400 and 3000 years (Wörner et al., 2000). Additionally, according to the hazard map of Parinacota recently published, its last eruption would have been in 1803 CE (Bertin et al., 2022). The Global Volcanism Program recognizes 6 Holocene eruptive periods with a maximum VEI of 0. However, sediment cores collected in the W basin of Lake Chungará show that many eruptions have occurred in the last 8 ka (Sáez et al., 2007; Guédron et al., 2019) and according to Clavero et al. (2004), PDC dating back 200 years would have been generated in a subplinian eruption of VEI 4. Bertin et al. (2022) recognize at least 38 Holocene eruptions. It is monitored by OVDAS (SERNAGEOMIN, 2021) and it is in the 22nd place of the last version of the Chilean volcanic risk ranking (SERNAGEOMIN, 2020a, b).

Hazard types

Debris avalanche deposits produced by a sector collapse located to the west of Parinacota volcano have been recognized (Francis and Self, 1987; Francis and Wells, 1988; Clavero et al., 2002; 2004). Since the collapse, the activity of Parinacota has been characterized by the emission of lavas and the generation of flows and pyroclastic fall, of andesitic composition, in addition to short-range lahars, which have built the current stratovolcano (Stern et al., 2007; Clavero et al., 2012). It should be noted that the permanent cover of snow and ice above 5,500 m a.s.l. warns about the potential generation of lahars (SERNAGEOMIN, 2021). There are records of seismic unrest (REAV Parinacota, 2020), while no ground deformation nor fumarolic and magmatic degassing (Lara et al., 2011).

According to SERNAGEOMIN (2021) a future reactivation could correspond to a flank eruption in the S-SW sector, with limited direct impact in the area, or an eruption in the main cone. Lava emissions and pyroclastic currents could be directed in any direction and would directly or indirectly affect the surrounding population. Pyroclastic emission in the atmosphere could spread to the east or west, depending on the season of the year (Amigo et al., 2012).

1.20 Guallatiri

Physical characteristics

Guallatiri is a 6071 m high stratovolcano of Holocene age, located in the Arica and Parinacota Region, northern Chile (GVP, 2013). Is the southernmost center of the Nevados de Quimsachata volcanic chain (García et al., 2004; Stern et al., 2007; Clavero et al., 2018) and is considered the second most active in northern Chile (SERNAGEOMIN, 2015). Its volcanic products cover an area of 27-292 km^2 and the main edifice has an estimated volume of 7-86 km^3 (Grosse et al., 2014; Aravena et al., 2015; SERNAGEOMIN, 2021).

Several geological (De Silva and Francis, 1991; García et al., 2004; Stern et al., 2007; Amigo and Bertin, 2013; Grosse et al., 2014; Aravena et al., 2015; Seynova et al., 2017; Clavero et al., 2018), petrographic (Watts et al., 2014), fluid geochemistry (Aguilera, 2008; Gliß et al., 2018; Inostroza et al., 2018; Arratia, 2019; Inostroza et al., 2020a; 2020b), surface deformation (Pritchard and Simons, 2004), thermal anomalies (Jay et al., 2013), geochronological (Watts, 2002; Montecinos, 2018), geological evolution (Sepúlveda, 2018; Sepúlveda et al., 2021), seismological (Henderson et al., 2012; Pritchard et al., 2014) and volcanic hazards works (Lara et al., 2011; Amigo et al., 2012; SERNAGEOMIN, 2015, 2020a, 2020b, 2021; ONEMI Arica y Parinacota, 2018; Jorquera et al., 2019; Reyes, 2019; Amigo, 2021; Reyes-Hardy et al., 2021; Aguilera et al., 2022) have been carried out.

Eruption frequency

A morphologicaly youthful lava flow on the northern flank of Acotango suggest possible Holocene activity (De Silva and Francis, 1991). The Global Volcanism Program recognizes 6 Holocene eruptive periods with a maximum VEI of 2. However, according to Jorquera et al. (2019), a Plinian eruption (VEI 4-5) occurred 2.6 ka BP. It is monitored by OVDAS (SERNAGEOMIN, 2021) and it is in the 30th place of the last version of the Chilean volcanic risk ranking (SERNAGEOMIN, 2020a, b).

Hazard types

In the SW flank of the volcano, Clavero et al. (2018) recognized distal block and ash flow deposits, although the lack of pyroclastic deposits and collapse scar suggests the absence of dome collapse (Walker et al., 2013). It retains a permanent ice-cap over 5,800 m a.s.l. (Lara et al., 2011; Amigo et al., 2012; Seynova et al., 2017; Jorquera et al., 2019) with a persistent and vigorous fumarolic activity steaming from two fumarolic fields (Aguilera, 2008; Inostroza et al., 2020a, 2020b). No deformation was detected at Guallatiri during a regional InSAR survey of Central Andean Volcanoes (Pritchard and Simons, 2004). There are also thermal fluid emissions, the volcano exhibits continuous seismic activity (Pritchard et al., 2014; SERNAGEOMIN, 2021), and according to ASTER images, it displays a permanent thermal hotspot anomaly (Jay et al., 2013).

A potential reactivation could be associated with the emplacement of lava flows or lava domes. A major explosive eruption would cause tephra fallout in distant areas even hundreds of kilometers (Amigo et al., 2012).

1.21 Tata Sabaya

Physical characteristics

Tata Sabaya is a 5430 m high stratovolcano of Holocene age, located above the northern end of the Salar de Coipasa in the Altiplano of Bolivia (GVP, 2013). It is a high-K, andesitic, composite-cone, that was built in at least four stages, and is the only one with Holocene activity which is not on the border with another country (De Silva et al., 1993); its volcanic products cover an area of ~ 37 km^2 and the main edifice has an estimated volume of ~ 10 km^3 (Grosse et al., 2014).

It is a scarcely investigated volcano, some geological (De Silva and Francis, 1991; González-Ferrán, 1995; Clavero et al., 2006; Grosse et al., 2014), petrographic (Deruelle and Brousse, 1984), surface deformation (Pritchard and Simons, 2004), geological evolution (Francis and Wells, 1988; De Silva et al., 1993; Godoy et al., 2012), and volcanic hazard works (Aguilera et al., 2022), have been carried out.

Eruption frequency

The present volcanic edifice has been rebuilt since a major cone collapse event ~ 12,000 years ago (De Silva et al., 1993) and since there are no moraines on the volcano, the subsequent healing events appear to have taken place after the Pleistocene Andean glaciation (Francis and Wells, 1988). Thus, despite the lack of reliable records of its eruptive activity in the last 10,000 years, Tata Sabaya has been classified as "'potentially active" by De Silva and Francis (1991). The Global Volcanism Program is not aware of any Holocene eruptions from Tata Sabaya and it is not monitored.

Hazard types

It suffered a partial sector collapse directed towards the S, covering ~ 300 km^2 and reaching a distance of more than 30 km (Francis and Wells, 1988; De Silva and Francis, 1991; González-Ferrán, 1995). Currently there are not characteristics which could represent primary lahar sources. No deformation was detected at Tata Sabaya during a regional InSAR survey of Central Andean Volcanoes (Pritchard and Simons, 2004). There are not records of observed seismic unrest nor fumarolic or magmatic degassing.

According to the geological surveys carried out in Tata Sabaya (Francis and Wells, 1988; De Silva and Francis, 1991; De Silva et al., 1993; González-Ferrán, 1995; Clavero et al., 2006; Godoy et al., 2012) the most characteristic volcanic processes which would be the most likely to occur in the event of an eruption, are lava domes and flows, pyroclastic flows and debris avalanches.

1.22 Isluga

Physical characteristics

Isluga is a 5501 m high stratovolcano of Holocene age, located ~ 7 km W of the Chile-Bolivia border (GVP, 2013). It has a well-preserved, 400-m-wide summit crater at the western end of the elongated, snow-covered summit region (De Silva and Francis, 1991); its volcanic products cover an area of 62-214 km^2 and the main edifice has an estimated volume of 15-113 km^3 (Grosse et al., 2014; Aravena et al., 2015; SERNAGEOMIN, 2021).

Several geological (De Silva and Francis, 1991; González-Ferrán, 1995; Grosse et al., 2014; Aravena et al., 2015), petrographic (Cascante et al., 2012), surface deformation (Pritchard and Simons, 2004), thermal anomalies (Jay et al., 2013), geochronological (Wörner et al., 2000), seismological (Henderson et al., 2012; Pritchard et al., 2014) and volcanic hazards works (Sapper, 1917; Casertano, 1963; Petit-Breuilh, 2004; Céspedes et al., 2004; Lara et al., 2011; Amigo et al., 2012; Bertin and Amigo, 2013; ONEMI Tarapacá, 2017; SERNAGEOMIN, 2020a, b, 2021; Amigo, 2021; Aguilera et al., 2022) have been carried out.

Eruption frequency

Activity from the summit crater was reported in the 19th and 20th centuries (Casertano, 1963). The Global Volcanism Program recognizes 8 Holocene eruptive periods with maximum VEI registered of 2 (GVP, 2013). It is monitored by OVDAS (SERNAGEOMIN, 2021), and it is in the 59th place of the last version of the Chilean volcanic risk ranking (SERNAGEOMIN, 2020a, b).

Hazard types

It suffered a partial sector collapse directed towards the NW (Cascante et al., 2012) and currently it has flank collapse potential but not to generating lahars (Lara et al., 2011). No deformation was detected at Isluga during a regional InSAR survey of Central Andean Volcanoes (Pritchard and Simons, 2004). According to Lara et al. (2011) there are no records of observed seismic unrest but Pritchard et al. (2014) reported an increase in seismicity and change in event locations in 2012 along with an increase in the temperature of a satellite hotspot. There are records of fumarolic activity in the central crater and about 150 m below the crater towards the SW (De Silva and Francis, 1991; González-Ferrán, 1995; Lara et al., 2011). According to ASTER images, it displays a permanent thermal hotspot anomaly (Jay et al., 2013).

A reactivation of the Isluga volcano could be related to the emission of short-range lava flows and the generation of pyroclastic density currents towards the north, west and south flanks, which could affect wetlands near Aravilla and Enquelga (Amigo et al., 2012). Occasional pyroclastic fallouts could affect the towns of Isluga, Colchane and sectors around the international route CH-15 (SERNAGEOMIN, 2021).

1.23 Irruputuncu

Physical characteristics

Irruputuncu is a 5165 m high stratovolcano of Holocene age, located in the Chile-Bolivia border (De Silva and Francis, 1991; González-Ferrán, 1995). It has two craters, the southernmost of which is fumarolically active and produces an ~200-m-high plume (Tassi et al., 2011); its volcanic products cover an area of 14-44 km^2 and the main edifice has an estimated volume of 3-12 km^3 (Grosse et al., 2014, 2018; SERNAGEOMIN, 2021).

Several geological (De Silva and Francis, 1991; González-Ferrán, 1995; Stern et al., 2007; Grosse et al., 2014, 2018), petrographic (Rodríguez et al., 2015), fluid geochemistry (Aguilera, 2008; Tassi et al., 2011; Pizarro et al., 2012), surface deformation (Pritchard and Simons, 2004), thermal anomalies (Jay et al., 2013), geochronological (Wörner et al., 2000), seismological (Henderson et al., 2012; Pritchard et al., 2014) and volcanic hazards works (Casertano, 1963; Petit-Breuilh, 2004; Lara et al., 2011; Amigo et al., 2012; Aguilera, 2008; Bertín and Amigo, 2013a; ONEMI Tarapacá, 2017; Amigo, 2021; Aguilera et al., 2022) have been carried out.

Eruption frequency

The first unambiguous historical eruption from Irruputuncu took place in November 1995, when phreatic explosions produced dark ash clouds (Stern et al., 2007). The Global Volcanism Program recognizes 2 Holocene eruptive periods with maximum VEI registered of 2. It is monitored by OVDAS (SERNAGEOMIN, 2021), and it is in the 47th place of the last version of the Chilean volcanic risk ranking (SERNAGEOMIN, 2020a, b).

Hazard types

It suffered a partial sector collapse directed towards the SW (De Silva and Francis, 1991) and currently it has flank collapse potential but not to generating lahars (Lara et al., 2011). No deformation was detected at Irruputuncu during a regional InSAR survey of Central Andean Volcanoes (Pritchard and Simons, 2004). There are records of observed seismic unrest and fumarolic and magmatic degassing (Lara et al., 2011; Pritchard et al., 2014). A thermal spring located 13 km west of the volcano disappeared after an earthquake (Mw 7.9) occurred in this area on June 13, 2005 (Tassi et al., 2011). The source of fluids present in the volcano is mainly dominated by magmatic origin (Aguilera, 2008) and shows permanent degassing activity, mainly through its central summit (Stern et al., 2007). According to ASTER images, it displays small thermal anomaly hotspots (Jay et al., 2013).

A reactivation of the Irruputuncu volcano would be associated to emission of lava flows or lava domes, as well as pyroclastic density currents and tephra fallout (Amigo et al., 2012). There are no towns near this eruptive center, however an important industrial movement is developing in the vicinity of its western flank, linked to large-scale mining activities (SERNAGEOMIN, 2021).

1.24 Olca-Paruma

Physical characteristics

Olca-Paruma is a 5450 m high volcanic complex of Holocene age, located in the Chile-Bolivia border (De Silva and Francis, 1991; González-Ferrán, 1995). It is formed by a 15-km-long E-W ridge comprised of several stratovolcanoes with Holocene lava flows (GVP, 2013); its volcanic products cover an area of ~80-2227 km^2 and the main edifice has an estimated volume of 19-74 km^3 (De Silva and Francis, 1991; Grosse et al., 2014).

Several geological (De Silva and Francis, 1991; González-Ferrán, 1995; Grosse et al., 2014), fluid geochemistry (Aguilera, 2008; Reyes et al., 2011; Tassi et al., 2011), surface deformation (Pritchard and Simons, 2004), thermal anomalies (Jay et al., 2013), geological evolution (Navas, 2019), seismological (Pritchard et al., 2014) and volcanic hazards works (Casertano, 1963; Lara et al., 2011; Amigo et al., 2012; Orozco and Bertín, 2013; ONEMI Tarapacá, 2017; Amigo, 2021; Aguilera et al., 2022) have been carried out.

Eruption frequency

The only known historical activity from the Olca-Paruma volcanic complex was a flank eruption of unspecified character between 1865 and 1867 (GVP, 2013). The Global Volcanism Program recognizes 1 Holocene eruptive period without maximum VEI registered. It is monitored by OVDAS (SERNAGEOMIN, 2021), and it is in the 49th place of the last version of the Chilean volcanic risk ranking (SERNAGEOMIN, 2020a, b).

Hazard types

Currently it has flank collapse potential but not to generating lahars (Lara et al., 2011). No deformation was detected at Olca-Paruma during a regional InSAR survey of Central Andean Volcanoes (Pritchard and Simons, 2004). There are no records of observed seismic unrest (Lara et al., 2011), although according to Pritchard et al. (2014) it had three potential swarms in 2010. The majority of other potential swarms for Olca were ruled out as they were probably associated with mining (Pritchard et al., 2014). There are records of fumarolic and magmatic degassing (Lara et al., 2011). The present fumarolic activity of Olca began within the last ~60 years. At present, the main fumarolic field is restricted to the dome within the summit crater (Tassi et al., 2011). According to ASTER images, it displays small thermal anomaly hotspots (Jay et al., 2013).

A reactivation of this complex would be mainly associated with the emission of andesitic to dacitic lavas as well as low explosive activity (Amigo et al., 2012). An important industrial movement is developing in the vicinity of its W flank linked to large mining activities (Coposa aerodrome and the Collahuasi thermoelectric plant) and therefore, there are mining settlements inhabited practically all year round (SERNAGEOMIN, 2021).

1.25 Aucanquilcha

Physical characteristics

Aucanquilcha is a 6176 m high stratovolcano of Pleistocene age (GVP, 2013), located at the center of a geomorphologically distinct cluster of around 20 volcanic centers in the Antofagasta Region, Chile, just west of the border with Bolivia (Walker et al., 2013). Located wholly within northern Chile, Aucanquilcha volcano was the site of the world's highest mine (sulphur) and permanent human habitation (De Silva and Francis, 1991) which finally closed its last camp in 1992: Amincha (Rivera, 2019); its volcanic products cover an area of 64-700 km^2 and the main edifice has an estimated volume of 24-327 km^3 (Aravena et al., 2015; Grosse et al., 2014, 2018).

Several geological (De Silva and Francis, 1991; González-Ferrán, 1995; Aravena et al., 2015; Grosse et al., 2014, 2018), petrographic (Walker et al., 2013), glaciological (Barcaza et al., 2017), surface deformation (Pritchard and Simons, 2004), thermal anomalies (Jay et al., 2013), geochronological (Wörner et al., 2000; Grunder et al., 2006; Klemetti and Grunder, 2008), geological evolution (Francis and Wells, 1988; Walker et al., 2010), and volcanic hazards works (Lara et al., 2011; Amigo et al., 2012; Amigo, 2021; Aguilera et al., 2022) have been carried out.

Eruption frequency

The Global Volcanism Program is not aware of any Holocene eruptions from Aucanquilcha, it is in the list of Pleistocene volcanoes and presently displays fumarolic activity (GVP, 2013). It is not monitored, and it is in the 70th place of the last version of the Chilean volcanic risk ranking (SERNAGEOMIN, 2020a, b).

Hazard types

It suffered a partial sector collapse directed towards the W side of the edifice (Klemetti and Grunder, 2008). Currently it has flank collapse potential but not to generating lahars (Lara et al., 2011), although large rock glaciers have been observed (Barcaza et al., 2017) and according to González-Ferrán (1995), the upper part of the volcano and part of the chain are permanently covered by ice, which constitutes a potential risk of avalanches in the event of a possible eruptive reactivation. No deformation was detected at Aucanquilcha during a regional InSAR survey of Central Andean Volcanoes (Pritchard and Simons, 2004). There are no records of observed seismic unrest (Lara et al., 2011), a feeble fumarolic activity persist to the present day (De Silva and Francis, 1991), and according to (Jay et al., 2013) it has potential hotspots that merit further study.

Despite the lack of reliable records of its eruptive activity in the last 10,000 years, Aucanquilcha is considered potentially active (De Silva and Francis, 1991), owing to its youthful morphology and faint steam emission in defunct sulphur mine workings near the summit (Grunder et al., 2006). In 2011 the Aucanquilcha volcano was considered a geologically active and potentially dangerous volcano, with very low specific risk level (Lara et al., 2011). A reactivation of this complex would be mainly associated with the emission of lavas as well as low explosive activity (Amigo et al., 2012).

1.26 Ollagüe

Physical characteristics

Ollagüe is a 5863 m high stratovolcano of Pleistocene age, located in the Chile-Bolivia border (GVP, 2013). It has a truncated appearance due to a large summit crater; its volcanic products cover an area of 113-260 km^2 and the main edifice has an estimated volume of 43-181 km^3 (Aravena et al., 2015; Grosse et al., 2014, Grosse et al., 2018; SERNAGEOMIN, 2021).

Several geological (De Silva and Francis, 1991; González-Ferrán, 1995; Aravena et al., 2015; Grosse et al., 2014, 2018), petrographic (Thorpe, 1984; Feeley et al., 1993; Feeley and Davidson, 1994; Mattioli et al., 2006), fluid geochemistry (Rojas, 2019), surface deformation (Tibaldi et al., 2006; Vezzoli et al., 2008), thermal anomalies (Jay et al., 2013), geochronological (Wörner et al., 2000), geological evolution (Francis and Wells, 1988; Clavero et al., 2004c; Ureta et al., 2019), seismological (Clavero et al., 2006; Henderson et al., 2012a; Pritchard et al., 2014) and volcanic hazards works (Casertano, 1963; Petit-Breuilh, 2004; Lara et al., 2011; Amigo et al., 2012; Bertin and Orozco, 2013; ONEMI Antofagasta, 2019; Amigo, 2021; Aguilera et al., 2022) have been carried out.

Eruption frequency

The Global Volcanism Program is not aware of any Holocene eruptions from Ollagüe and it is in the list of Pleistocene volcanoes (GVP, 2013). However, there are suggestions of unconfirmed historical eruptions thought to have been mistaken for intense fumarolic activity (Feeley et al., 1993; Petit-Breuilh, 2004) and a parasitic Holocene scoria cone, La Poruñita was erupted through its debris-avalanche (Thorpe, 1984; González-Ferrán, 1995). It is monitored by OVDAS (SERNAGEOMIN, 2021), and it is in the 60th place of the last version of the Chilean volcanic risk ranking (SERNAGEOMIN, 2020a, b).

Hazard types

It suffered a partial sector collapse of its SW flank, the deposits extended W from the volcano and separated the Salar de San Martín from the Salar de Ollagüe (De Silva and Francis, 1991). Currently it has flank collapse potential but not to generating lahars (Lara et al., 2011). No deformation was detected at Ollagüe during a regional InSAR survey of Central Andean Volcanoes (Pritchard and Simons, 2004), while according to Vezzoli et al. (2008) its volcanological evolution is characterized by four stages of volcano building separated by three main events of deformation and collapse of the cone. There are records of observed seismic unrest, fumarolic degassing and satellite thermal hotspots (Lara et al., 2011; Jay et al., 2013; Pritchard et al., 2014). Thus, despite the lack of reliable records of its eruptive activity in the last 10,000 years, it is considered a potentially active volcano.

A reactivation of this volcano would be linked to the extrusion of domes or viscous lavas, with the possible generation of pyroclastic density currents mainly directed towards the west flank (Amigo and Bertin, 2013). A larger eruption, with a low probability of occurrence, could affect the town of Ollagüe (SERNAGEOMIN, 2021).

1.27 Cerro del Azufre (Apacheta-Aguilucho)

Physical characteristics

Cerro del Azufre is a 5846 m high volcanic complex of Holocene age, located ~105 km NE and ~55 km NW from the city of Calama and El Tatio Geothermal Field, respectively, in the Antofagasta Region of Chile just west of the Bolivian border (Godoy et al., 2008). Is the largest and youngest volcanic center of a complex volcanic chain with 100 km in length (González-Ferrán, 1995); its volcanic products cover an area of ~ 96 km^2 and the main edifice has an estimated volume of ~ 33 km^3 (Grosse et al., 2014).

Several geological (De Silva and Francis, 1991; González-Ferrán, 1995; Grosse et al., 2014), fluid geochemistry (Tassi et al., 2010; Aguilera et al., 2020), thermal anomalies (Jay et al., 2013), geochronological (Francis and Rundle, 1976; Urzúa et al., 2002), geological evolution (Roobol et al., 1976; Godoy et al., 2008; Rivera and Zavala, 2015), and volcanic hazards works (Lara et al., 2011; Amigo et al., 2012; Amigo, 2021; Aguilera et al., 2022) have been carried out.

Eruption frequency

It has two youthful-looking craters on the main edifice that could be Holocene and the postglacial silicic domes on the E flank represent the most recent activity from this system (De Silva and Francis, 1991). The Global Volcanism Program is not aware of any Holocene eruptions from Cerro del Azufre, but it is in the list of Holocene volcanoes (GVP, 2013), it is not monitored, and it is in the 76th place of the last version of the Chilean volcanic risk ranking (SERNAGEOMIN, 2020a, b).

Hazard types

It has flank collapse potential but not to generating lahars (Lara et al., 2011). There are not records of ground deformation or observed seismic unrest (Lara et al., 2011), but intense fumarolic activity without historical eruptions (Aguilera et al., 2020). According to Jay et al. (2013) it has potential hotspots that merit further study.

Despite the lack of reliable records of its eruptive activity in the last 10,000 years, in 2011 the Cerro del Azufre volcano was considered a geologically active and potentially dangerous volcano, with low specific risk level (Lara et al., 2011). A reactivation of this center could correspond to a minor eruption, probably of a phreatic type, with a local impact (Amigo et al., 2012).

1.28 San Pedro

Physical characteristics

San Pedro is a 6145 m high stratovolcano of Holocene age, located in the Antofagasta Region, ~ 35 km away from the Chile-Bolivia border (Bertin and Amigo, 2015). San Pedro is composed of two superimposed coalescent cones, denominated the "young cone" (~5971 m a.s.l.) and the "old cone" (~6149 m a.s.l.), where the active fumarole is located (Francis et al., 1974; O'Callaghan and Francis, 1986); its volcanic products cover an area of 124-150 km^2 and the main edifice has an estimated volume of 40-56 km^3 (De Silva and Francis, 1991; Grosse et al., 2014; Aravena et al., 2015; SERNAGEOMIN, 2021).

Several geological (De Silva and Francis, 1991; González-Ferrán, 1995; Grosse et al., 2014; Aravena et al., 2015), petrographic (Francis et al., 1974; Godoy et al., 2014), glaciological (Barcaza et al., 2017), surface deformation (Pritchard and Simons, 2004), thermal anomalies (Jay et al., 2013), geochronological (Wörner et al., 2000; Delunel et al., 2016), geological evolution (O'Callaghan and Francis, 1986; Francis and Wells, 1988), and volcanic hazards works (Casertano, 1963; Petit-Breuilh, 2004; Lara et al., 2011; Amigo and Bertin, 2012; Amigo et al., 2012; Bertin and Amigo, 2015, 2019; ONEMI Antofagasta, 2019; Alcozer, 2020; Amigo, 2021; Aguilera et al., 2022; (Alcozer-Vargas et al., 2022) have been carried out.

Eruption frequency

San Pedro is the only one in the area which has a record of historic activity (Casertano, 1963; Francis et al., 1974). The Global Volcanism Program recognizes 10 Holocene eruptive periods with maximum VEI registered of 2 (GVP, 2013). It is monitored by OVDAS (SERNAGEOMIN, 2021), and it is in the 41st place of the last version of the Chilean volcanic risk ranking (SERNAGEOMIN, 2020a, b).

Hazard types

It suffered a partial sector collapse which generated a large debris avalanche deposited to the western pampa of the volcano (González-Ferrán, 1995). Currently it has flank collapse potential but not to generating lahars (Lara et al., 2011), although large rock glaciers have been observed (Barcaza et al., 2017). No deformation was detected at the San Pedro-San Pablo Volcanic Complex during a regional InSAR survey of Central Andean Volcanoes (Pritchard and Simons, 2004). There are no records of observed seismic unrest but fumarolic and magmatic degassing (Lara et al., 2011), and small thermal anomaly hotspots (Jay et al., 2013).

According to the volcanic hazard maps (Amigo et al., 2012; Bertin and Amigo, 2015, 2019) and SERNAGEOMIN (2021) the most characteristic volcanic processes of the San Pedro volcano, which would be the most likely to occur in the event of an eruption, are tephra fallout, pyroclastic density currents, lava flows, volcanic ballistic projectiles, and lahars.

1.29 Uturuncu

Physical characteristics

Uturuncu is a 6008 m high stratovolcano of Pleistocene age (Sparks et al., 2008), located in the Lipez area, in the most southern part of the Bolivian Altiplano (Blard et al., 2014). It is the highest peak of SW Bolivia and is part of a large regional cluster of volcanoes, nested calderas and ignimbrite sheets termed the Altiplano-Puna volcanic complex (de Silva, 1989); its volcanic products cover an area of 174 km^2 and the main edifice has an estimated volume of 54 km^3 (Grosse et al., 2014).

Several geological (Kussmaul et al., 1977; de Silva, 1989; Grosse et al., 2014), petrographic (Fernandez et al., 1973; Sparks et al., 2008; Muir et al., 2014, 2015), glaciological (Alcalá-Reygosa, 2017), fluid geochemistry (Sunagua, 2004), surface deformation (Pritchard and Simons, 2002; Fialko and Pearse, 2012; Henderson and Pritchard, 2013; Hickey et al., 2013;Gottsmann et al., 2017; Barone et al., 2019; Pritchard et al., 2018; Morand et al., 2021), geochronological (Blard et al., 2014), geological evolution (Michelfelder et al., 2014), seismological (Jay et al., 2012; Comeau, 2015; Comeau et al., 2015; Alvizuri and Tape, 2016; Farrell et al., 2017; Kukarina et al., 2017; Maher and Kendall, 2018; McFarlin et al., 2018; MacQueen et al., 2021; Hudson et al., 2022) and volcanic hazards works (Sánchez, 2017; Amigo, 2021; Aguilera et al., 2022) have been carried out.

Eruption frequency

Geochronological analysis outcomes reveal the activity range around Uturuncu is about 10–15 Ma (Sparks et al., 2008). Although there are no recent eruptions, Uturuncu has been showing signs of unrest in recent years through surface deformation and fumarolic activity (Kussmaul et al., 1977; Sparks et al., 2008; Jay et al., 2012). The Global Volcanism Program is not aware of any Holocene eruptions from Uturuncu (GVP, 2013), it is not monitored and it is not included in any volcanic risk ranking.

Hazard types

It has not flank collapse potential nor characteristics which could represent primary lahar sources. The 0°C annual isotherm is located at 5000m, but there are no glaciers today at the top of Uturuncu and surrounding summits (Blard et al., 2014). Large-scale ground deformation was observed beginning in May 1992 (Pritchard and Simons, 2002) surrounded by subsidence to create a sombrero- shaped deformation pattern (Fialko and Pearse, 2012; Henderson and Pritchard, 2013; Hickey et al., 2013), indicating, along with seismicity detected in 2009-10 (Jay et al., 2012), that a magmatic system is still present. Active fumaroles

(Sparks et al., 2008) and geothermal fields in the region also suggest active magmatic activity (de Silva, 1989). Thus, despite the Uturuncu last erupted 250,000 y.a. (Muir et al., 2015), the volcano has been deforming for at least 50yrs, at a rate of up to 1 cm/yr between 1992 and 2004 (Gottsmann et al., 2017; Henderson et al., 2017; Pritchard et al., 2018), suggesting that the volcano might be a potentially active volcano.

known eruptive products from Uturuncu consist entirely of effusive dacitic lava flows (Sparks et al., 2008; Muir et al., 2014). The eruptive episodes have spanned ~620,000 years with a total of ~105 lava flows and domes identified and with repose intervals of 6000–8000 years (Sparks et al., 2008; Michelfelder et al., 2014; McFarlin et al., 2018). According to Walter and Motagh (2009) extended magma bodies may exist under Uturuncu may bear a major hazard potential because of the considerable dimensions and volumes of magma temporarily stored in the shallow crust. Following the hazard map of Sánchez (2017) the most characteristic volcanic processes of Uturruncu volcano, which would be the most likely to occur in the event of an eruption, are pyroclastic flows, lava flows, ballistic projectiles, gases and tephrafallout. In the event of a super-explosion, Bolivian cities and populations located in northern Chile and Argentina would be potentially affected (Sánchez, 2017).

1.30 Putana

Physical characteristics

Putana is a 5890 m high stratovolcano of Holocene age, located on the southern border between Bolivia and Chile (GVP, 2013). Is one component of a much larger complex which extends as far as Sairecabur and includes several unnamed volcanic centers (De Silva and Francis, 1991); its volcanic products cover an area of 57-600 km^2 and the main edifice has an estimated volume of ~ 17 km^3 (González-Ferrán, 1995; Grosse et al., 2014).

Several geological (De Silva and Francis, 1991; González-Ferrán, 1995; Grosse et al., 2014), fluid geochemistry (Aguilera, 2008; Tassi et al., 2011; Stebel et al., 2015), surface deformation (Pritchard and Simons, 2004; Henderson and Pritchard, 2013), thermal anomalies (Jay et al., 2013), geochronological (Lahsen and Munizaga, 1983), geological evolution (Marinovic and Lahsen, 1984), seismological (Henderson et al., 2012; Soler and Amigo, 2012) and volcanic hazards works (Rudolph, 1955; Casertano, 1963; Petit-Breuilh, 2004; Amigo et al., 2012; Amigo, 2021; Aguilera et al., 2022) have been carried out.

Eruption frequency

Casertano (1963) lists fumarolic activity in 1886-1888, 1900 and 1960, and González-Ferrán (1995) described more than twenty eruptive centers of thick postglacial dacitic domes that suggest Holocene activity. The Global Volcanism Program recognizes 2 Holocene eruptive periods with maximum VEI registered of 2 (GVP, 2013). It is not monitored and is in the 78th place of the last version of the Chilean volcanic risk ranking (SERNAGEOMIN, 2020a, b).

Hazard types

Currently it has no flank collapse potential nor to generating lahars (Lara et al., 2011). No deformation was detected at Putana during a regional InSAR survey of Central Andean Volcanoes (Pritchard and Simons, 2004), although it underwent a short-lived episode of uplift between 13 Sep 2009 and 31 Jan 2010, with a maximum uplift of 4.0 cm (Henderson and Pritchard, 2013). There are records of observed seismic unrest, fumarolic and magmatic degassing (Tassi et al., 2011; Henderson and Pritchard, 2013; Pritchard et al., 2014), and small thermal anomaly hotspots (Jay et al., 2013).

In 2011 the Putana volcano was considered a geologically active and potentially dangerous volcano, with very low specific risk level (Lara et al., 2011). According to Amigo et al. (2012) the most characteristic volcanic processes which would be the most likely to occur in the event of an eruption, are the emission of viscous lavas with a reduced generation of pyroclastic material.

1.31 Escalante-Sairecabur

Physical characteristics

Escalante-Sairecabur is a 5971 m high volcanic complex of Holocene age, located along the Chile-Bolivia border (De Silva and Francis, 1991). This chain of andesitic-dacitic volcanoes extends for ~22 km north-south and contains at least 10 postglacial centers, all of which have several youthful lava flows associated (De Silva and Francis, 1991); its volcanic products cover an area of 216 km^2 and the main edifice has an estimated volume of 79 km^3 (Grosse et al., 2014).

It is scarcely investigated, some geological (De Silva and Francis, 1991; González-Ferrán, 1995; Grosse et al., 2014), petrographic (Deruelle, 1978; Harmon et al., 1984; Figueroa and Figueroa, 2006), surface deformation (Henderson and Pritchard, 2013), geological evolution (Marinovic and Lahsen, 1984), and volcanic hazards works (Lara et al., 2011; Amigo et al., 2012; Amigo, 2021; Aguilera et al., 2022) have been carried out.

Eruption frequency

Postglacial activity began south of the Sairecabur summit, and other eruptive centers have also produced Holocene lava flows (GVP, 2013). The Global Volcanism Program is not aware of any Holocene eruptions from Escalante-Sairecabur, it is not monitored and is in the 77th place of the last version of the Chilean volcanic risk ranking (SERNAGEOMIN, 2020a, b).

Hazard types

According to Lara et al. (2011) it has not flank collapse potential nor characteristics which could represent primary lahar sources. No deformation was detected at Escalante-Sairecabur during a regional InSAR survey of Central Andean Volcanoes (Henderson and Pritchard, 2013). There are not records of observed seismic unrest (Lara et al., 2011) and currently there is no fumarolic activity; however, this seems to have been intense in the past due to the presence of disturbed rocks on the eastern slope and the existence of abundant sulfur deposits (González-Ferrán, 1995).

Despite the lack of reliable records of its eruptive activity in the last 10,000 years Escalante-Sairecabur volcanic complex is considered potentially active (De Silva and Francis, 1991) and a potentially dangerous volcano, with low specific risk level (Lara et al., 2011). A reactivation of this complex could occur at any point in the cordon, although with greater probability in the surroundings of the Sairecabur volcano, which would be mainly related to the emission of lavas or the construction of a dome (Amigo et al., 2012).

1.32 Licancabur

Physical characteristics

Licancabur is a 5916 m high stratovolcano of Holocene age (GVP, 2013), located on the western border of the Bolivia-Chile Altiplano (Figueroa et al., 2009). It has one of the world's highest lakes in its 400-m-wide summit crater (De Silva and Francis, 1991); its volcanic products cover an area of ~ 28 km^2 and the main edifice has an estimated volume of 10-39 km^3 (Grosse et al., 2014; Aravena et al., 2015).

It is a scarcely investigated volcano, some geological (De Silva and Francis, 1991; González-Ferrán, 1995; Grosse et al., 2014; Aravena et al., 2015), petrographic (Figueroa et al., 2009), thermal anomalies (Jay et al., 2013), geological evolution (Marinovic and Lahsen, 1984), and volcanic hazards works (Rudolph, 1955; Lara et al., 2011; Amigo et al., 2012; Amigo, 2021; Aguilera et al., 2022) have been carried out.

Eruption frequency

Youthful lava flows, a well-preserved summit crater and absence of glacial geomorphic features are evidence of Holocene activity (De Silva and Francis, 1991). The Global Volcanism Program is not aware of any Holocene eruptions from Licancabur (GVP, 2013), it is not monitored and is in the 69th place of the last version of the Chilean volcanic risk ranking (SERNAGEOMIN, 2020a, b).

Hazard types

According to Lara et al. (2011) it has not flank collapse potential nor characteristics which could represent primary lahar sources, although it has a shallow freshwater summit lake (Amigo et al., 2012). There are not records of ground deformation, observed seismic unrest, nor fumarolic and magmatic degassing (Lara et al., 2011). According to ASTER images, it has potential hotspots that merit further study (Jay et al., 2013).

Despite the lack of current activity, the presence of the crater lake at an altitude close to 6000m with bottom temperature of 6°C, may indicate a mild thermal source maintaining the lake water temperature above freezing and supporting fauna (De Silva and Francis, 1991). In 2011 the Licancabur volcano was considered a geologically active and potentially dangerous volcano, with low specific risk level (Lara et al., 2011). The most characteristic volcanic processes of Licancabur volcano, which would be the most likely to occur in the event of an eruption, are emission of lavas from the central crater, with possible generation of pyroclastic density currents towards the west flank (Amigo et al., 2012).

1.33 Chascón-Purico Complex

Physical characteristics

Chascón-Purico is a 5703 m high dome complex of Holocene age, located ~ 30 km E from San Pedro de Atacama village in the Antofagasta Region, Chile (De Silva and Francis, 1991). It consists of a roughly circular, gently inclined apron of ignimbrites 25 km in diameter, capped by a summit complex of andesite lavas and dacite domes (Francis et al., 1984); its volcanic products cover an area of ~16 km^2 and the main edifice has an estimated volume of 5-22 km^3 (Grosse et al., 2014; Aravena et al., 2015).

Several geological (De Silva and Francis, 1991; Grosse et al., 2014; Aravena et al., 2015), petrographic (Hawkesworth et al., 1982; Schmitt et al., 2001; Burns et al., 2015, 2020), surface deformation (Henderson and Pritchard, 2013), geochronological (Brown et al., 2021), geological evolution (Harmon et al., 1984; Cesta and Ward, 2016), seismological (Otárola et al., 2002) and volcanic hazards works (SERNAGEOMIN, 2020a, b; Amigo, 2021; Aguilera et al., 2022) have been carried out.

Eruption frequency

There are two Holocene dacite-rhyolite domes overlying the large moraines on the summit region of Purico (De Silva and Francis, 1991). According to Burns et al. (2020) these youngest centers are the 0.18 Ma Cerro Chascon and Cerro Aspero domes. The Global Volcanism Program is not aware of any Holocene eruptions from Chascón-Purico volcanic complex (GVP, 2013), it is not monitored and is in the 79th place of the last version of the Chilean volcanic risk ranking (SERNAGEOMIN, 2020a, b).

Hazard types

There is no further information on potential or records of partial sector collapse. Lahars and debris flows from the volcanoes have covered parts of the ignimbrite shield with gravels (Cesta and Ward, 2016). No deformation was detected at the Purico Complex during a regional InSAR survey of Central Andean Volcanoes (Henderson and Pritchard, 2013). There are no records of superficial seismic unrest in the Purico area (Otárola et al., 2002), the lavas of Cerro Purico and Toco are deeply weathered, exposing extensive fumarolic alteration deposits (Francis et al., 1984), and a water spring system (Aguada Pajaritos) is present on the north flank of the Purico Volcano (Otárola et al., 2002).

According to the geological studies made in Chascón-Purico complex the most characteristic volcanic processes, which would be the most likely to occur in the event of an eruption, are lava flows, extrusion of domes, and minor pyroclastic activity (De Silva and Francis, 1991).

1.34 Colachi

Physical characteristics

Colachi is a 5631 m high stratovolcano of Pleistocene-Holocene age, located in the Antofagasta Region, Chile (Ramírez and Gardeweg, 1982). Is a symmetrical cone with a degraded summit crater and some flow features especially on its E flank and summit region (De Silva and Francis, 1991); its volcanic products cover an area of ~ 8 km^2 and the main edifice has an estimated volume of ~ 1 km^3 (Grosse et al., 2014).

It is a scarcely investigated volcano, some geological (De Silva and Francis, 1991; González-Ferrán, 1995; Grosse et al., 2014), surface deformation (Pritchard, 2003; Henderson and Pritchard, 2013), geological evolution (Ramírez and Gardeweg, 1982), and volcanic hazards works (Lara et al., 2011; Amigo et al., 2012; Amigo, 2021; Aguilera et al., 2022) have been carried out.

Eruption frequency

Most recent activity corresponds to the eruption of two small siliceous lava flows at its W base, which according to Ramírez and Gardeweg (1982) would be indicating a clearly postglacial age (González-Ferrán, 1995). The Global Volcanism Program is not aware of any Holocene eruptions from Colachi, it is not monitored, and it is in the 74th place of the last version of the Chilean volcanic risk ranking (SERNAGEOMIN, 2020a, b).

Hazard types

According to Lara et al. (2011) it has not flank collapse potential nor characteristics which could represent primary lahar sources. No deformation was detected at Colachi during a regional InSAR survey of Central Andean Volcanoes (Henderson and Pritchard, 2013). There are not records of observed seismic unrest, nor fumarolic and/or magmatic degassing (Lara et al., 2011).

Despite the lack of reliable records of its eruptive activity in the last 10,000 years, in 2011 the Colachi volcano was considered a geologically active and potentially dangerous volcano, with very low specific risk level (Lara et al., 2011). A reactivation of this volcano would be mainly associated with the emission of lavas or the construction of a dome, the impact of which would only cover neighboring areas (Amigo et al., 2012).

1.35 Acamarachi (Pili)

Physical characteristics

Acamarachi is a 6046 m high stratovolcano of Pleistocene-Holocene age, located ~ 6 km apart from Colachi, in the Antofagasta Region, Chile (Ramírez and Gardeweg, 1982). It is the highest peak in the region, with steep-sided slopes that reach about 45° (González-Ferrán, 1995); its volcanic products cover an area of ~ 18 km^2 and the main edifice has an estimated volume of ~ 5 km^3 (Grosse et al., 2014).

It is a scarcely investigated volcano, some geological (De Silva and Francis, 1991; González-Ferrán, 1995; Grosse et al., 2014), fluid geochemistry (Aguilera, 2008), surface deformation (Pritchard, 2003), geological evolution (Ramírez and Gardeweg, 1982), and volcanic hazards works (Lara et al., 2011; Amigo et al., 2012; Amigo, 2021; Aguilera et al., 2022) have been carried out.

Eruption frequency

Some flows associated with the central crater suggest Holocene activity (González-Ferrán, 1995). The Global Volcanism Program is not aware of any Holocene eruptions from Acamarachi, it is not monitored and is in the 87th place of the last version of the Chilean volcanic risk ranking (SERNAGEOMIN, 2020a, b).

Hazard types

According to Lara et al. (2011) it has not flank collapse potential nor characteristics which could represent primary lahar sources, although the central crater contains a lake of 10-15 m in diameter (Aguilera, 2008). No deformation was detected at Colachi during a regional InSAR survey of Central Andean Volcanoes (Pritchard, 2003). There are not records of observed seismic unrest, nor fumarolic and/or magmatic degassing (Lara et al., 2011). However, the summit crater lake, which despite its height, remains in a liquid state suggests the existence of a remnant magmatic heat flow (Aguilera, 2008).

Despite the lack of reliable records of its eruptive activity in the last 10,000 years, in 2011 the Acamarachi volcano was considered a geologically active and potentially dangerous volcano, with very low specific risk level (Lara et al., 2011). A reactivation of this volcano would be mainly associated with the emission of lavas or the construction of a dome (Amigo et al., 2012).

1.36 Lascar

Physical characteristics

Lascar is a 5592 m high stratovolcano of Holocene age, located ~ 70 km SE of San Pedro de Atacama town in the Antofagasta Region, Chile (Esquivel, 2018). It is the most active volcano of the central Andes of Chile and is characterized by persistent fumarolic activity and occasional vulcanian and steam eruptions

(De Silva and Francis, 1991); its volcanic products cover an area of 33-62 km^2 and the main edifice has an estimated volume of 10-28 km^3 (Aravena et al., 2015; Grosse et al., 2014, 2018; SERNAGEOMIN, 2021).

Several geological (De Silva and Francis, 1991; Gardeweg and Medina, 1994; González-Ferrán, 1995; Sparks et al., 1997; Calder et al., 2000; Stern et al., 2007; Aravena et al., 2015; Grosse et al., 2014, 2018), fluid geochemistry (Aguilera et al., 2006; Tassi et al., 2009; Bredemeyer et al., 2018), surface deformation (Pritchard and Simons, 2004; Pavez et al., 2006; Whelley et al., 2012; Henderson and Pritchard, 2013, de Zeeuw-van Dalfsen et al., 2017; Richter et al., 2018), thermal anomalies (Jay et al., 2013; González et al., 2015), geological evolution (Matthews et al., 1994, 1999; Gardeweg et al., 1998a; 2011), seismological (Asch et al., 1996; Pritchard et al., 2014; Gaete et al., 2019) and volcanic hazards works (Casertano, 1963; Viramonte et al., 1995; Lara et al., 2011; Amigo et al., 2012; Gardeweg and Amigo, 2015; Bertin, 2017; Esquivel, 2018; ONEMI Antofagasta, 2019; Amigo, 2021; Aguilera et al., 2022) have been carried out.

Eruption frequency

Since 1993 eruption, activity has been dominated by passive degassing and occasional minor and short-lived explosive events (Bertin, 2017). The Global Volcanism Program recognizes 37 Holocene eruptive periods with maximum VEI registered of 4 (GVP, 2023). It is monitored by OVDAS (SERNAGEOMIN, 2021), and it is in the 14th place of the last version of the Chilean volcanic risk ranking (SERNAGEOMIN, 2020a, b).

Hazard types

It suffered a partial sector collapse directed towards the NE, leaving a horseshoe shape (Matthews et al., 1994). Currently it has flank collapse potential but not to generating lahars (Lara et al., 2011). There are records of ground deformation, but most notably related to co-eruptive subsidence in the crater (Pavez et al., 2006) and compaction of pyroclastic flow deposits (Whelley et al., 2012). There are records of observed seismic unrest (Gaete et al., 2019) and fumarolic and magmatic degassing (Matthews et al., 1997; Aguilera et al., 2006; Tassi et al., 2009; Bredemeyer et al., 2018). Additionally, it displays thermal anomaly hotspots (Jay et al., 2013; González et al., 2015).

According to the geological and volcanic hazard maps of the Lascar volcano (Gardeweg et al., 2011; Lara et al., 2011; Amigo et al., 2012; Gardeweg and Amigo, 2015) the most characteristic volcanic processes which would be the most likely to occur in the event of an eruption, are pyroclastic density currents, ballistic projectiles, tephra fallout and debris avalanches.

1.37 Puntas Negras

Physical characteristics

Puntas Negras is a 5852 m high volcanic complex of Holocene age, located on the junction between the E-W trending Cordón Puntas Negras and N-S trending Cordón Chalviri, in the Antofagasta Region, Chile (De Silva and Francis, 1991).

It is scarcely investigated, some geological (De Silva and Francis, 1991; González-Ferrán, 1995), surface deformation (Pritchard, 2003), geological evolution (Ramírez and Gardeweg, 1982), and volcanic hazards works (Lara et al., 2011; Amigo, 2021; Aguilera et al., 2022) have been carried out.

Eruption frequency

The Global Volcanism Program just mention it within the Cordón Puntas Negras-Chalviri volcanic complex profile, it is not monitored and is in the 80th place of the last version of the Chilean volcanic risk ranking (SERNAGEOMIN, 2020a, b).

Hazard types

There are not records of flank collapse potential nor characteristics which could represent primary lahar sources (Lara et al., 2011). No deformation was detected at Puntas Negras during a regional InSAR survey of Central Andean Volcanoes (Pritchard, 2003). There are not records of observed seismic unrest nor fumarolic and magmatic degassing (Lara et al., 2011).

Despite the lack of reliable records of its eruptive activity in the last 10,000 years, according to González-Ferrán (1995) the morphological characteristics of domes and thick flows of andesitic-dacitic lavas, clearly reflect a Holocene eruptive activity. In 2011 the Puntas Negras volcano was considered a geologically active and potentially dangerous volcano, with very low specific risk level (Lara et al., 2011) and is still considered in the latest version of the Chilean volcanic risk ranking (SERNAGEOMIN, 2020a, b). There is no information about the hazards that Puntas Negras could pose in the event of an eruption, but according to its geological records it may be inferred that a reactivation would be mainly associated with the emission of lava flows and hot avalanches (De Silva and Francis, 1991).

1.38 Chiliques

Physical characteristics

Chiliques is a 5778 m high volcanic complex of Pleistocene-Holocene age, located immediately south of Laguna Lejía in the Antofagasta Region, Chile (Amigo et al., 2012). It occupies an interesting position at the intersection of two of the major volcano tectonic lineaments in this region (De Silva and Francis, 1991); its volcanic products cover an area of ~19 km^2 and the main edifice has an estimated volume of ~ 5 km^3 (Grosse et al., 2014).

Several geological (De Silva and Francis, 1991; González-Ferrán, 1995; Grosse et al., 2014), fluid geochemistry (Aguilera, 2008), surface deformation (Pritchard, 2003; Henderson and Pritchard, 2013), thermal anomalies (Pieri and Abrams, 2004; Pritchard and Simons, 2004; Jay et al., 2013), geological evolution (Ramírez and Gardeweg, 1982), and volcanic hazards works (Lara et al., 2011; Amigo et al., 2012; Amigo, 2021; Aguilera et al., 2022) have been carried out.

Eruption frequency

This volcano had previously been considered to be dormant; however, in 2002 a NASA nighttime thermal infrared satellite image from the Advanced Spaceborne Thermal Emission and Reflection Radiometer (ASTER) showed low-level hot spots in the summit crater and upper flanks (Pieri and Abrams, 2004). The Global Volcanism Program is not aware of any Holocene eruptions from Chiliques (GVP, 2013), it is not monitored and is in the 83rd place of the last version of the Chilean volcanic risk ranking (SERNAGEOMIN, 2020a, b).

Hazard types

According to Lara et al. (2011) it has not flank collapse potential nor characteristics which could represent primary lahar sources; however, it has a crater lake at almost 6000 m (González-Ferrán, 1995). No deformation was detected at Chiliques during a regional InSAR survey of Central Andean Volcanoes (Henderson and Pritchard, 2013). There are not records of observed seismic unrest (Lara et al., 2011) and fumarolic degassing was recorded during an aircraft overflight, by the Chilean Geologic Survey (Pieri and Abrams, 2004). ASTER images indicated a short-lived thermal anomaly at Chiliques volcano (Pritchard and Simons, 2004), while MODVOLC did not (Jay et al., 2013).

Despite the lack of reliable records of its eruptive activity in the last 10,000 years, the very fresh morphological features of the central lava flow, the maar, and the presence of a lagoon in the central crater, evidence a very recent eruptive activity (González-Ferrán, 1995). In 2011 the Chiliques volcano was considered a geologically active and potentially dangerous volcano, with very low specific risk level (Lara et al., 2011). A reactivation would be mainly linked to the emission of lavas and the routes that connect Socaire with Laguna Lejía and Paso Huaytiquina, could be affected if the eruptive event were of medium to high intensity (Amigo et al., 2012).

1.39 Alitar

Physical characteristics

Alitar is a 5346 m high maar of Pleistocene age (Amigo et al., 2012), located ~ 10 km N of Colachi volcano in the Antofagasta Region, Chile (González-Ferrán, 1995). It has a 500-m-wide, 50-m-deep maar (broad, low relief) crater at the base of its SW flank (Tassi et al., 2011).

Little is known about Alitar because of its remote location and the limited accessibility. Some geological (González-Ferrán, 1995), fluid geochemistry (Aguilera, 2008; Tassi et al., 2011), surface deformation (Henderson and Pritchard, 2013), and volcanic hazards works (Lara et al., 2011; Amigo et al., 2012; SERNAGEOMIN, 2020a, b; Amigo, 2021; Aguilera et al., 2022) have been carried out.

Eruption frequency

Alítar has no documented historical activity (Tassi et al., 2011). The Global Volcanism Program just mention it within the Purico complex profile as a subfeature (GVP, 2013), it is not monitored, and is in the 89th place of the last version of the Chilean volcanic risk ranking (SERNAGEOMIN, 2020a, b).

Hazard types

According to Lara et al. (2011) it has not flank collapse potential nor characteristics which could represent primary lahar sources. No deformation was detected at Alitar during a regional InSAR survey of Central Andean Volcanoes (Henderson and Pritchard, 2013), and there are not records of observed seismic unrest (Lara et al., 2011). Fumarolic activity has been recognized in the northern sector of the Alitar maar and in a small area 400 m NW of the maar. Its current thermal activity also includes six pools that discharge thermal water and gas along a small, NS-oriented creek that is located ~200 m west of the maar (Aguilera, 2008).

In 2011 the Alitar volcano was considered a geologically active and potentially dangerous volcano, with low specific risk level (Lara et al., 2011). According to Amigo et al. (2012), a reactivation of this center would probably be related to a phreatic event and would only have a local impact. Accordingly, the most characteristic volcanic processes, which would be the most likely to occur in the event of a phreatic eruption, are tephra fallout and ballistic projectiles.

1.40 Caichinque

Physical characteristics

Caichinque is a 4458 m high stratovolcano of Pleistocene-Holocene age, located between Salar de Talar and Salar de Capur, in the Antofagasta Region, Chile (González-Ferrán, 1995). More than a half-dozen vents produced andesitic-to-dacitic lava flows, with young flows descending to the NE and SE from the summit (GVP, 2013); its volcanic products cover an area of ~ 6 km^2 and the main edifice has an estimated volume of ~ 0.5 km^3 (Grosse et al., 2014).

It is a scarcely investigated volcanic complex, some geological (González-Ferrán, 1995; Grosse et al., 2014), surface deformation (Henderson and Pritchard, 2013), geological evolution (Ramírez and Gardeweg, 1982), and volcanic hazards works (Lara et al., 2011; Amigo et al., 2012; SERNAGEOMIN, 2020a, b; Amigo, 2021; Aguilera et al., 2022) have been carried out.

Eruption frequency

There is no record of historical activity. However, according to González-Ferrán (1995), the very fresh morphological features of some lava flows suggest that they probably occurred in prehistoric times. The Global Volcanism Program is not aware of any Holocene eruptions from Caichinque, it is not monitored and is in the 84th place of the last version of the Chilean volcanic risk ranking (SERNAGEOMIN, 2020a, b).

Hazard types

According to Lara et al. (2011) it has not flank collapse potential nor characteristics which could represent primary lahar sources. No deformation was detected at Caichinque during a regional InSAR survey of

Central Andean Volcanoes (Henderson and Pritchard, 2013). There are not records of observed seismic unrest nor fumarolic and magmatic degassing (Lara et al., 2011).

Despite the lack of reliable records of its eruptive activity in the last 10,000 years, in 2011 Caichinque was considered a geologically active and potentially dangerous volcanic complex, with very low specific risk level (Lara et al., 2011). A reactivation of this volcano would be associated with the emission of lavas, with an impact only in neighboring areas and in some sectors of the international route CH-23 (Amigo et al., 2012).

1.41 Tuzgle

Physical characteristics

Tuzgle is a 5486 m high stratovolcano of Holocene age, located ~ 120 km E of the main volcanic arc in the Jujuy Province, Argentina (De Silva and Francis, 1991). Is the easternmost young volcano of the central Andes (GVP, 2013); its volcanic products cover an area of ~33 km^2 and the main edifice has an estimated volume of ~9 km^3 (Grosse et al., 2014).

Several geological (De Silva and Francis, 1991; González-Ferrán, 1995; Blasco et al., 1996; Grosse et al., 2014), petrographic (Coira and Kay, 1993; Coira and Rosas, 2008), fluid geochemistry (Mon, 1987; Giordano et al., 2013), surface deformation (Sainato and Pomposiello, 1997; Henderson and Pritchard, 2013), geological evolution (Norini et al., 2014), seismological (Schurr et al., 2003) and volcanic hazards works (Elissondo et al., 2016; Amigo, 2021; Garcia and Badi, 2021; Aguilera et al., 2022) have been carried out.

Eruption frequency

There are no known historical eruptions, however, it is worth noting the existence of hot thermal waters 6 km NW of the volcano (González-Ferrán, 1995). The Global Volcanism Program is not aware of any Holocene eruptions from Tuzgle, it is not monitored, and it is in the 11th place of the relative risk ranking of Argentine and neighboring volcanoes (Elissondo et al., 2016).

Hazard types

It suffered a catastrophic sector collapse of the summit, directed towards the NNE (Norini et al., 2014) and currently there are not characteristics which could represent primary lahar sources. No deformation was detected at Tuzgle during a regional InSAR survey of Central Andean Volcanoes (Henderson and Pritchard, 2013). There are not records of observed seismic unrest nor fumarolic degassing. Its associated geothermal field constitutes one of the most important of the region, besides exploitation of the geothermal resources, there exist potential for mining (Coira and Rosas, 2008).

There is not information about the hazards that Tuzgle could pose in the event of an eruption, but according to its geological records it may be inferred that a reactivation would be mainly associated with the emission of lava flows and debris avalanches (De Silva and Francis, 1991).

1.42 Pular-Pajonales

Physical characteristics

Pular and Pajonales (6233 and 5958 m high, respectively) are two stratovolcanoes of Holocene age, located ~ 15 km W of the Argentinian border in the Antofagasta Region, Chile (De Silva and Francis, 1991). They form a 12-km-long volcanic ridge with a NE-SW trending which has about ten craters (González-Ferrán, 1995); its volcanic products cover an area of 301 km^2 and the main edifice has an estimated volume of 160 km^3 (Grosse et al., 2014).

It is a scarcely investigated volcanic complex, some geological (De Silva and Francis, 1991; González-Ferrán, 1995; Grosse et al., 2014), surface deformation (Pritchard, 2003; Henderson and Pritchard, 2013), thermal anomalies (Jay et al., 2013), geological evolution (Ramírez, 1988; Ramírez et al., 1991), and volcanic hazards works (Lara et al., 2011; Amigo et al., 2012; Amigo, 2021; Aguilera et al., 2022) have been carried out.

Eruption frequency

It is mostly pre-Holocene but show evidence for some Holocene activity related to Pajonales Norte, a satellite vent slightly offset 1.5 km NW from the axis of the main chain (De Silva and Francis, 1991; Ramírez et al., 1991). The Global Volcanism Program just mention 1 uncertain Holocene eruptive event probably false with maximum VEI registered of 1 (GVP, 2013); it is not monitored and is in the 81st place of the last version of the Chilean volcanic risk ranking (SERNAGEOMIN, 2020a, b).

Hazard types

According to Lara et al. (2011) it has not flank collapse potential nor characteristics which could represent primary lahar sources, although some craters of the Pajonales have interior lagoons (De Silva and Francis, 1991). No deformation was detected at Pular-Pajonales during a regional InSAR survey of Central Andean Volcanoes (Henderson and Pritchard, 2013). There are not records of observed seismic unrest nor fumarolic degassing (Lara et al., 2011), and according to ASTER images it displays a permanent thermal hotspot anomaly (Jay et al., 2013).

In 2011 Pular-Pajonales was considered a geologically active and potentially dangerous volcano, with very low specific risk level (Lara et al., 2011). A reactivation of this volcano would be mainly associated with the emission of lavas and extensive pyroclastic density currents (Amigo et al., 2012).

1.43 Aracar

Physical characteristics

Aracar is a 6095 m high stratovolcano of Holocene age (GVP, 2013), located in the Salta province, northwestern Argentina, just east of the Chilean border (Maisonnave and Page, 1997). It is a steep-sided stratovolcano with a youthful-looking summit crater 1-1.5 km in diameter that contains a small lake (GVP, 2013); its volcanic products cover an area of 113 -192 km^2 and the main edifice has an estimated volume of 50 - 62 km^3 (Karátson et al., 2012; Grosse et al., 2014).

It is a scarcely investigated volcano, some geological (González-Ferrán, 1995; Zappettini and Blasco, 2001; Karátson et al., 2012; Grosse et al., 2014), petrographic (Koukharsky and Etcheverria, 1997; Maisonnave and Page, 1997), surface deformation (Fournier et al., 2010; Henderson and Pritchard, 2013), and volcanic hazards works (Elissondo et al., 2016; Amigo, 2021; Garcia and Badi, 2021; Aguilera et al., 2022) have been carried out.

Eruption frequency

There were reports of possible ash columns from the summit in 1993, which suggest possible Holocene activity (González-Ferrán, 1995), but it is not known whether these were rockfall dust or eruption plumes (GVP, 2013). The Global Volcanism Program recognizes 1 Holocene eruptive period with maximum VEI registered of 2. It is not monitored, and it is in the 17th place of the relative risk ranking of Argentine and neighboring volcanoes (Elissondo et al., 2016).

Hazard types

There is no further information or records on partial sector collapse or lahar potential. No deformation was detected at Aracar during a regional InSAR survey of Central Andean Volcanoes (Fournier et al., 2010; Henderson and Pritchard, 2013), and there are no records on observed seismic unrest nor fumarolic and magmatic degassing.

There is not information about the hazards that Aracar could pose in the event of an eruption, but according to its geological records it may be inferred that a reactivation would be mainly associated with the emission of lava flows (Koukharsky and Etcheverria, 1997; Maisonnave and Page, 1997; González-Ferrán, 1995).

1.44 Socompa

Physical characteristics

Socompa is a 6031 m high stratovolcano of Holocene age, located along the Chile-Argentina border (GVP, 2013). It is the largest of a chain of volcanoes on a NE-SW trending portion of the active front of the Andes (De Silva and Francis, 1991); its volcanic products cover an area of 158 km^2 and the main edifice has an estimated volume of 81-179 km^3 (Grosse et al., 2014; Aravena et al., 2015).

Several geological (De Silva and Francis, 1991; González-Ferrán, 1995; Zappettini and Blasco, 2001; Stern et al., 2007; Grosse et al., 2014; Aravena et al., 2015; Seggiaro and Apaza, 2018), fluid geochemistry (Lelli, 2018; Raco, 2018; Conde et al., 2020), surface deformation (Pritchard, 2003; Henderson and Pritchard, 2013; Liu et al., 2022, 2023), geological evolution (Francis et al., 1985; Francis and Wells, 1988; Wadge et al., 1995; Kelfoun et al., 2008), and volcanic hazards works (van Wyk de Vries et al., 2001; Kelfoun and Druitt, 2005; Lara et al., 2011; Amigo et al., 2012; Elissondo et al., 2016; Amigo, 2021; Garcia and Badi, 2021; Aguilera et al., 2022) have been carried out.

Eruption frequency

According to De Silva and Francis (1991), five small explosion craters at the vent region of the extrusive dacites in the summit region represent its youngest eruptive activity. And although there is no recognized historical activity, González-Ferrán (1995) mentioned that sulfurous gas emanations have been detected about 100 m below the summit of the crater. The Global Volcanism Program recognizes 1 Holocene eruptive event without maximum VEI registered (GVP, 2013). It is not monitored, is in the 57th place of the last version of the Chilean volcanic risk ranking (SERNAGEOMIN, 2020a, b), and the 13th place of the relative risk ranking of Argentine and neighboring volcanoes (Elissondo et al., 2016).

Hazard types

It suffered a partial sector collapse of the original cone, causing a debris avalanche that descended nearly 3000 m vertically and traveled more than 35 km from the volcano (Francis et al., 1985). Currently it has flank collapse potential but not to generating lahars (Lara et al., 2011). No deformation was detected at Socompa during a regional InSAR survey of Central Andean Volcanoes (Henderson and Pritchard, 2013). However, a steady uplift at a rate of ~18mm/yr was detected from Dec 2019 (Liu et al., 2022, 2023). There are not records of observed seismic unrest but fumarolic and magmatic degassing (De Silva and Francis, 1991; González-Ferrán, 1995; Lara et al., 2011; Seggiaro and Apaza, 2018).

In 2011 the Socompa volcano was considered a geologically active and potentially dangerous volcano, with low specific risk level (Lara et al., 2011). A reactivation would be mainly associated with the emission of lava flows, tephra fallout, pyroclastic density currents and debris avalanches (De Silva and Francis, 1991). High-magnitude explosive eruptions could disperse pyroclastic material to distant areas of the volcano, although mainly located to the east; however, during the summer months the probability of dispersal to the west increases considerably (Amigo et al., 2012).

1.45 Arizaro volcanic field

Physical characteristics

Arizaro is a 5736 m high volcanic field of Upper Miocene-Holocene age (Viramonte et al., 1984), located ~ 20 km SW of the Aracar volcano and ~ 20 km E-SE of Socompa, in the Salta province of Argentina. It is limited to the W by the fault that gave rise to the edge of Caipe, which conditioned its asymmetric shape, characterized by a greater development of its flows towards the SE sector (Zappettini and Blasco, 2001); its volcanic products cover an area of 6 x 4 km (Dow and Hitzman, 2002) and the main edifice has an estimated volume of 0.4-59 km^3 (Viramonte et al., 1984; Grosse et al., 2017).

It is a scarcely investigated volcanic field, some geological (Zappettini and Blasco, 2001; Grosse et al., 2017), petrographic (Viramonte et al., 1984; Dow and Hitzman, 2002), geochronological (Schoenbohm and

Carrapa, 2015), and volcanic hazards works (Elissondo et al., 2016; Amigo, 2021; Garcia and Badi, 2021; Aguilera et al., 2022) have been carried out.

Eruption frequency

According to Viramonte et al. (1984), the Arizaro volcanites are undoubtedly Holocene, they cover a recent foothill scour and preserve their flow structures without conspicuous evidence of erosional action. It is not included in the catalogs of Holocene/Pleistocene volcanoes of the Global Volcanism Program. It is not monitored, and it is in the 37th place of the relative risk ranking of Argentine and neighboring volcanoes (Elissondo et al., 2016).

Hazard types

No further information or records were found on partial sector collapse, lahar potential, ground deformation, observed seismic unrest and fumarolic and/or magmatic degassing.

According to its geological records, the volcanic processes of Arizaro most likely to occur in the event of an eruption, would be mainly associated with the emission of high viscosity lava flows and tephra fallout (Viramonte et al., 1984).

1.46 Llullaillaco

Physical characteristics

Llullaillaco is a 6739 m high stratovolcano of Holocene age, located on the Chilean-Argentine border (GVP, 2013). It is considered the second highest active volcano summit in the world (De Silva and Francis, 1991; González-Ferrán, 1995; Stern et al., 2007); its volcanic products cover an area of ~88 km^2 and the main edifice has an estimated volume of 37-144 km^3 (Grosse et al., 2014, 2018; Aravena et al., 2015).

Several geological (De Silva and Francis, 1991; González-Ferrán, 1995; Zappettini and Blasco, 2001; Stern et al., 2007; Grosse et al., 2014, 2018; Aravena et al., 2015), petrographic (Gardeweg et al., 1984; Zapettini and Blasco, 1998), surface deformation (Pritchard, 2003), geochronological (Richards and Villeneuve, 2001), geological evolution (Francis and Wells, 1988), and volcanic hazards works (Casertano, 1963; Lara et al., 2011; Amigo et al., 2012; Elissondo et al., 2016) have been carried out.

Eruption frequency

Although it shows no signs of current fumarolic activity, there are records of at least three eruptions during the nineteenth century (Stern et al., 2007). The Global Volcanism Program recognizes 3 Holocene eruptive periods with maximum VEI registered of 2 (GVP, 2013). It is not monitored, it is in the 88th place of the last version of the Chilean volcanic risk ranking (SERNAGEOMIN, 2020a, b) and the 16th place of the relative risk ranking of Argentine and neighboring volcanoes (Elissondo et al., 2016).

Hazard types

According to Francis and Wells (1988) it suffered a partial sector collapse directed towards the E. Currently it has flank collapse and lahar potential (Lara et al., 2011). No deformation was detected at Llullaillaco during a regional InSAR survey of Central Andean Volcanoes (Pritchard, 2003). There are no records of observed seismic unrest nor fumarolic and magmatic degassing (Lara et al., 2011).

In 2011 the Llullaillaco was considered a geologically active and potentially dangerous volcano, with low specific risk level (Lara et al., 2011) and is still considered in the latest version of the Chilean volcanic risk ranking (SERNAGEOMIN, 2020a, b). A reactivation would be associated with the emission of viscous lavas and the generation of pyroclastic density currents (Amigo et al., 2012).

1.47 Sin nombre (unnamed)

Physical characteristics

Sin nombre (unnamed) is a 4652 m high cinder cone of possibly Holocene age, located E of Corrida de Cori range in the Salta Region, Argentine (Richards and Villeneuve, 2002). It has a basaltic andesite composition, it was constructed on top of Early-Middle Miocene lavas and ignimbrites, and it has a second smaller vent ~ 800 m NW of the cinder cone (Richards and Villeneuve, 2002).

It is very scarcely investigated, some geological (Richards and Villeneuve, 2002; Seggiaro et al., 2007), surface deformation (Henderson and Pritchard, 2013), and volcanic hazards works (Elissondo et al., 2016; Amigo, 2021; Garcia and Badi, 2021; Aguilera et al., 2022) have been carried out.

Eruption frequency

Its relatively fluid lava flows, which display surficial breadcrust textures, suggest possible Holocene activity (GVP, 2013). The Global Volcanism Program is not aware of any Holocene eruptions from Sin nombre (unnamed) , it is not monitored, and it is in the 38th place of the relative risk ranking of Argentine and neighboring volcanoes (Elissondo et al., 2016).

Hazard types

There is no further information or records on partial sector collapse or lahar potential. No deformation was detected at this unnamed volcano during a regional InSAR survey of Central Andean Volcanoes (Henderson and Pritchard, 2013). No information or records were found on observed seismic unrest and fumarolic and/or magmatic degassing.

According to Richards and Villeneuve (2002) the most characteristic volcanic process of Sin nombre (unnamed) volcano, which would be the most likely to occur in the event of an eruption, is fluid lava flows of basaltic andesite composition.

1.48 Escorial (Corrida de Cori)

Physical characteristics

Escorial is a 5451 m high stratovolcano of Pleistocene-Holocene age, located on the Chilean-Argentine border (Amigo et al., 2012). It represents the most recent active vent of a NW-SE trending chain called Corrida de Cori (De Silva and Francis, 1991); its volcanic products cover an area of ~25 km^2 and the main edifice has an estimated volume of ~4 km^3 (Grosse et al., 2014).

Several geological (De Silva and Francis, 1991; González-Ferrán, 1995; Seggiaro et al., 2007; Stern et al., 2007; Grosse et al., 2014), petrographic (Richards and Villeneuve, 2002; Fiedrich et al., 2020), geological evolution (Naranjo and Cornejo, 1992), and volcanic hazards works (Lara et al., 2011; Amigo et al., 2012; Elissondo et al., 2016; Amigo, 2021; Garcia and Badi, 2021; Aguilera et al., 2022) have been carried out.

Eruption frequency

According to Richards and Villeneuve (2002), warm springs (frozen at surface), mud vents, and well-preserved fumarole spires attest to recent activity on Cerro Escorial, also the well-preserved summit crater postdates the lava flows and could be of Holocene age. The Global Volcanism Program is not aware of any Holocene eruptions from Cerro Escorial (GVP, 2013). It is not monitored, it is not included in the Chilean volcanic risk ranking, and it is in the 28th place of the relative risk ranking of Argentine and neighboring volcanoes (Elissondo et al., 2016).

Hazard types

Currently it has not flank collapse potential nor characteristics which could represent primary lahar sources (Lara et al., 2011). No deformation was detected at Llullaillaco during a regional InSAR survey of Central Andean Volcanoes (Pritchard, 2003). There are not records of observed seismic unrest nor fumarolic and magmatic degassing (Lara et al., 2011), but fumarolic deposits on the NE of the summit indicate extensive hydrothermal alteration there (De Silva and Francis, 1991).

Despite the lack of reliable records of its eruptive activity in the last 10,000 years, according to González-Ferrán (1995) the fresh morphological features of the effusive and the hydrothermal alteration reflect Holocene activity. In 2011 the Escorial volcano was considered a geologically active and potentially dangerous volcano, with very low specific risk level (Lara et al., 2011). A reactivation of this volcano would be associated with the emission of lavas (Amigo et al., 2012).

1.49 Lastarria

Physical characteristics

Lastarria is a 5706 m high stratovolcano of Holocene age, located on the Chilean-Argentine border (GVP, 2013). It is a NNW trending edifice with an oval basal plan, about 12 km long and 8 km wide (de Silva and Francis, 1991); its volcanic products cover an area of 37-105 km^2 and the main edifice has an estimated volume of 8-31 km^3 (Grosse et al., 2014; Aravena et al., 2015; SERNAGEOMIN, 2021).

Several geological (De Silva and Francis, 1991; González-Ferrán, 1995; Seggiaro et al., 2007; Stern et al., 2007; Grosse et al., 2014; Aravena et al., 2015), petrographic (Naranjo, 1992; Robidoux et al., 2020), fluid geochemistry (Naranjo, 1985; Aguilera, 2008, Aguilera et al., 2012, 2016; Inostroza et al., 2020b), surface deformation (Pritchard, 2003; Pritchard and Simons, 2002, 2004; Froger et al., 2007; Ruch et al., 2008, 2009; Anderssohn et al., 2009; Ruch and Walter, 2010; Budach et al., 2011; Henderson and Pritchard, 2013; Díaz et al., 2015), thermal anomalies (Jay et al., 2013), geological evolution (Francis and Wells, 1988; Naranjo, 1985, 1992, 2010), seismological (Spica et al., 2012; Pritchard et al., 2014) and volcanic hazards works (Casertano, 1963; Lara et al., 2011; Amigo et al., 2012; Amigo and Bertín, 2013; Elissondo et al., 2016; ONEMI Antofagasta, 2019; Amigo, 2021; Garcia and Badi, 2021; Aguilera et al., 2022) have been carried out.

Eruption frequency

The Global Volcanism Program is not aware of any Holocene eruptions from Lastarria, it is monitored by OVDAS (SERNAGEOMIN, 2021), it is in the 64th place of the last version of the Chilean volcanic risk ranking (SERNAGEOMIN, 2020a, b), and 9th place of the relative risk ranking of Argentine and neighboring volcanoes (Elissondo et al., 2016).

Hazard types

Currently it has flank collapse potential but not to generating lahars (Lara et al., 2011). There are records of ground deformation since 1997 (Pritchard and Simons, 2002; Froger et al., 2007; Ruch et al., 2008, 2009; Anderssohn et al., 2009) probably related to a growing magmatic chamber located about 10 km deep and magmas in the process of ascent from the asthenospheric wedge, which would feed a potential magmatic reservoir (Ruch and Walter, 2010; Budach et al., 2011). There are records of observed seismic unrest (Lara et al., 2011; Spica et al., 2012; Pritchard et al., 2014) and fumarolic and magmatic degassing (Naranjo, 1985; Aguilera, 2008, Aguilera et al., 2012, 2016; Robidoux et al., 2020; Inostroza et al., 2020b). Additionally, it displays continuous thermal anomaly hotspots (Jay et al., 2013).

Although no historical eruptions have been recorded, the youthful morphology of deposits suggest activity during historical time (González-Ferrán, 1995). And on its N flank there are extensive block and ash and column collapse pyroclastic deposits of 2.46 ± 0.06 ka (^{14}C, Naranjo, 2010). A reactivation in the Lastarria volcano would probably be linked to explosive activity with dispersion of pyroclastic material and generation of pyroclastic density currents (Amigo et al., 2012).

1.50 Cordón del Azufre

Physical characteristics

Cordón del Azufre is a 5481 m high volcanic complex of Holocene age, located on the Chile-Argentina border (GVP, 2013). It corresponds to a complex set of stratovolcanoes and monogenetic eruptive centers, which have been structured on an ancient stratovolcano, along a N-S fracture of ~6 km in length (González-Ferrán, 1995); its volcanic products cover an area of ~42 km^2 and the main edifice has an estimated volume of ~6 km^3 (Grosse et al., 2014).

Several geological (De Silva and Francis, 1991; González-Ferrán, 1995; Seggiaro et al., 2007; Stern et al., 2007; Grosse et al., 2014), petrographic (Trumbull et al., 1999), surface deformation (Pritchard and Simons, 2002; Froger et al., 2007; Ruch and Walter, 2010; Pearse and Lundgren, 2013; Henderson and Pritchard, 2013; Henderson et al., 2017), and volcanic hazards works (Lara et al., 2011; Amigo et al., 2012; Elissondo et al., 2016; Amigo, 2021; Garcia and Badi, 2021; Aguilera et al., 2022) have been carried out.

Eruption frequency

The most recent eruption is considered to be a small explosive eruption, which generated a small deposit of pyroclasts (González-Ferrán, 1995). The Global Volcanism Program is not aware of any Holocene eruptions from Cordón del Azufre, and it is not monitored. Is in the 91st place of the last version of the Chilean volcanic risk ranking (SERNAGEOMIN, 2020a, b), and in the 21st place of the relative risk ranking of Argentine and neighboring volcanoes (Elissondo et al., 2016).

Hazard types

Currently it has not flank collapse potential nor characteristics which could represent primary lahar sources (Lara et al., 2011). No ground deformation was detected at Cordón del Azufre but lying between Lastarria and Cordon del Azufre (Lazufre) (Pritchard and Simons, 2002; Pritchard, 2003; Froger et al., 2007; Henderson and Pritchard, 2013). There are not records of observed seismic unrest nor fumarolic and magmatic degassing (Lara et al., 2011).

Despite the lack of reliable records of its eruptive activity in the last 10,000 years, according to González-Ferrán (1995) given the characteristics of the latest effusive and the explosive eruption, it may have occurred in very recent time, probably historical. In 2011 the Cordón del Azufre was considered a geologically active and potentially dangerous volcanic complex, with very low specific risk level (Lara et al., 2011). It is scored for the latest Chilean volcanic risk ranking because it had unrest-type superficial fumarolic activity. A reactivation of this volcano would be associated with the emission of lavas and pyroclastic emission (Amigo et al., 2012).

1.51 Cerro Bayo

Physical characteristics

Cerro Bayo is a 5413 m high volcanic complex of partial Holocene age, located along the Chile-Argentina border (GVP, 2013). It is a relatively small, weathered edifice (basal diameter ~ 8 km) composed of andesitic tuffs and lavas and dacitic-riodacitic domes (Seggiaro et al., 2015); its volcanic products cover an area of 116 km^2 and the main edifice has an estimated volume of 33 km^3 (Grosse et al., 2014).

It is a scarcely investigated volcanic complex, some geological (De Silva and Francis, 1991; González-Ferrán, 1995; Seggiaro et al., 2007; Grosse et al., 2014; Benison, 2019), petrographic (Naranjo, 1988; Seggiaro et al., 2015), surface deformation (Pritchard, 2003; Henderson and Pritchard, 2013), and volcanic hazards works (Elissondo et al., 2016; SERNAGEOMIN, 2020a, b; Amigo, 2021; Garcia and Badi, 2021; Aguilera et al., 2022) have been carried out.

Eruption frequency

There is no Holocene evidence of activity, according to SERNAGEOMIN (*pers. Comm*) however there is doubt due to geothermal activity. The Global Volcanism Program is not aware of any Holocene eruptions from Cerro Bayo and it is not monitored. It is in the 90th place of the last version of the Chilean volcanic risk ranking (SERNAGEOMIN, 2020a, b), and in the 22nd place of the relative risk ranking of Argentine and neighboring volcanoes (Elissondo et al., 2016).

Hazard types

Currently it has no flank collapse potential nor characteristics which could represent primary lahar sources (Lara et al., 2011). No deformation was detected at Cerro Bayo during a regional InSAR survey of Central Andean Volcanoes (Pritchard, 2003; Henderson and Pritchard, 2013). There are not records of observed seismic unrest nor fumarolic and magmatic degassing (Lara et al., 2011). However, according to Naranjo (1988), fumarolic activity would have been concentrated in the past in the S and SW sectors of the main crater.

Despite the lack of reliable records of its eruptive activity in the last 10,000 years, De Silva and Francis (1991) suggest possible Holocene activity based in the summit of the complex, source of two viscous dacitic lava flows which represent the most recent activity of the complex; additionally, during a fieldwork in Salar Gorbea and Ignorado, Benison (2019) observed a small steam from Cerro Bayo. There is no information about the hazards that Cerro Bayo could pose in the event of an eruption, but according to its geological records it may be inferred that a reactivation would be mainly associated with the emission of lava flows, pyroclastic flows and tephra fallout (De Silva and Francis, 1991).

1.52 Antofagasta de la Sierra (Antofagasta volcanic field)

Physical characteristics

Antofagasta de la Sierra is a 3495 m high volcanic complex of Holocene age, located W of Beltran volcano, between the Salar de Antofalla on the W and the massive Cerro Galán caldera on the E, in the Catamarca Province, Argentina (GVP, 2013). It is formed by the La Laguna, Jote and Alumbrera volcanoes. The Alumbrera cone has a volume of 0.12 km^3 and its lava flows cover an area of 41.3 km^2; while the La Laguna cone has a volume of 0.12 km^3 and its lava flows occupy an area of 6.8 km^2 (Báez et al., 2016).

It is a scarcely investigated volcanic field, some geological (De Silva and Francis, 1991), petrographic (Francis et al., 1978; Hörmann et al., 1973), surface deformation (Henderson and Pritchard, 2013), geochronological (Risse et al., 2008), geological evolution (Báez et al., 2016), and volcanic hazards works (Elissondo et al., 2016; Amigo, 2021; Garcia and Badi, 2021; Aguilera et al., 2022) have been carried out.

Eruption frequency

The field contains several very youthful looking basaltic-andesite scoria cones and fresh-looking lava flows, suggesting possible Holocene activity (De Silva and Francis, 1991). Ar-Ar age dates for 22 samples taken by Risse et al. (2008) from throughout the main part of the field ranged from 7.3 to less than 0.1 Ma, and there is no report of an historical eruption (Báez et al., 2016). The Global Volcanism Program is not aware of any Holocene eruptions from Antofagasta de la Sierra volcanic field, it is not monitored, and it is in the 34th place of the relative risk ranking of Argentine and neighboring volcanoes (Elissondo et al., 2016).

Hazard types

A collapse scarp affecting only the external layers of the cone was identified on the NW flank of the Alumbrera volcano, showing a high degree of hydrothermal alteration (Báez et al., 2016). Currently it has not characteristics which could represent primary lahar sources. No deformation was detected at the Antofagasta volcanic field during a regional InSAR survey of Central Andean Volcanoes (Henderson and Pritchard, 2013). There are no records on observed seismic unrest nor fumarolic and magmatic degassing.

According to the geological map of the Báez et al. (2016), the occurrence of violent strombolian eruptions could cause extensive economic and social disruption as far as hundreds of kilometers from the vent because of ash dispersion. In addition, the occurrence of a high-explosive phreatomagmatic phase could generate pyroclastic density currents.

1.53 Sierra Nevada

Physical characteristics

Sierra Nevada is a 6173 m high volcanic complex of partial Holocene age, located in one of the most inaccessible parts of the Central Andes along the Chile-Argentina border (GVP, 2013). It consists of at least 12 volcanic vents with associated lava flows (De Silva and Francis, 1991); its volcanic products cover an area of 198-285 km^2 and the main edifice has an estimated volume of 73-100 km^3 (De Silva and Francis, 1991; Grosse et al., 2014, 2018).

It is a scarcely investigated volcanic complex, some geological (De Silva and Francis, 1991; González-Ferrán, 1995; Seggiaro et al., 2006; Grosse et al., 2014, 2018), petrographic (Schnurr et al., 2007), surface deformation (Pritchard, 2003), thermal anomalies (Jay et al., 2013), and volcanic hazards works (Elissondo et al., 2016; SERNAGEOMIN, 2020a, b; Amigo, 2021; Garcia and Badi, 2021; Aguilera et al., 2022) have been carried out.

Eruption frequency

There is no Holocene evidence of activity, but according to SERNAGEOMIN (*pers. Comm.*), the oldest lavas have been dated to ca. 400 ka, and the youngest ages have been obtained in the Cuyanos Azufrera Complex (ca. 140 ka). The Global Volcanism Program is not aware of any Holocene eruptions from Sierra Nevada, it is not monitored, is in the 92nd place of the last version of the Chilean volcanic risk ranking (SERNAGEOMIN, 2020a, b), and in the 31st place of the relative risk ranking of Argentine and neighboring volcanoes (Elissondo et al., 2016; Amigo, 2021; Garcia and Badi, 2021; Aguilera et al., 2022).

Hazard types

There is no further information or records on partial sector collapse or lahar potential. No deformation was detected at Sierra Nevada during a regional InSAR survey of Central Andean Volcanoes (Pritchard, 2003). There are not records of observed seismic unrest nor fumarolic and magmatic degassing. According to ASTER images, it has potential hotspots that merit further study (Jay et al., 2013).

There is no information about the hazards that Sierra Nevada could pose in the event of an eruption, but according to its geological records it may be inferred that a reactivation would be mainly associated with the emission of lava flows (De Silva and Francis, 1991).

1.54 Peinado

Physical characteristics

Peinado is a 5741 m high stratovolcano of Holocene age, located to the S of the Salar de Antofalla and Laguna del Peinado in Argentina. It is in the heart of the most tectonically and volcanically active region in the Central Andes (De Silva and Francis, 1991); its volcanic products cover an area of 44-93 km^2 and the main edifice has an estimated volume of 15-20 km^3 (Grosse et al., 2014, 2018).

It is a very scarcely investigated volcano, some geological (De Silva and Francis, 1991; Seggiaro et al., 2006; Grosse et al., 2014, 2018, 2020), surface deformation (Pritchard, 2003), and volcanic hazards works (Elissondo et al., 2016; Amigo, 2021; Garcia and Badi, 2021; Aguilera et al., 2022) have been carried out.

Eruption frequency

The Global Volcanism Program is not aware of any Holocene eruptions from Peinado, it is not monitored, and it is in the 29th place of the relative risk ranking of Argentine and neighboring volcanoes (Elissondo et al., 2016).

Hazard types

There is no further information or records on partial sector collapse or lahar potential. No deformation was detected at Peinado during a regional InSAR survey of Central Andean Volcanoes (Pritchard, 2003), and there are no records on observed seismic unrest nor fumarolic and magmatic degassing.

According to its geological records, the volcanic processes of Peinado most likely to occur in the event of an eruption, would be mainly associated with the emission of lava flows and pyroclastic density currents (De Silva and Francis, 1991).

1.55 Cerro El Cóndor

Physical characteristics

Cerro El Cóndor is a 6373 m high stratovolcano of Holocene age, located north of Falso Azufre volcano, which straddles the Chile-Argentina border (GVP, 2013). It is one of the few major stratovolcanoes located wholly in Argentina (De Silva and Francis, 1991); its volcanic products cover an area of 128-281 km^2 and the main edifice has an estimated volume of 41-109 km^3 (Grosse et al., 2014, 2018).

It is a very scarcely investigated volcano, some geological (De Silva and Francis, 1991; González-Ferrán, 1995; Seggiaro et al., 2006; Grosse et al., 2014, 2018), surface deformation (Pritchard, 2003), and volcanic hazards works (Elissondo et al., 2016; Amigo, 2021; Garcia and Badi, 2021; Aguilera et al., 2022) have been carried out.

Eruption frequency

The morphologically youthful lava flows and pristine summit crater imply a Holocene age (GVP, 2013), and according to Grosse et al. (2018) its main constructive phase may still be ongoing. The Global Volcanism Program is not aware of any Holocene eruptions from Cerro El Cóndor, it is not monitored, and it is in the 30th place of the relative risk ranking of Argentine and neighboring volcanoes (Elissondo et al., 2016).

Hazard types

Grosse et al. (2018) suggest a catastrophic, sector collapse event, directed towards the NW. Currently there are no characteristics which could represent primary lahar sources. No deformation was detected at Cerro El Cóndor during a regional InSAR survey of Central Andean Volcanoes (Pritchard, 2003), and there is no further information or records on observed seismic unrest nor fumarolic and magmatic degassing.

According to its geological records, the volcanic processes of Cerro El Cóndor most likely to occur in the event of an eruption, would be mainly associated with the emission of lava flows, volcanic avalanches and explosive activity (De Silva and Francis, 1991; Grosse et al., 2018).

1.56 Cerro Blanco

Physical characteristics

It has been named simply Robledo (Simkin and Siebert, 1994), De Silva and Francis (1991) refer to its silicic dome in the western part of the caldera as Cerro Blanco, Arnosio et al. (2005) and Brunori et al. (2013) use “Cerro Blanco/Robledo Caldera” (CBRC) for the whole structures which includes two 4–5 km wide coalescent circular features, and Fernandez-Turiel et al. (2019) used Cerro Blanco Volcanic Complex (CBVC).

Cerro Blanco is a 4670 m high caldera of Holocene age (GVP, 2013; Aguilera et al., 2022), that belongs to an SW-NE prolongation of the CVZ towards the back-arc region (Lamberti et al., 2021), located in the southern limit of Andean plateau of the Catamarca Province in Argentina (Báez et al., 2015). Four calderas have been recognized in the CBVC: El Niño, Pie de San Buenaventura, Robledo, and Cerro Blanco (Báez et al., 2015; Montero López et al., 2010).

Several geological (Seggiaro et al., 2006; Di Filippo et al., 2008; de Silva et al., 2022; Barcelona et al., 2023), petrographic (Arnosio et al., 2005; Montero López et al., 2010; Fernandez-Turiel et al., 2019; de Silva et al., 2022; Barcelona et al., 2023), fluid geochemistry (Viramonte et al., 2005a; Chiodi et al., 2019; Lamberti et al., 2021), surface deformation (Pritchard and Simons, 2002, 2004; Viramonte et al., 2005b; Brunori et al., 2013, Henderson and Pritchard, 2013; Vélez et al., 2021), geological evolution (Báez et al., 2015, 2020), seismological (Mulcahy et al., 2010) and volcanic hazards works (Elissondo et al., 2016; Amigo, 2021; Garcia and Badi, 2021; Aguilera et al., 2022) have been carried out.

Eruption frequency

Based on Fernandez-Turiel et al. (2019) results, the Cerro Blanco eruption is among the largest volcanic eruptions of the Holocene globally, exceeding the magnitude of the 1600 Huaynaputina eruption. The Global Volcanism Program recognizes 1 Holocene eruptive period with maximum VEI registered of 7. It is not monitored, and it is in the 8th place of the relative risk ranking of Argentine and neighboring volcanoes (Elissondo et al., 2016).

Hazard types

Currently it has not flank collapse potential nor characteristics which could represent primary lahar sources. There is evidence of ground deformation (Pritchard and Simons, 2002, 2004; Viramonte et al., 2005b; Brunori et al., 2013; Henderson and Pritchard, 2013; Vélez et al., 2021), it is subsiding with an average velocity of 0.87 cm/year (Báez et al., 2015). There are records of seismic swarms during the years 2007-2009 in the upper crust (Mulcahy et al., 2010) and it hosts an active, small geothermal field, fumaroles, diffuse degassing of CO_2, hot springs and mud volcanoes (Viramonte et al., 2005a; Chiodi et al., 2019; Lamberti et al., 2021).

According to Báez et al. (2015), two possible scenarios would be the most likely to occur in the event of an eruption: i) eruptive style with generation of PDCs without vertical development of an eruptive column (boiling over), and ii) Plinian / subplinian eruptive style with generation of PDCs.

1.57 Falso Azufre

Physical characteristics

Falso Azufre is a 5906 m high volcanic complex of Holocene age, located along the Chile-Argentina border (GVP, 2013). It is the main edifice of a 15 km W-E trending complex of approximately 6 overlapping craters, lava domes, and composite cones extending from Chile into Argentina (De Silva and Francis, 1991); its volcanic products cover an area of 310-387 km^2 and the main edifice has an estimated volume of 83–101 km^3 (Grosse et al., 2014, 2018).

It is a very scarcely investigated volcano, some geological (De Silva and Francis, 1991; Seggiaro et al., 2006; Grosse et al., 2014, 2018), surface deformation (Pritchard, 2003), thermal anomalies (Jay et al., 2013), and volcanic hazards works (Elissondo et al., 2016; Amigo, 2021; Garcia and Badi, 2021; Aguilera et al., 2022) have been carried out.

Eruption frequency

Two small composite cones and two lava domes appear to represent the most recent activity of the complex and may be of Holocene age (De Silva and Francis, 1991). The Global Volcanism Program is not aware of any Holocene eruptions from Falso Azufre (GVP, 2013), it is not monitored, and it is in the 32nd place of the relative risk ranking of Argentine and neighboring volcanoes (Elissondo et al., 2016).

Hazard types

There is no further information or records on partial sector collapse or lahar potential. No deformation was detected at Falso Azufre during a regional InSAR survey of Central Andean Volcanoes (Pritchard, 2003), and there are no records on observed seismic unrest nor fumarolic and magmatic degassing. According to ASTER images, it has potential hotspots that merit further study (Jay et al., 2013).

Despite the lack of reliable records of its eruptive activity in the last 10,000 years, according to Grosse et al. (2018), Falso Azufre has an intermediate long-term eruptive potential and a minor felsic phase may be ongoing. The volcanic processes of Falso Azufre most likely to occur in the event of an eruption, would be mainly associated with the emission of lava flows, pyroclastic density currents and tephra fallout (De Silva and Francis, 1991).

1.58 Nevado de Incahuasi

Physical characteristics

Nevado de Incahuasi is a 6638 m high volcanic complex of Holocene age, located ENE of Nevados Ojos del Salado volcano at the Chile-Argentina border (GVP, 2013). It has two stratocones whose amalgamated craters opened in a calderic amphitheater of about 3.5 km in diameter southward (González-Ferrán, 1995); its volcanic products cover an area of 125-207 km^2 and the main edifice has an estimated volume of 54–231 km^3 (Grosse et al., 2014, 2018; Aravena et al., 2015).

Several geological (González-Ferrán, 1995; Rubiolo et al., 2003; Aravena et al., 2015; Grosse et al., 2014, 2018), petrographic (Kay et al., 2008, 2013), glaciological (Gspurning et al., 2006), surface deformation (Henderson and Pritchard, 2013), geological evolution (Seggiaro and Hongn, 1999), and volcanic hazards works (Lara et al., 2011; Amigo et al., 2012; Perucca and Moreiras, 2009; Elissondo et al., 2016; SERNAGEOMIN, 2020a, b; Amigo, 2021; Garcia and Badi, 2021; Aguilera et al., 2022) have been carried out.

Eruption frequency

The youngest activity recorded at Incahuasi is from the NE mafic center, with an age of 0.35 ± 0.03 Ma (Grosse et al., 2018). The Global Volcanism Program is not aware of any Holocene eruptions from Nevado de Incahuasi and it is not monitored. It is in the 85th place of the last version of the Chilean volcanic risk ranking (SERNAGEOMIN, 2020a, b) and the 27th place of the relative risk ranking of Argentine and neighboring volcanoes (Elissondo et al., 2016).

Hazard types

Currently it has not flank collapse potential nor characteristics which could represent primary lahar sources (Lara et al., 2011). There are some small areas of firn and ice (6620 m), but their total extent is very low, and it is also noticeable that there is no ice in the wind-protected crater (Gspurning et al., 2006). No deformation was detected at Nevado de Incahuasi during a regional InSAR survey of Central Andean Volcanoes (Henderson and Pritchard, 2013). There are not records of observed seismic unrest (Lara et al., 2011), nor fumarolic or magmatic degassing.

The main edifice of Incahuasi has been inactive since ~ 0.7 Ma and hence future activity seems unprobable. It can be considered a young extinct volcano following the classification of Szakács (1994), although future activity cannot be completely ruled out as other volcanoes in the CVZ have shown repose periods in the order of 1 Ma, and because there seems to be availability of magma in the area (Grosse et al., 2018). According to González-Ferrán (1995), there are possibilities of violent explosive eruptions of dacitic-rhyolitic nature, in which the most characteristic volcanic processes most likely to occur would be tephra fallout over remote regions and eventual pyroclastic flows. And according to (Amigo et al., 2012), a reactivation of this volcano would be linked to the emission of lavas and less pyroclastic emission, from limited to zero impact in populated areas, although it could affect the international route CH-31.

1.59 Nevado Tres Cruces

Physical characteristics

Nevado Tres Cruces is a 6620 m high stratovolcano of Pliocene-Pleistocene age, located along the Chile-Argentina border (GVP, 2013). It has 30 eruptive centers, controlled by a fracture system heading N70ºE and N10ºW (González-Ferrán, 1995), three coalescing cones aligned in a N-S direction and a series of dacitic to riodacitic lavas, domes, explosion craters, small volume pyroclastic flows, and tephra fallout deposits (Amigo et al., 2012); its volcanic products cover an area of 126-1000 km^2 and the main edifice has an estimated volume of 38-225 km^3 (González-Ferrán, 1995; Aravena et al., 2015; Grosse et al., 2014, 2018).

Several geological (González-Ferrán, 1995; Rubiolo et al., 2003; Aravena et al., 2015; Grosse et al., 2014, 2018), petrographic (Fernandez-Turiel et al., 2016), glaciological (Haselton et al., 2002; Masiokas et al., 2009; García et al., 2017; Flores et al., 2018), geological evolution (Gardeweg et al., 2000) and volcanic hazards works (Amigo et al., 2012; SERNAGEOMIN, 2020a, b; Amigo, 2021; Aguilera et al., 2022) have been carried out.

Eruption frequency

According to Fernandez-Turiel et al. (2016), it is the strongest candidate to be the source of the Upper Holocene pyroclastic deposits found in the Fiambalá basin. The Global Volcanism Program is not aware of any Holocene eruptions from Nevado Tres Cruces, it is not monitored, and it is in the 82nd place of the last version of the Chilean volcanic risk ranking (SERNAGEOMIN, 2020a, b).

Hazard types

Currently it has not flank collapse potential nor characteristics which could represent primary lahar sources. However, it is covered by glaciers mainly on its southeastern slope (González-Ferrán, 1995), with 1.1 km^2 of ice in 2000 (Masiokas et al., 2009), which according to Flores et al. (2018) is the fastest shrinking glacier of the Alto Andina basin. No further information or records were found on ground deformation, observed seismic unrest and fumarolic and/or magmatic degassing.

The existence of activity until ca. 30 Ka and the period of rest of approximately 40 Ka that separates it from the previous eruptive event (Ignimbrita de Pampa Blanca) allowed Gardeweg et al. (2000) to postulate that it is a potentially active center, of high hazard but low risk. According to Amigo et al. (2012), a reactivation could be related to explosive activity with dispersion of pyroclastic material and generation of pyroclastic density currents, although of limited impact in populated areas. The international route CH-31 could be affected, depending on the eruption magnitude.

1.60 El Solo

Physical characteristics

El Solo is a 6205 m high stratovolcano of Holocene age, located W of Nevados Ojos del Salado and SE of Nevado Tres Cruces, along the Chile-Argentina border (GVP, 2013). It has nine eruptive centers that structure an imposing pyramidal cone (González-Ferrán, 1995); its volcanic products cover an area of 15-19 km^2 and the main edifice has an estimated volume of 4-11 km^3 (Grosse et al., 2014, 2018; Aravena et al., 2015).

It is a very scarcely investigated volcano, some geological (González-Ferrán, 1995; Rubiolo et al., 2003; Aravena et al., 2015; Grosse et al., 2014, 2018), petrographic (Mpodozis et al., 1996; Gardeweg et al., 1997), and volcanic hazards works (Lara et al., 2011; Elissondo et al., 2016; Amigo, 2021; Garcia and Badi, 2021; Aguilera et al., 2022) have been carried out.

Eruption frequency

It was source of major rhyodacitic pyroclastic-flow deposits estimated to be post-Holocene which currently are filling the adjacent valleys (González-Ferrán, 1995). The Global Volcanism Program is not aware of any Holocene eruptions from El Solo, it is not monitored, and it is in the 33rd place of the relative risk ranking of Argentine and neighboring volcanoes (Elissondo et al., 2016).

Hazard types

It has not flank collapse potential nor characteristics which could represent primary lahar sources (Lara et al., 2011). No deformation was detected at El Solo during a regional InSAR survey of Central Andean Volcanoes (Henderson and Pritchard, 2013). There are not records of observed seismic unrest nor fumarolic and magmatic degassing (Lara et al., 2011).

In 2011 El Solo was considered a geologically active and potentially dangerous volcano, with very low specific risk level (Lara et al., 2011). According to the geological surveys carried out in this area, the most characteristic volcanic processes of El Solo volcano, which would be the most likely to occur in the event of an eruption, are tephra fallout and pyroclastic density currents.

1.61 Nevado Ojos del Salado

Physical characteristics

Nevado Ojos del Salado is a 6879 m high volcanic complex of Holocene age, located along the Chile-Argentina border (GVP, 2013). It is the highest active volcano in the world (De Silva and Francis, 1991); its volcanic products cover an area of 70-148 km^2 and the main edifice has an estimated volume of 40-54 km^3 (Grosse et al., 2014, 2018).

Several geological (De Silva and Francis, 1991; González-Ferrán, 1995; Rubiolo et al., 2003; Stern et al., 2007; Grosse et al., 2014, 2018), petrographic (Baker et al., 1987; Gardeweg et al., 1997; 1998b), surface deformation (Pritchard, 2003; Pritchard and Simons, 2004), and volcanic hazards works (Casertano, 1963; Lara et al., 2011; Amigo et al., 2012; Elissondo et al., 2016; Amigo, 2021; Garcia and Badi, 2021; Aguilera et al., 2022) have been carried out.

Eruption frequency

There are no records of historic activity, but climbers reported fumarolic activity in 1937 and 1956 (Casertano, 1963). A major rhyodacitic explosive eruption took place about 1000-1500 years ago, producing pumiceous pyroclastic flows and there was an unconfirmed report of minor gas-and-ash emission in 1993 (GVP, 2013). The Global Volcanism Program recognizes 2 Holocene eruptive periods with maximum VEI registered of 1 and it is not monitored. It is in the 75th place of the last version of the Chilean volcanic risk ranking (SERNAGEOMIN, 2020a, b) and the 14th place of the relative risk ranking of Argentine and neighboring volcanoes (Elissondo et al., 2016).

Hazard types

Currently it has not flank collapse potential nor characteristics which could represent primary lahar sources (Lara et al., 2011). No deformation was detected at Nevados Ojos del Salado during a regional InSAR survey of Central Andean Volcanoes (Pritchard, 2003). There are not records of observed seismic unrest (Lara et al., 2011), but intermittent fumarolic activity and magmatic degassing (Gardeweg et al., 1998b; Jay et al., 2013).

In 2011 the Nevados Ojos del Salado was considered a geologically active and potentially dangerous volcano, with very low specific risk level (Lara et al., 2011). A reactivation could be related to minor explosive activity and the emission of lava or construction of domes, associated with possible pyroclastic currents (Amigo et al., 2012).

1.62 Cerro Tipas (Walker Penk)

Physical characteristics

Cerro Tipas is a 6658 m high volcanic complex of Holocene age, located in Argentina, immediately SSW of Nevados Ojos del Salado, and S of the Chilean border (GVP, 2013). It is the world's third highest active volcano but remains largely unknown (De Silva and Francis, 1991); its volcanic products cover an area of 25-211 km^2 and the main edifice has an estimated volume of 43-52 km^3 (De Silva and Francis, 1991; Grosse et al., 2014, 2018).

Some geological (De Silva and Francis, 1991; Rubiolo et al., 2003; Stern et al., 2007; Grosse et al., 2014, 2018), surface deformation (Pritchard, 2003; Henderson and Pritchard, 2013), and volcanic hazards works (Perucca and Moreiras, 2009; Elissondo et al., 2016; Amigo, 2021; Garcia and Badi, 2021; Aguilera et al., 2022) have been carried out.

Eruption frequency

It displays a youthful morphology, and its latest eruptions were considered to be of Holocene age (De Silva and Francis, 1991). The Global Volcanism Program is not aware of any Holocene eruptions from Tipas

(GVP, 2013), it is not monitored, and it is in the 20th place of the relative risk ranking of Argentine and neighboring volcanoes (Elissondo et al., 2016).

Hazard types

There is no further information or records on partial sector collapse or lahar potential. No deformation was detected at Tipas during a regional InSAR survey of Central Andean Volcanoes (Henderson and Pritchard, 2013), and there are not records of observed seismic unrest, nor fumarolic or magmatic degassing.

There is not information about the hazards that Tipas could pose in the event of an eruption, but according to its geological records it may be inferred that a reactivation would be mainly associated with the emission of lava flows, pyroclastic flows and tephra fallout as its better-known neighbour Nevados Ojos del Salado (De Silva and Francis, 1991).

2 References

Adams, N., de Silva, S., Self, S., Salas, G., Schubring, S., Permenter, J., et al. (2001). The physical volcanology of the 1600 eruption of Huaynaputina, southern Peru. *Bull. Volcanol.* 62, 493–518. doi: 10.1007/s004450000105.

Aguilar, R., Taipe Maquerhua, E., Antayhua Vera, Y., Ortega Gonzales, M., Apaza Choquehuayta, F., and Cruz Mamani, L. (2021). Hazard assessment studies and multiparametric volcano monitoring developed by the Instituto Geológico, Minero y Metalúrgico in Peru. *Volcanica* 4, 73–92. doi: 10.30909/vol.04.S1.7392.

Aguilar, R., Thouret, J.-C., and Samaniego, P. (2016). Actividad eruptiva en sistemas de larga duración: relaciones entre el complejo post-caldérico Chachani y las ignimbritas Plio-cuaternarias de la cuenca de Arequipa (Perú). *XVIII Congr. Peru. Geol.*, 1–4. Available at: https://repositorio.ingemmet.gob.pe/handle/20.500.12544/1597?locale=en#.XbwWoJcjFlQ.mendeley.

Aguilar, R., Thouret, J.-C., Samaniego, P., Wörner, G., Jicha, B., Paquette, J.-L., et al. (2022). Growth and evolution of long-lived, large volcanic clusters in the Central Andes: The Chachani Volcano Cluster, southern Peru. *J. Volcanol. Geotherm. Res.* 426, 107539. doi: 10.1016/j.jvolgeores.2022.107539.

Aguilera, F. (2008). Origen y naturaleza de los fluidos en los sistemas volcánicos, geotermales y termales de baja entalpía de la Zona Volcánica Central entre los 17°43´S y 25°10´S, Chile. *Ph.D. Thesis. Univ. Católica del Norte. (In Spanish)*, 393.

Aguilera, F., Apaza, F., Del Carpio, J., Grosse, P., Jiménez, N., Ureta, G., et al. (2022). Advances in scientific understanding of the Central Volcanic Zone of the Andes: a review of contributing factors. *Bull. Volcanol.* 84, 1–8. doi: 10.1007/s00445-022-01526-y.

Aguilera, F., Layana, S., Rodríguez-Díaz, A., González, C., Cortés, J., and Inostroza, M. (2016). Hydrothermal alteration, fumarolic deposits and fluids from Lastarria Volcanic Complex: A multidisciplinary study. *Andean Geol.* 43, 166. doi: 10.5027/andgeoV43n2-a02.

Aguilera, F., Layana, S., Rojas, F., Arratia, P., Wilkes, T. C., González, C., et al. (2020). First measurements of gas flux with a low-cost smartphone sensor-based uv camera on the volcanoes of Northern Chile. *Remote Sens.* 12. doi: 10.3390/rs12132122.

Aguilera, F., Tassi, F., Darrah, T., Moune, S., and Vaselli, O. (2012). Geochemical model of a magmatic–hydrothermal system at the Lastarria volcano, northern Chile. *Bull. Volcanol.* 74, 119–134. doi: 10.1007/s00445-011-0489-5.

Aguilera, F., Viramonte, J., Medina, E., Guzmán, K., Becchio, R., Delgado, H., et al. (2006). Eruptive Activity From Lascar Volcano (2003 – 2005). *XI Congr. Geológico Chil. Antofagasta, II Región, Chile* 2, 397–400.

Alcalá-Reygosa, J. (2017). El Último Máximo Glaciar local y la deglaciación de la Zona Volcánica Central Andina: El caso del volcán HualcaHualca y del altiplano de Patapampa (Sur de Perú). *Cuad. Investig. Geográfica* 43, 649. doi: 10.18172/cig.3231.

Alcozer-Vargas, N., Reyes-Hardy, M.-P., Esquivel, A., and Aguilera, F. (2022). A GIS-based multi-hazard assessment at the San Pedro volcano, Central Andes, northern Chile. *Front. Earth Sci.* 10, 25. doi: 10.3389/feart.2022.897315.

Alvizuri, C., and Tape, C. (2016). Full moment tensors for small events (M w < 3) at Uturuncu volcano, Bolivia. *Geophys. J. Int.* 206, 1761–1783. doi: 10.1093/gji/ggw247.

Amigo, A. (2021). Volcano monitoring and hazard assessments in Chile. *Volcanica* 4, 1–20. doi: 10.30909/vol.04.S1.0120.

Amigo, A., and Bertin, D. (2013). Mapa preliminar de peligros volcánicos volcán Guallatiri, escala 1:75.000. *Programa Riesgo Volcánico. Serv. Nac. Geol. y Minería, Chile*.

Amigo, Á., and Bertin, D. (2012). Mapa Preliminar De Peligros Volcánicos Volcán San Pedro, escala 1:75.000. *Serv. Nac. Geol. y Minería, Cart. Geológica Chile, Ser. Geol. Ambient.*

Amigo, Á., and Bertín, D. (2013). Mapa Preliminar De Peligros Volcánicos Volcán Lastarria, escala 1:50.000. *Serv. Nac. Geol. y Minería, Cart. Geológica Chile, Ser. Geol. Ambient.*, 542000.

Amigo, A., Bertin, D., and Orozco, G. (2012). Peligros volcanicos de la zona norte de Chile, Regiones de Arica y Parinacota, Tarapacá, Antofagasta y Atacama. Servicio Nacional de Geología y Minería, Carta Geológica de Chile, Serie Geología Ambiental. 45, 1 mapa en 5 hojas escala 1:250.000, 1 mapa esc.

Anderssohn, J., Motagh, M., Walter, T. R., Rosenau, M., Kaufmann, H., and Oncken, O. (2009). Surface deformation time series and source modeling for a volcanic complex system based on satellite wide swath and image mode interferometry: The Lazufre system, central Andes.

Remote Sens. Environ. 113, 2062–2075. doi: 10.1016/j.rse.2009.05.004.

Andrés, N., Palacios, D., Úbeda, J., and Alcalá, J. (2011). Ground thermal conditions at chachani volcano, southern peru. *Geogr. Ann. Ser. A, Phys. Geogr.* 93, 151–162. doi: 10.1111/j.1468-0459.2011.00424.x.

Antayhua, Y., Ramos, D., and Masías, P. (2011). Monitoreo sísmico temporal y caracterización geoquímica de fumarolas y fuentes termales del volcán Huaynaputina. *INGEMMET, Inf. Técnico N° 6576*, 63.

Antayhua, Y., Ramos, D., and Masías, P. (2013). Monitoreo de los volcanes Ticsani, Sabancaya y Huaynaputina: Periodo 2006-2012. *INGEMMET, Boletín No 53 Ser. C Geodinámica e Ing. Geológica*, 124.

Apaza, F., Kern, C., Ortega, M., and Miranda, R. (2021). The July 2019 explosive activity of Ubinas Volcano , Peru. *EGU21-3529*, 1. doi: https://doi.org/10.5194/egusphere-egu21-3529.

Apaza, F., Miranda, R., Ccallata, B., Masías, P., Cruz, L., Valdivia, D., et al. (2019). Informe Técnivo Anual: Vigilancia de los Volcanes Misti y Coropuna, Periodo 2019. *INGEMMET, Inf. Técnico N° A6997*, 36.

Apaza, F., Miranda, R., and Ramos, D. (2015). Monitoreo de los Volcanes Coropuna, Ticsani y Tutupaca, 2015. in *INGEMMET, Informe técnico* (Arequipa: Observatorio Volcanológico del INGEMMET), 32.

Aravena, D., Villalón, I., and Sánchez, P. (2015). Igneous Related Geothermal Resource in the Chilean Andes. in *World Geothermal Congress 2015* (Melbourne), 8.

Arnosio, M., Becchio, R., Viramonte, J. G., Groppelli, G., Norini, G., and Corazzato, C. (2005). Geología del Complejo Volcánico Cerro Blanco (26° 45´ LS- 67° 45´ LO), Puna Austral. *16º Congr. Geológico Argentino La Plata, Buenos Aires, Asoc. Geológica Argentina*, 851–858.

Arratia, P. (2019). Estimación de las emisiones de dióxido de azufre mediante una cámara UV de bajo costo en los volcanes Guallatiri, Isluga e Irruputuncu, Chile. *Undergrad. Thesis. Univ. Católica del Norte, Chile.*, 85.

Asch, G., Kurt, W., Hellweg, M., Seidl, D., and Rademacher, H. (1996). Observations of rapid-fire event tremor at Lascar volcano, Chile. *Ann. di Geofis.* XXXIX, 273–282.

Ayala-Arenas, J. S., Cano, N. F., Rivera-Porras, M., Gonzales-Lorenzo, C. D., and Watanabe, S. (2019). Dating volcanic ash and pumice stones from volcano El Misti, Peru, by thermoluminescence. *Quat. Int.* 512, 1–5. doi: 10.1016/j.quaint.2018.11.013.

Báez, W., Arnosio, M., Chiodi, A., Ortiz-Yañes, A., Viramonte, J. G., Bustos, E., et al. (2015). Stratigraphy and evolution of the Cerro Blanco Volcanic Complex, Puna Austral, Argentina. *Rev. Mex. Ciencias Geológicas* 32, 29–49.

Báez, W., Bustos, E., Chiodi, A., Reckziegel, F., Arnosio, M., de Silva, S., et al. (2020). Eruptive style and flow dynamics of the pyroclastic density currents related to the Holocene Cerro Blanco eruption (Southern Puna plateau, Argentina). *J. South Am. Earth Sci.* 98, 102482. doi: 10.1016/j.jsames.2019.102482.

Báez, W., Carrasco Nuñez, G., Giordano, G., Viramonte, J. G., and Chiodi, A. (2016). Polycyclic scoria cones of the Antofagasta de la Sierra basin, Southern Puna plateau, Argentina. *Geol. Soc. London, Spec. Publ.* 446, 311–336. doi: 10.1144/SP446.3.

Baker, P. E., González-Ferrán, O., and Rex, D. C. (1987). Geology and geochemistry of the Ojos del Salado volcanic region, Chile. *J. Geol. Soc. London.* 144, 85–96.

Barcaza, G., Nussbaumer, S. U., Tapia, G., Valdés, J., García, J.-L., Videla, Y., et al. (2017). Glacier inventory and recent glacier variations in the Andes of Chile, South America. *Ann. Glaciol.* 58, 166–180. doi: 10.1017/aog.2017.28.

Barcelona, H., Chiodi, A., Yagupsky, D., Peri, G., Winocur, D., and Kleiman, P. (2023). Resource assessment of the Cerro Blanco geothermal system. *J. South Am. Earth Sci.* 123, 104247. doi: 10.1016/j.jsames.2023.104247.

Barone, A., Fedi, M., Tizzani, P., and Castaldo, R. (2019). Multiscale Analysis of DInSAR Measurements for Multi-Source Investigation at Uturuncu Volcano (Bolivia). *Remote Sens.* 11, 703. doi: 10.3390/rs11060703.

Barrientos, J. A. (2013). Evaluación y zonificación preliminar del peligro volcánico del volcán Tacora, XV Región de Arica y Parinacota, Andes Centrales del Norte de Chile. *Mem. para optar al título geólogo.*, 150.

Benison, K. C. (2019). The Physical and Chemical Sedimentology of Two High-Altitude Acid Salars in Chile: Sedimentary Processes In An Extreme Environment. *J. Sediment. Res.* 89, 147–167.

doi: 10.2110/jsr.2019.9.

Bernard, K., Thouret, J.-C., and van Wyk de Vries, B. (2017). Emplacement and transformations of volcanic debris avalanches-A case study at El Misti volcano, Peru. *J. Volcanol. Geotherm. Res.* 340, 68–91. doi: 10.1016/j.jvolgeores.2017.04.009.

Bertin, D. (2017). 3-D ballistic transport of ellipsoidal volcanic projectiles considering horizontal wind field and variable shape-dependent drag coefficients. *J. Geophys. Res. Solid Earth* 122, 1126–1151. doi: 10.1002/2016JB013320.

Bertin, D., and Amigo, A. (2013). Mapa preliminar de peligros volcánicos volcán Isluga, escala 1:50.000. *Serv. Nac. Geol. y Minería, Programa Riesgo Volcánico, Chile*.

Bertin, D., and Amigo, Á. (2015). Geología y peligros del volcán San Pedro, II Región, escalada 1:50.000. *Serv. Nac. Geol. y Minería, Subdirección Nac. Geol. Cart. Geológica Chile, Ser. Geol. Ambient. N° 25*.

Bertín, D., and Amigo, Á. (2013a). Mapa Preliminar De Peligros Volcánicos Volcán Irruputuncu, escala 1:50.000. *Serv. Nac. Geol. y Minería, Programa Riesgo Volcánico, Chile*.

Bertín, D., and Amigo, Á. (2013b). Mapa Preliminar De Peligros Volcánicos Volcán Parinacota, escala 1:75.000. *Cart. Geológica Chile, Ser. Geol. Ambient.*

Bertín, D., and Amigo, Á. (2019). Geología del volcán San Pedro, Región de Antofagasta. *Serv. Nac. Geol. y Minería, Cart. Geológica Chile, Ser. Geol. Básica*, 73.

Bertin, D., and Orozco, G. (2013). Mapa Preliminar De Peligros Volcánicos Volcán Ollagüe, escala 1:75.000. *Serv. Nac. Geol. y Minería, Programa Riesgo Volcánico*.

Bertin, L. ., Jara, G. ., and Toloza, V. (2022). Peligros del volcán Parinacota, región de Arica y Parinacota. Servicio Nacional de Geología y Minería, Carta Geológica de Chile, Serie de Geología Ambiental: X p., 1 mapa escala 1:50.000, Santiago.

BGVN (2021). Report on Sabancaya (Peru) (Crafford, A.E., and Venzke, E., eds.). *Glob. Volcanism Program, 2021. Bull. Glob. Volcanism Network. Smithson. Institution.* 46. Available at: https://volcano.si.edu/showreport.cfm?doi=10.5479/si.GVP.BGVN202104-354006.

Birnie, R., and Hall, J. (1974). The geochemistry of El Misti volcano, Peru fumaroles. *Bull. Volcanol.* 38, 1–15. doi: 10.1007/BF02597797.

Blard, P.-H., Lave, J., Farley, K. A., Ramirez, V., Jimenez, N., Martin, L. C. P., et al. (2014). Progressive glacial retreat in the Southern Altiplano (Uturuncu volcano, 22°S) between 65 and 14 ka constrained by cosmogenic 3 He dating. *Quat. Res.* 82, 209–221. doi: 10.1016/j.yqres.2014.02.002.

Blasco, G., Zappettini, E., and Hongn, F. (1996). Hoja Geológica 2566-I, San Antonio de los Cobres. Provincias de Jujuy y de Salta. Escala 1:250.000. *Serv. Geológico Min. Argentino. Inst. Geol. y Recur. Miner. Programa Nac. Cart. Geológicas la República. Buenos Aires,* 131.

Boixart, G., Cruz, L. F., Miranda Cruz, R., Euillades, P. A., Euillades, L. D., and Battaglia, M. (2020). Source Model for Sabancaya Volcano Constrained by DInSAR and GNSS Surface Deformation Observation. *Remote Sens.* 12, 1852. doi: 10.3390/rs12111852.

Bourdon, B., Wörner, G., and Zindler, A. (2000). U-series evidence for crustal involvement and magma residence times in the petrogenesis of Parinacota volcano, Chile. *Contrib. to Mineral. Petrol.* 139, 458–469. doi: 10.1007/s004100000150.

Bredemeyer, S., Ulmer, F.-G., Hansteen, T., and Walter, T. (2018). Radar Path Delay Effects in Volcanic Gas Plumes: The Case of Láscar Volcano, Northern Chile. *Remote Sens.* 10, 1514. doi: 10.3390/rs10101514.

Bromley, G. R. M., Thouret, J.-C., Schimmelpfennig, I., Mariño, J., Valdivia, D., Rademaker, K., et al. (2019). In situ cosmogenic 3He and 36Cl and radiocarbon dating of volcanic deposits refine the Pleistocene and Holocene eruption chronology of SW Peru. *Bull. Volcanol.* 81, 64. doi: 10.1007/s00445-019-1325-6.

Brown, L., Singer, B. S., and Barquero-Molina, M. (2021). Paleomagnetism and 40Ar/39Ar chronology of ignimbrites and lava flows, Central Volcanic Zone, Northern Chile. *J. South Am. Earth Sci.* 106, 103037. doi: 10.1016/j.jsames.2020.103037.

Brunori, C. A., Bignami, C., Stramondo, S., and Bustos, E. (2013). 20 years of active deformation on volcano caldera: Joint analysis of InSAR and AInSAR techniques. *Int. J. Appl. Earth Obs. Geoinf.* 23, 279–287. doi: 10.1016/j.jag.2012.10.003.

Budach, I., Brasse, H., and Díaz, D. (2011). Imaging of conductivity anomalies at Lazufre volcanic complex , Northern Chile , through 3-D inversion of magnetotelluric data. *Schmucker-Weidelt-Kolloquium Neustadt an der Weinstraße*, 27–34.

Bullard, F. M. (1962). Volcanoes of Southern Peru. *Bull. Volcanol.* 24, 443–453. doi: 10.1007/BF02599360.

Bulmer, M., Johnston, A., and Engle, F. (1999). Analysis of Sabancaya volcano, souther Peru using Radarsat and Landsat TM data. *Appl. Dev.* .... Available at: http://airandspace.si.edu/research/ceps/research/bulmer/pdf/ADRORELATEDii.pdf.

Burns, D. H., de Silva, S. L., Tepley, F. J., and Schmitt, A. K. (2020). Chasing the mantle: Deciphering cryptic mantle signals through Earth's thickest continental magmatic arc. *Earth Planet. Sci. Lett.* 531, 115985. doi: 10.1016/j.epsl.2019.115985.

Burns, D. H., de Silva, S. L., Tepley, F., Schmitt, A. K., and Loewen, M. W. (2015). Recording the transition from flare-up to steady-state arc magmatism at the Purico–Chascon volcanic complex, northern Chile. *Earth Planet. Sci. Lett.* 422, 75–86. doi: 10.1016/j.epsl.2015.04.002.

Byrdina, S., Ramos, D., Vandemeulebrouck, J., Masias, P., Revil, A., Finizola, A., et al. (2013). Influence of the regional topography on the remote emplacement of hydrothermal systems with examples of Ticsani and Ubinas volcanoes, Southern Peru. *Earth Planet. Sci. Lett.* 365, 152–164. doi: 10.1016/j.epsl.2013.01.018.

Cabrera, M., and Thouret, J.-C. (2000). Volcanismo monogenético en el sur del Perú. *X Congr. Peru. Geol. Soc. Geológica del Perú, Lima* 186.

Calder, E. S., Sparks, R. S. J., and Gardeweg, M. C. (2000). Erosion, transport and segregation of pumice and lithic clasts in pyroclastic flows inferred from ignimbrite at Lascar Volcano, Chile. *J. Volcanol. Geotherm. Res.* 104, 201–235. doi: 10.1016/S0377-0273(00)00207-9.

Capaccioni, B., Aguilera, F., Tassi, F., Darrah, T., Poreda, R. J., and Vaselli, O. (2011). Geochemical and isotopic evidences of magmatic inputs in the hydrothermal reservoir feeding the fumarolic discharges of Tacora volcano (northern Chile). *J. Volcanol. Geotherm. Res.* 208, 77–85. doi: 10.1016/j.jvolgeores.2011.09.015.

Cascante, M., Polanco, E., Castruccio, A., and Clavero, J. (2012). Geología , geoquímica y petrografía del Volcán Isluga (19°09'S), Altiplano de la I Región , Chile : resultados preliminares. *XIII Congr. Geológico Chil. Antofagasta*, 612–614.

Casertano, L. (1963). GENERAL AND A CHARACTERISTICS OF ACTIVE ANDEAN VOLCANOES SUMMARY OF THEIR ACTIVITIES DURING RECENT CENTURIES. *Bull.*

Seismol. Soc. Am. 53, 1415–1433.

Centeno, R., Anccasi, R., and Macedo, O. (2013). Sismos distales de fractura observados en la zona de los Volcanes Misti y Chachani. 4.

Centeno, R., and Rivera, M. (2020). Reconocimiento automatico de señales sísmicas de origen volcánico para la alerta temprana de eurpciones volcánicas del sur del Perú. Available at: http://repositorio.igp.gob.pe/handle/IGP/4783.

Céspedes, L., Clavero, J., and Cayupi, J. (2004). Hazard management at Isluga volcano, northern Chile: preliminary results. International Association of Volcanology and Chemistry of the Earth's Interior (IAVCEI). *Gen. Assem. 6, Symp. 05, Poster 5a, No. 107. Pucón, Chile.*

Cesta, J. M., and Ward, D. J. (2016). Timing and nature of alluvial fan development along the Chajnantor Plateau, northern Chile. *Geomorphology* 273, 412–427. doi: 10.1016/j.geomorph.2016.09.003.

Charbonnier, S. J., Thouret, J.-C., Gueugneau, V., and Constantinescu, R. (2020). New Insights Into the 2070calyrBP Pyroclastic Currents at El Misti Volcano (Peru) From Field Investigations, Satellite Imagery and Probabilistic Modeling. *Front. Earth Sci.* 8, 1–20. doi: 10.3389/feart.2020.557788.

Chávez Chávez, J. (1992). La erupción del volcán Misti. Pasado, Presente, Futuro. *Imprenta Zenit, Arequipa*, 158.

Chiodi, A., Tassi, F., Báez, W., Filipovich, R., Bustos, E., Glok Galli, M., et al. (2019). Preliminary conceptual model of the Cerro Blanco caldera-hosted geothermal system (Southern Puna, Argentina): Inferences from geochemical investigations. *J. South Am. Earth Sci.* 94, 102213. doi: 10.1016/j.jsames.2019.102213.

Clavero, J. (2007). Peligros Volcánicos Complejo Volcánico Tarapacá. *Serv. Nac. Geol. y Minería, Cart. Geológica Chile, Ser. Geol. Ambient. 10.*

Clavero, J., Droguett, B., Quiroga, R., and Alvarez, P. (2018). Carta Lago Chungará, Región de Arica y Parinacota. Escala 1:100.000. *Serv. Nac. Geol. y Minería, Cart. Geológica Chile, Ser. Geol. Básica n.194*, 96.

Clavero, J. E., and Sparks, R. S. J. (2005). Geología del Complejo Volcánico Taapaca, Región de Tarapacá. *Serv. Nac. Geol. y Minería, Cart. Geológica Chile, Ser. Geol. Básica* 93, 23.

Clavero, J. E., Sparks, R. S. J., and Polanco, E. (2012). Geología del Volcán Parinacota, Región de Arica y Parinacota, escala 1:50.000. *Serv. Nac. Geol. y Minería, Cart. Geológica Chile, Ser. Geol. Básica 132*, 31.

Clavero, J., Polanco, E., Godoy, E., Aguilar, G., Sparks, R. S. J., van Wyk de Vries, B., et al. (2004a). Substrata infuence in the transport and emplacement mechanism of the Ollague debris avalanche (Northern Chile). *Acta Vulcanol.* 16, 59–76.

Clavero, J., Soler, V., and Amigo, A. (2006). Caracterización preliminar de la actividad sísmica y de desgasificación pasiva de volcanes activos de los Andes Centrales del Norte de Chile. *XI Congr. Geológico Chil. Antofagasta, II Reg. Chile* 2, 443–446.

Clavero, J., Sparks, R., Huppert, H., and Dade, W. (2002). Geological constraints on the emplacement mechanism of the Parinacota debris avalanche, northern Chile. *Bull. Volcanol.* 64, 40–54. doi: 10.1007/s00445-001-0183-0.

Clavero, J., Sparks, R. S. J., Pringle, M. S., Polanco, E., and Gardeweg, M. C. (2004b). Evolution and volcanic hazards of Taapaca Volcanic Complex, Central Andes of Northern Chile, escala 1:50.000. *J. Geol. Soc. London.* 161, 603–618. doi: 10.1144/0016-764902-065.

Clavero, J., Sparks, S., Polanco, E., and Pringle, M. (2004c). Evolution of Parinacota volcano, Central Andes, Northern Chile. *Rev. geológica Chile* 31, 317–347. doi: 10.4067/S0716-02082004000200009.

Cobeñas, G., Thouret, J.-C., Bonadonna, C., and Boivin, P. (2012). The c.2030yr BP Plinian eruption of El Misti volcano, Peru: Eruption dynamics and hazard implications. *J. Volcanol. Geotherm. Res.* 241–242, 105–120. doi: 10.1016/j.jvolgeores.2012.06.006.

Coira, B., and Kay, S. M. (1993). Implications of Quaternary volcanism at Cerro Tuzgle for crustal and mantle evolution of the Puna Plateau, Central Andes, Argentina. *Contrib. to Mineral. Petrol.* 113, 40–58. doi: 10.1007/BF00320830.

Coira, B., and Rosas, S. (2008). El Tuzgle. Algo más que un volcán. Sitios de Interés Geológico de la República Argentina. *Inst. Geol. y Recur. Miner. Serv. Geológico Min. Argentino, An.* 46, 446.

Comeau, M. J. (2015). Electrical Resistivity Structure of the Altiplano-Puna Magma Body and Volcan Uturuncu from Magnetotelluric Data. *A thesis Submitt. Partial fulfillment Requir.*

degree Dr. Philos. Physics. Dep. Physics, Univ. Alberta, 337.

Comeau, M. J., Unsworth, M. J., Ticona, F., and Sunagua, M. (2015). Magnetotelluric images of magma distribution beneath Volcán Uturuncu, Bolivia: Implications for magma dynamics. *Geology* 43, 243–246. doi: 10.1130/G36258.1.

Conde, A., Seggiaro, R. E., Apaza, F. D., Castro, S. E., Marquetti, C., Masa, S., et al. (2020). Modelo Conceptual Geotérmico preliminar del Volcán Socompa, Departamento de los Andes, Provincia de Salta. Argentina. *Inst. Geol. y Recur. Miner. Serv. GeológicoMinero Argentino. Ser. Contrib. Técnicas Geoterm. N° 2, Buenos Aires*, 92.

Contreras, Á. (2013). Caracterización de la mineralogía de alteración hidrotermal en superficie del Volcán Tacora y sus alrededores, Región de Arica y Parinacota. *Mem. para optar al título geólogo*, 98.

Coppola, D., Macedo, O., Ramos, D., Finizola, A., Delle Donne, D., del Carpio, J., et al. (2015). Magma extrusion during the Ubinas 2013–2014 eruptive crisis based on satellite thermal imaging (MIROVA) and ground-based monitoring. *J. Volcanol. Geotherm. Res.* 302, 199–210. doi: 10.1016/j.jvolgeores.2015.07.005.

Costa, F., Scaillet, B., and Gourgaud, A. (2003). Massive atmospheric sulfur loading of the AD 1600 Huaynaputina eruption and implications for petrologic sulfur estimates. *Geophys. Res. Lett.* 30, 1–4. doi: 10.1029/2002GL016402.

Cotrina, G., Olarte, Y., Peña, F., Vargas, V., Sánchez, M., and Pari, W. (2009). Hidrogeología de la cuenca del Río Locumba. *INGEMMET, Ser. H. Hidrogeol. N° 2*, 117.

Cruz, J. (2020). Análisis de la actividad sísmica en el volcán Ticsani y su variación temporal, periodo 1999-2019. *Inf. vulcanológico IGP/CENVUL-TIC/IV 2020-0001*, 72.

Cruz, J., Macedo, O., Del Carpio, J. A., Ali, L., Alvarado, W., Centeno, R., et al. (2018). Estado Actual de la Actividad del Volán Ticsani. Resultados del monitoreo y vigilancia 2014 - 2018. *Serv. Vulcanológico Nac. Inf. Espec. N ° 01 – 2018*, 55.

Cruz, V., Flores, R., and Velarde, Y. (2020). Caracterización y evaluación del potencial geotérmico de la zona geotermal Casiri- Kallapuma, Región Tacna. *NGEMMET, Boletín Ser. B Geol. Económica N° 69*, 250.

Cruz, V., Gonzales, K., Macedo, O., and Fournier, N. (2009). Caracterización Geoquímica de las

Fuentes Termales y Frías asociadas al Volcán Ubinas en el Sur del Perú. *Bol. Soc. Geol. Perú SGP* 103, 265–281.

Cruz, V., Pajuelo, D., and Yupa, G. (2019). Caracterización de los sistemas Geotermales asociados a los volcanes activos Ubinas y Huaynaputina, región Moquegua. Lima.

Cruz, V., Vargas, V., and Matsuda, K. (2010). Geochemical Characterization of Thermal Waters in the Calientes Geothermal Field, Tacna, South of Peru. *Proc. World Geotherm. Congr. 2010*, 7.

Cueva, K. (2016). Estudio geológico, petrográfico y geoquímico del Volcán Sara Sara (Ayacucho).

Cueva, K., Mariño, J., Thouret, J., Japura, S., and Macedo, L. (2018a). Pueblos enterrados por la erupción de 1600 d . C . del volcán Huaynaputina : geología del sector de Calicanto y Chimpapampa. *Foro Int. Los volcanes y su impacto*, 96–100.

Cueva, K., Rivera, M., Samaniego, P., Pennec, J. Le, and Lourzu, C. (2018b). Preliminary study into geology, petrography and geochemistry of the Sara Sara volcano (Ayacucho) in south Peru.

Davidson, J., McMillan, N., Moorbath, S., Wörner, G., Harmon, R., and Lopez-Escobar, L. (1990). The Nevados de Payachata volcanic region (18°S/69°W, N. Chile) II. Evidence for widespread crustal involvement in Andean magmatism. *Contrib. to Mineral. Petrol.* 105, 412–432. doi: 10.1007/BF00286829.

De la Cruz, N., and De la Cruz, O. (2001). Memoria explicativa de la revisión geológica cuadrángulo de Tarata. *INGEMMET, Boletín N°36*, 20.

De Silva, S., Davidson, J. P., Croudace, I. W., and Escobar, A. (1993). Volcanological and petrological evolution of Volcan Tata Sabaya, SW Bolivia. *J. Volcanol. Geotherm. Res.* 55, 305–335. doi: 10.1016/0377-0273(93)90043-Q.

De Silva, S., and Francis, P. (1990). Potentially active volcanoes of Peru - Observations using Landsat Thematic Mapper and Space Shuttle imagery. *Bull. Volcanol.* 52, 286–301.

De Silva, S., and Francis, P. (1991). *Volcanoes of the Central Andes*. Berlin: Springer Verlag, Berlín, 216 p.

de Silva, S. L. (1989). Geochronology and stratigraphy of the ignimbrites from the 21°30′S to 23°30′S portion of the Central Andes of northern Chile. *J. Volcanol. Geotherm. Res.* 37, 93–131. doi: 10.1016/0377-0273(89)90065-6.

de Silva, S. L., Roberge, J., Bardelli, L., Báez, W., Ortiz, A., Viramonte, J. G., et al. (2022). Magmatic evolution and architecture of an arc-related, rhyolitic caldera complex: The late Pleistocene to Holocene Cerro Blanco volcanic complex, southern Puna, Argentina. *Geosphere* 18, 394–423. doi: 10.1130/GES02294.1.

De Silva, S. L., and Zielinski, G. A. (1998). Global influence of the AD1600 eruptionofHuaynaputina,Peru. *Nature* 393, 455–458.

de Zeeuw-van Dalfsen, E., Richter, N., González, G., and Walter, T. R. (2017). Geomorphology and structural development of the nested summit crater of Láscar Volcano studied with Terrestrial Laser Scanner data and analogue modelling. *J. Volcanol. Geotherm. Res.* 329, 1–12. doi: 10.1016/j.jvolgeores.2016.09.018.

Degg, M., and Chester, D. (2005). Seismic and volcanic hazards in Peru: changing attitudes to disaster mitigation. *Geogr. J.* 171, 125–145. doi: 10.1111/j.1475-4959.2005.00155.x.

Del Carpio, J. A., and Tavera, H. (2019). Evaluacion Del Proceso Eruptivo del Volcán Ubinas de Julio 2019. *IInstituto Geofísico del Perú*, 49.

Del Carpio, J. A., and Torres, J. L. (2020). La actividad sísmica en el volcán Ubinas y su variación temporal (1998-2019) para la identificación de patrones de sismicidad a ser considerados en la gestión del riesgo de desastres. 71.

Delacour, A., Gerbe, M.-C., Thouret, J.-C., Wörner, G., and Paquereau-Lebti, P. (2007). Magma evolution of Quaternary minor volcanic centres in southern Peru, Central Andes. *Bull. Volcanol.* 69, 581–608. doi: 10.1007/s00445-006-0096-z.

Delacour, A., Paquereau, P., Gerbe, M.-C., Thouret, J., and Wörner, G. (2002). Quaternary Minor Volcanic Centres in Southern Peru : Volcanology, Petrology, and Geochemistry. 175–178.

Delaite, G., Thouret, J. C., Sheridan, M., Labazuy, P., Stinton, A., Souriot, T., et al. (2005). Assessment of volcanic hazards of El Misti and in the city of Arequipa, Peru, based on GIS and simulations, with emphasis on lahars. *Zeitschrift fur Geomorphol. Suppl.* 140, 209–231.

Delunel, R., Blard, P.-H., Martin, L. C. P., Nomade, S., and Schlunegger, F. (2016). Long term low latitude and high elevation cosmogenic 3He production rate inferred from a 107 ka-old lava flow in northern Chile; 22°S-3400 m a.s.l. *Geochim. Cosmochim. Acta* 184, 71–87. doi: 10.1016/j.gca.2016.04.023.

Deruelle, B. (1978). Calc-alkaline and shoshonitic lavas from five Andean volcanoes (between latitudes 21° 45′ and 24° 30′ S) and the distribution of the Plio-Quaternary volcanism of the south-central and southern Andes. *J. Volcanol. Geotherm. Res.* 3, 281–298. doi: 10.1016/0031-9201(76)90082-0.

Deruelle, B., and Brousse, R. (1984). "Nuee ardente" deposits at Tata Sabaya volcano (Bolivian-Chilean Andes): pumices and lava blocks crystallization from single magma at different depths. *Nuee ardente Depos. Tata Sabaya volcano (Bolivian-Chilean Andes) pumices lava blocks Cryst. from single magma Differ. depths*, 3–15. doi: 10.5027/andgeoV11n2-a01.

Di Filippo, M., Di Nezza, M., Colombi, A., Viramonte, J., and Toro, B. (2008). Estructura gravimetrica preliminar del Complejo volcanico Cerro Blanco, Puna Austral, Argentina. *XVII Congr. Geològico Argentino, San Salvador Jujuy*.

Díaz, D., Heise, W., and Zamudio, F. (2015). Three-dimensional resistivity image of the magmatic system beneath Lastarria volcano and evidence for magmatic intrusion in the back arc (northern Chile). *Geophys. Res. Lett.* 42, 5212–5218. doi: 10.1002/2015GL064426.

Dietterich, H., and de Silva, S. (2010). Sulfur yield of the 1600 eruption of Huaynaputina, Peru: Contributions from magmatic, fluid-phase, and hydrothermal sulfur. *J. Volcanol. Geotherm. Res.* 197, 303–312. doi: 10.1016/j.jvolgeores.2010.01.003.

Domingues, A. B., Scorzelli, R. B., and Mattievich, E. (1988). Mössbauer studies in volcanic material of the peruvian volcano Quimsachata. *Hyperfine Interact.* 41, 763–766. doi: 10.1007/BF02400502.

Douglas, J. (1914). Geological Sections through the Andes of Peru and Bolivia: I—From the Coast at Arica in the North of Chile to La Paz and the Bolivian 'Yungas'. *Q. J. Geol. Soc.* LXX, 63.

Dow, R. J., and Hitzman, M. W. (2002). Geology of the Arizaro and Lindero prospects, Salta Province, northwest Argentina: Mid-Miocene hydrothermal Fe-Ox copper-gold mineralization. *Hydrothermal iron oxide copper-gold Relat. Depos. a Glob. Perspect.* 2, 153–161.

Eash, N. S., and Sandor, J. A. (1995). Soil chronosequence and geomorphology in a semi-arid valley in the Andes of southern Peru. *Geoderma* 65, 59–79. doi: 10.1016/0016-7061(94)00025-6.

Elissondo, M., Farías, C., and Collini, E. (2016). Evaluacion del riesgo volcanico relativo en argentina. *Cities Volcanoes 9, Puerto Varas, Chile.*, Poster.

Entenmann, J. (1994). Magmatic evolution of the Nevados de Payachata complex and the petrogenesis of basaltic andesites in the Central Volcanic Zone of northern Chile. *Dr. Diss. Johannes Gutenberg-Universität Mainz*, 177.

Esquivel, A. (2018). Evaluación de los Peligros asociados a la actividad de los Volcanes Isluga y Láscar, Norte de Chile. *Mem. para optar al Título Geólogo. Undergrad. Thesis, Univ. Católica del Norte, Chile.*, 135.

Farrell, A. K., McNutt, S. R., and Thompson, G. (2017). Seismic attenuation, time delays, and raypath bending of teleseisms beneath Uturuncu volcano, Bolivia. *Geosphere* 13, 699–722. doi: 10.1130/GES01354.1.

Feeley, T. C., and Davidson, J. P. (1994). Petrology of Calc-Alkaline Lavas at Volc n Ollag e and the Origin of Compositional Diversity at Central Andean Stratovolcanoes. *J. Petrol.* 35, 1295–1340. doi: 10.1093/petrology/35.5.1295.

Feeley, T. C., Davidson, J. P., and Armendia, A. (1993). The volcanic and magmatic evolution of Volcán Ollagüe, a high-K, late quaternary stratovolcano in the Andean Central Volcanic Zone. *J. Volcanol. Geotherm. Res.* 54, 221–245. doi: 10.1016/0377-0273(93)90065-Y.

Fei, J., Zhang, D. D., and Lee, H. F. (2016). 1600 AD Huaynaputina Eruption (Peru), Abrupt Cooling, and Epidemics in China and Korea. *Adv. Meteorol.* 2016, 1–12. doi: 10.1155/2016/3217038.

Fei, J., and Zhou, J. (2009). The possible climatic impact in North China of the AD 1600 Huaynaputina eruption, Peru. *Int. J. Climatol.* 29, 927–933. doi: 10.1002/joc.1776.

Fernandez-Turiel, J. L., Perez–Torrado, F. J., Rodriguez-Gonzalez, A., Saavedra, J., Carracedo, J. C., Rejas, M., et al. (2019). La gran erupción de hace 4.2 ka cal en Cerro Blanco, Zona Volcánica Central, Andes: nuevos datos sobre los depósitos eruptivos holocenos en la Puna sur y regiones adyacentes. *Estud. Geológicos* 75, 088. doi: 10.3989/egeol.43438.515.

Fernandez-Turiel, J. L., Ratto, N., Perez-Torrado, F. J., Rodriguez-Gonzalez, A., Rejas, M., and Lobo, A. (2016). A large eruption convulsed in prehistoric times an extensive area of Catamarca, Southern Central Andes, NW Argentina. *Geophys. Res. Abstr.* 18, 1.

Fernandez, A. C., Hormann, P. K., Kussmaul, S., Meave, J., Pichler, H., and Subieta, T. (1973). First petrologic data on young volcanic rocks of SW-Bolivia. *TMPM Tschermaks Mineral. und Petrogr. Mitteilungen* 19, 149–172. doi: 10.1007/BF01167425.

Fialko, Y., and Pearse, J. (2012). Sombrero Uplift Above the Altiplano-Puna Magma Body: Evidence of a Ballooning Mid-Crustal Diapir. *Science (80-.).* 338, 250–252. doi: 10.1126/science.1226358.

Fídel, L., and Huamaní, A. (2001). Mapa preliminar de amenaza volcánica potencial del Volcán Yucamane. *INGEMMET, Boletín N° 26 Ser. C Geodinámica e Ing. Geológica*, 165.

Fídel, L., Morche, W., and Núñez, S. (1997a). Inventario de volcanes del Peru.

Fídel, L., Morche, W., and Núñez, S. (1997b). Riesgo Volcánico en el Sur del Perú. *INGEMMET, Boletín N° 16 Ser. C Geodinámica e 1 ngeniería Geológica*, 106.

Fidel, L., and Zavala, B. (2001). Mapa preliminar de amenaza volcánica potencial del Volcán Tutupaca. *INGEMMET, Boletín N° 24 Ser. C Geodinámica e Ing. Geológica*, 124.

Fiedrich, A. M., Heinrich, C. A., and Bachmann, O. (2020). Evolution from magmatic to hydrothermal activity beneath the Cerro Escorial volcano (NW Argentina) as sampled by erupted quartz and brines. *Lithos* 374–375, 105706. doi: 10.1016/j.lithos.2020.105706.

Figueroa, J., and Figueroa, O. (2006). Petrografía y geoquímica de las lavas del volcán Sairecabur, Andes Centrales, Chile. *XI Congr. Geológico Chil. Antofagasta, II Región, Chile* 2, 459–462.

Figueroa, O., Déruelle, B., and Demaiffe, D. (2009). Genesis of adakite-like lavas of Licancabur volcano (Chile—Bolivia, Central Andes). *Comptes Rendus Geosci.* 341, 310–318. doi: 10.1016/j.crte.2008.11.008.

Finizola, A., Lénat, J.-F., Macedo, O., Ramos, D., Thouret, J.-C., and Sortino, F. (2004). Fluid circulation and structural discontinuities inside Misti volcano (Peru) inferred from self-potential measurements. *J. Volcanol. Geotherm. Res.* 135, 343–360. doi: 10.1016/j.jvolgeores.2004.03.009.

Flores, B., García, A., and Ulloa, C. (2018). Evolución espacial y temporal de glaciares descubiertos en la Región de Atacama, Chile. *XV Congr. Geológico Chil. Concepción, Chile*, 5. doi: 10.13140/RG.2.2.26769.38249.

Forget, M.-E., Thouret, J.-C., Kuentz, A., and Fontugne, M. (2008). Héritages glaciaires, périglaciaires et évolution récente : le cas du Nevado Coropuna (Andes centrales, sud du Pérou). *Géomorphologie Reli. Process. Environ.* 14, 113–132. doi: 10.4000/geomorphologie.6383.

Fournier, T. J., Pritchard, M. E., and Riddick, S. N. (2010). Duration, magnitude, and frequency of subaerial volcano deformation events: New results from Latin America using InSAR and a global synthesis. *Geochemistry, Geophys. Geosystems* 11, n/a-n/a. doi: 10.1029/2009GC002558.

Francis, P., and Self, S. (1987). Collapsing Volcanoes. *Sci. Am.* 256, 90–99. Available at: https://www.jstor.org/stable/10.2307/24979404.

Francis, P. W., Gardeweg, M., Ramirez, C. F., and Rothery, D. A. (1985). Catastrophic debris avalanche deposit of Socompa volcano, northern Chile. *Geology* 13, 5. doi: 10.1130/0091-7613(1985)13<600:CDADOS>2.0.CO;2.

Francis, P. W., Hammill, M., Kretzschmar, G., and Thorpe, R. S. (1978). The Cerro Galan Caldera, North-west Argentina and its tectonic setting. *Nature* 274, 749–751. doi: 10.1038/274749a0.

Francis, P. W., McDonough, W. F., Hammill, M., O'Callaghan, L. J., and Thorpe, R. S. (1984). "The Cerro Purico Shield Complex, North Chile," in *Andean Magmatism* (Boston, MA: Birkhäuser Boston), 106–123. doi: 10.1007/978-1-4684-7335-3_8.

Francis, P. W., Roobol, M. J., Walker, G. P. L., Cobbold, P. R., and Coward, M. (1974). The San Pedro and San Pablo volcanoes of northern Chile and their hot avalanche deposits. *Geol. Rundschau* 63, 357–388. doi: 10.1007/BF01820994.

Francis, P. W., and Rundle, C. C. (1976). Rates of production of the main magma types in the central Andes. *Geol. Soc. Am. Bull.* 87, 474. doi: 10.1130/0016-7606(1976)87<474:ROPOTM>2.0.CO;2.

Francis, P., and Wells, G. (1988). Landsat Thematic Mapper observations of debris avalanche deposits in the Central Andes. *Bull. Volcanol.* 50, 258–278.

Frangipane, M. (1976). Studio geochimico-petrográfico del Nevado de Coropuna (Peru meridionale). *Ph.D. Thesis no.5790 ETH, Univ. Zurich*. doi: https://doi.org/10.3929/ethz-a-000116555 Rights.

Froger, J.-L., Remy, D., Bonvalot, S., and Legrand, D. (2007). Two scales of inflation at Lastarria-Cordon del Azufre volcanic complex, central Andes, revealed from ASAR-ENVISAT interferometric data. *Earth Planet. Sci. Lett.* 255, 148–163. doi: 10.1016/j.epsl.2006.12.012.

Gaete, A., Cesca, S., Franco, L., San Martin, J., Cartes, C., and Walter, T. R. (2019). Seismic activity during the 2013–2015 intereruptive phase at Lascar volcano, Chile. *Geophys. J. Int.* 219, 449–463. doi: 10.1093/gji/ggz297.

Gałaś, A. (2011). The extent and volcanic structures of the quaternary andahua group, andes, southern Peru. *Ann. Soc. Geol. Pol.* 81, 1–19.

Gałaś, A., Panajew, P., and Cuber, P. (2014). Stratovolcanoes in the Western Cordillera – Polish Scientifi c Expedition to Peru 2003–2012 reconnaissance research. *Geotourism/Geoturystyka* 37, 61. doi: 10.7494/geotour.2014.37.61.

García, A., Ulloa, C., Amigo, G., Milana, J. P., and Medina, C. (2017). An inventory of cryospheric landforms in the arid diagonal of South America (high Central Andes, Atacama region, Chile). *Quat. Int.* 438, 4–19. doi: 10.1016/j.quaint.2017.04.033.

García, F., Chorowicz, J., and Legros, F. (1997). La caldera Chachani , gran centro explosivo Plioceno-Holoceno del Sur del Peru: Identification y evolution en imagenes Landsat y radar ERS. *IX Congr. Peru. Geol. Resúmenes Extendidos.*, 449–454.

Garcia, M. (2001). Evolution oligo-miocène de l' Altiplano occidental (arc et avant arc du nord du Chili , Arica) : tectonique , volcanisme , sédimentation , géomorphologie et bilan érosion-sédimentation . To cite this version : HAL Id : tel-00546057. *Géologie appliquée. Univ. Joseph-Fourier - Grenoble I.*

García, M., Clavero, J., and Gardeweg, M. (2012). Cartas Visviri y Villa Industrial, Región de Arica y Parinacota. *Cart. Geológica Chile. Ser. Geol. Básica Escala 1100.000.*

García, M., Gardeweg, M., Clavero, J., and Hérail, G. (2004). Hoja Arica, Región de Tarapacá. *Serv. Nac. Geol. y Minería. Cart. Geológica Chile, Ser. Geol. Básica.*

Garcia, M., Hérail, G., and Charrier, R. (1999). Age and structure of the Oxaya anticline: a major feature of the Miocene compressive structures of northernmost Chile. *Proc. Int. Symp. Andean Geodyn.*, 249–252.

Garcia, S., and Badi, G. (2021). Towards the development of the first permanent volcano observatory in Argentina. *Volcanica* 4, 21–48. doi: 10.30909/vol.04.S1.2148.

García, S., Sruoga, P., and Elissondo, M. (2018). Programa de Evaluación de Amenazas Volcánicas del SEGEMAR, Argentina. in *Foro Internacional: Los volcanes y su impacto*, 174–178.

Gardeweg, M., and Amigo, Á. (2015). Peligros del volcán Láscar, Región de Antofagasta, escala 1:50.000. *Serv. Nac. Geol. y Minería, Cart. Geológica Chile, Ser. Geol. Ambient.*

Gardeweg, M. C., Clavero, J., Mpodozis, C., Pérez de A., C., and Villanueuve, M. (2000). El Macizo Tres Cruces: un complejo volcanico longevo y potencialmente activo en la alta cordillera de Copiapo, Chile. *IX Congr. Geológico Chil. Puerto Varas, Chile* 2, 291–295.

Gardeweg, M. C., Mpodozis, C., Clavero, J., and Cuitiño, L. (1997). Mapa Geológico de la Hoja Nevado Ojos del Salado, versión preliminar, escala 1:100.000. *Serv. Nac. Geol. y Minería*.

Gardeweg, M. C., Sparks, R. S. J., and Matthews, S. J. (1998a). Evolution of Lascar volcano, northern Chile. *J. Geol. Soc. London.* 155, 89–104. doi: 10.1144/gsjgs.155.1.0089.

Gardeweg, M., Cornejo Peláez, P., and Davidson, J. (1984). Geología del volcán Llullaillaco, altiplano de Antofagasta, Chile (Andes Centrales). *Rev. geológica Chile An Int. J. andean Geol.*, 21–37.

Gardeweg, M., Matthews, S. J., Sparks, R. S. J., and R, J. C. (2011). Geología del volcán láscar, Región de Antofagasta. *Serv. Nac. Geol. y Minería, Cart. Geológica Chile, Ser. Geol. Básica, Santiago*, 40 p., 1 mapa escala 1:50.000.

Gardeweg, M., and Medina, E. (1994). La erupción subpliniana del 19–20 de Abril de 1993 del Volcán Láscar, N. De Chile. *Actas 7th Chil. Geol. Congr. Concepción*, 299–304.

Gardeweg, M., Mpodozis, C., and Clavero, J. (1998b). The Ojos del Salado complex: the highest active volcano of the world, Central Andes. *Proc. IAVCE, Abstr. Magmat. Divers. Volcanoes their roots*, 21.

Gerbe, M.-C., and Thouret, J.-C. (2004). Role of magma mixing in the petrogenesis of tephra erupted during the 1990–98 explosive activity of Nevado Sabancaya, southern Peru. *Bull. Volcanol.* 66, 541–561. doi: 10.1007/s00445-004-0340-3.

Giordano, G., Pinton, A., Cianfarra, P., Baez, W., Chiodi, A., Viramonte, J., et al. (2013). Structural control on geothermal circulation in the Cerro Tuzgle–Tocomar geothermal volcanic area (Puna plateau, Argentina). *J. Volcanol. Geotherm. Res.* 249, 77–94. doi: 10.1016/j.jvolgeores.2012.09.009.

Gliß, J., Stebel, K., Kylling, A., and Sudbø, A. (2018). Improved optical flow velocity analysis in SO₂ camera images of volcanic plumes –

implications for emission-rate retrievals investigated at Mt Etna, Italy and Guallatiri, Chile. *Atmos. Meas. Tech.* 11, 781–801. doi: 10.5194/amt-11-781-2018.

Godoy, B., Aguilera, F., and Medina, E. (2008). The Debris-Avalanche Deposit (DAD) of Aguilucho-Apacheta Volcanic Complex, Northern Chile. 2.

Godoy, B. G., Clavero, J., Rojas, C., and Godoy, E. (2012). Volcanic facies of the debris avalanche deposit of Tata Sabaya Volcano, Central Andes. *Andean Geol.* 39, 394–406. doi: 10.5027/andgeoV39n3-a03.

Godoy, B., Wörner, G., Kojima, S., Aguilera, F., Simon, K., and Hartmann, G. (2014). Low-pressure evolution of arc magmas in thickened crust: The San Pedro–Linzor volcanic chain, Central Andes, Northern Chile. *J. South Am. Earth Sci.* 52, 24–42. doi: 10.1016/j.jsames.2014.02.004.

Gonzales, K. (2009). Monitoreo INSAR de los volcanes Misti, Ubinas y Ticsani - 2009. 8.

Gonzales, K., Finizola, A., Lénat, J.-F., Macedo, O., Ramos, D., Thouret, J.-C., et al. (2014). Asymmetrical structure, hydrothermal system and edifice stability: The case of Ubinas volcano, Peru, revealed by geophysical surveys. *J. Volcanol. Geotherm. Res.* 276, 132–144. doi: 10.1016/j.jvolgeores.2014.02.020.

Gonzáles, K., Froger, J., Rivera, M., and Audin, L. (2006). Deformación co-sísmica producida por el sismo Mb=5.4 del 01 de Octubre de 2005 (Carumas-Moquegua), detectada por interferometría radar - InSAR. *XIII Congr. Peru. Geolgía. Resúmenes Extendidos Soc. Geológica del Perú*, 488–489.

González-Ferrán, O. (1995). *Volcanes de Chile*. Instituto Geográfico Militar.

González, C., Inostroza, M., Aguilera, F., González, R., Viramonte, J., and Menzies, A. (2015). Heat and mass flux measurements using Landsat images from the 2000–2004 period, Lascar volcano, northern Chile. *J. Volcanol. Geotherm. Res.* 301, 277–292. doi: 10.1016/j.jvolgeores.2015.05.009.

Gottsmann, J., Blundy, J., Henderson, S., Pritchard, M. E., and Sparks, R. S. J. (2017). Thermomechanical modeling of the Altiplano-Puna deformation anomaly: Multiparameter insights into magma mush reorganization. *Geosphere* 13, GES01420.1. doi: 10.1130/GES01420.1.

Grosse, P., Euillades, P. A., Euillades, L. D., and van Wyk de Vries, B. (2014). A global database of composite volcano morphometry. *Bull. Volcanol.* 76, 784. doi: 10.1007/s00445-013-0784-4.

Grosse, P., Guzmán, S., and Petrinovic, I. (2017). *Del Noroeste Argentino*.

Grosse, P., Ochi Ramacciotti, M. L., Escalante Fochi, F., Guzmán, S., Orihashi, Y., and Sumino, H. (2020). Geomorphology, morphometry, spatial distribution and ages of mafic monogenetic volcanoes of the Peinado and Incahuasi fields, southernmost Central Volcanic Zone of the Andes. *J. Volcanol. Geotherm. Res.* 401, 106966. doi: 10.1016/j.jvolgeores.2020.106966.

Grosse, P., Orihashi, Y., Guzmán, S. R., Sumino, H., and Nagao, K. (2018). Eruptive history of Incahuasi, Falso Azufre and El Cóndor Quaternary composite volcanoes, southern Central Andes. *Bull. Volcanol.* 80, 44. doi: 10.1007/s00445-018-1221-5.

Grunder, A. L., Klemetti, E. W., Feeley, T. C., and McKee, C. M. (2006). Eleven million years of arc volcanism at the Aucanquilcha Volcanic Cluster, northern Chilean Andes: implications for the life span and emplacement of plutons. *Trans. R. Soc. Edinb. Earth Sci.* 97, 415–436. doi: 10.1017/S0263593300001541.

Gspurning, J., Lazar, R., and Sulzer, W. (2006). Regional Climate and Snow/Glacier Distribution in Southern Upper Atacama (Ojos del Salado)-an integrated statistical, GIS and RS based approach. *8th Int. Symp. High Moutain Remote Sens. Cartogr.*, 59–70. Available at: http://www.kfunigraz.ac.at/geowww/hmrsc/pdfs/hmrsc8/8_lazar_gspurning_sulzer.pdf.

Guédron, S., Tolu, J., Brisset, E., Sabatier, P., Perrot, V., Bouchet, S., et al. (2019). Late Holocene volcanic and anthropogenic mercury deposition in the western Central Andes (Lake Chungará, Chile). *Sci. Total Environ.* 662, 903–914. doi: 10.1016/j.scitotenv.2019.01.294.

GVP (2013). Global Volcanism Program. *Volcanoes World, v. 4.9.2. Venzke, E (ed.). Smithson. Institution.* Available at: https://doi.org/10.5479/si.GVP.VOTW4-2013.

GVP (2017). Report on Sabancaya (Peru) (Crafford, A.E., and Venzke, E., eds.). *Glob. Volcanism Program. Bull. Glob. Volcanism Network, 425. Smithson. Institution.*

GVP (2023). Global Volcanism Program, 2023. Pleistocene Volcanoes of the World (v. 5.1.1; 17 Aug 2023). Distributed by Smithsonian Institution, compiled by Venzke, E. doi: https://doi.org/10.5479/si.GVP.VOTW5-2023.5.1.

Hantke, G. (1939). Resumen de la actividad volcánica (de abril a diciembre de 1938). *Rev. la Soc. Geológica Alem.* 91, 757–765. Available at:

https://www.schweizerbart.de/papers/zdgg/detail/91/69844/Ubersicht_uber_die_vulkanische_Tatigkeit_vom_April?l=EN.

Harmon, R. S., Barreiro, B. A., Moorbath, S., Huefs, J., Francis, P. W., Thorpe, R. S., et al. (1984). Regional O-, Sr-, and Pb-isotope relationships in late Cenozoic calc-alkaline lavas of the Andean Cordillera. *J. Geol. Soc. London.* 141, 803–822.

Haselton, K., Hilley, G., and Strecker, M. R. (2002). Average Pleistocene Climatic Patterns in the Southern Central Andes: Controls on Mountain Glaciation and Paleoclimate Implications. *J. Geol.* 110, 211–226. doi: 10.1086/338414.

Hawkesworth, C. J., Hammill, M., Gledhill, A. R., van Calsteren, P., and Rogers, G. (1982). Isotope and trace element evidence for late-stage intra-crustal melting in the High Andes. *Earth Planet. Sci. Lett.* 58, 240–254. doi: 10.1016/0012-821X(82)90197-2.

Henderson, S. T., Delgado, F., Elliott, J., Pritchard, M. E., and Lundgren, P. R. (2017). Decelerating uplift at Lazufre volcanic center, Central Andes, from A.D. 2010 to 2016, and implications for geodetic models. *Geosphere* 13, 1489–1505. doi: 10.1130/GES01441.1.

Henderson, S. T., and Pritchard, M. E. (2013). Decadal volcanic deformation in the Central Andes Volcanic Zone revealed by InSAR time series. *Geochemistry, Geophys. Geosystems* 14, 1358–1374. doi: 10.1002/ggge.20074.

Henderson, S. T., Pritchard, M. E., Jay, J. a, Welch, M., Mares, P. J., Mnich, M. E., et al. (2012). Searching for Activity in the Andean Central Volcanic Zone : Thermal Anomalies , Seismicity , and Deformation Over a Timespan of 1-20 years. in, 588–590.

Hickey, J., Gottsmann, J., and del Potro, R. (2013). The large-scale surface uplift in the Altiplano-Puna region of Bolivia: A parametric study of source characteristics and crustal rheology using finite element analysis. *Geochemistry, Geophys. Geosystems* 14, 540–555. doi: 10.1002/ggge.20057.

Holtkamp, S. G., Pritchard, M. E., and Lohman, R. B. (2011). Earthquake swarms in South America. *Geophys. J. Int.* 187, 128–146. doi: 10.1111/j.1365-246X.2011.05137.x.

Hora, J. M., Singer, B. S., and Worner, G. (2007). Volcano evolution and eruptive flux on the thick crust of the Andean Central Volcanic Zone: 40Ar/39Ar constraints from Volcan Parinacota, Chile. *Geol. Soc. Am. Bull.* 119, 343–362. doi: 10.1130/B25954.1.

Hörmann, P. K., Pichler, H., and Zeil, W. (1973). New Data on the Young Volcanism in the Puna of NW-Argentina. *Geol. Rundschau* 62, 397–418. doi: 10.1007/BF01840106.

Hudson, T. S., Kendall, J. M., Pritchard, M. E., Blundy, J. D., and Gottsmann, J. H. (2022). From slab to surface: Earthquake evidence for fluid migration at Uturuncu volcano, Bolivia. *Earth Planet. Sci. Lett.* 577, 117268. doi: 10.1016/j.epsl.2021.117268.

IGP/CENVUL (2021). Boletín IGP/CENVUL-SAB/BV 2021-0015, Volcán Sabancaya. 1.

IGP (2021). Instituto Geofísico del Perú. *Cent. vulcanológico Nac. Volcanes Monit. Perú*. Available at: https://www.igp.gob.pe/servicios/centro-vulcanologico-nacional/volcanes-monitoreados.

Ilanko, T., Pering, T., Wilkes, T., Apaza Choquehuayta, F., Kern, C., Díaz Moreno, A., et al. (2019). Degassing at Sabancaya volcano measured by UV cameras and the NOVAC network. *Volcanica* 2, 239–252. doi: 10.30909/vol.02.02.239252.

INGEMMET, and ELECTROPERÚ (1994). Estudio geovolcanológico e inventario sistemático de manifestaciones geotermales del lote Tutupaca: hidrogeología, hidrogeoquímica y áreas de interés. *Inf. inédito. Conv. INGEMMETELECTROPERU. Lima*, 325.

Inostroza, M., Aguilera, F., Menzies, A., Layana, S., González, C., Ureta, G., et al. (2020a). Deposition of metals and metalloids in the fumarolic fields of Guallatiri and Lastarria volcanoes, northern Chile. *J. Volcanol. Geotherm. Res.* 393, 106803. doi: 10.1016/j.jvolgeores.2020.106803.

Inostroza, M., Aguilera, F., and Tassi, F. (2018). Preliminary Assessment of the Origin and Evolution of Fluids Discharged From Guallatiri Volcano. 2–3. doi: 10.13140/RG.2.2.32990.89925.

Inostroza, M., Tassi, F., Aguilera, F., Sepúlveda, J. P., Capecchiacci, F., Venturi, S., et al. (2020b). Geochemistry of gas and water discharge from the magmatic-hydrothermal system of Guallatiri volcano, northern Chile. *Bull. Volcanol.* 82, 57. doi: 10.1007/s00445-020-01396-2.

Inostroza, M., Tassi, F., Sepúlveda, J., Capecchiacci, F., Rizzo, A. L., and Aguilera, F. (2020c). Geochemical survey of the Colpitas-Taapaca volcanic-hydrothermal system, northern Chile. *Ital. J. Geosci.* 139, 359–373. doi: 10.3301/IJG.2020.09.

Jaén, H. (1965). Geologia Del Cuadrangulo De Tarata (Hoja 35-v). *INGEMMET, Boletín N° 11*, 91.

Jay, J. A., Delgado, F. J., Torres, J. L., Pritchard, M. E., Macedo, O., and Aguilar, V. (2015).

Deformation and seismicity near Sabancaya volcano, southern Peru, from 2002 to 2015. *Geophys. Res. Lett.* 42, 2780–2788. doi: 10.1002/2015GL063589.

Jay, J. A., Pritchard, M. E., West, M. E., Christensen, D., Haney, M., Minaya, E., et al. (2012). Shallow seismicity, triggered seismicity, and ambient noise tomography at the long-dormant Uturuncu Volcano, Bolivia. *Bull. Volcanol.* 74, 817–837. doi: 10.1007/s00445-011-0568-7.

Jay, J. A., Welch, M., Pritchard, M. E., Mares, P. J., Mnich, M. E., Melkonian, A. K., et al. (2013). Volcanic hotspots of the central and southern Andes as seen from space by ASTER and MODVOLC between the years 2000 and 2010. *Geol. Soc. London, Spec. Publ.* 380, 161–185. doi: 10.1144/SP380.1.

Jorquera, C., Rodríguez, I., Lizette, B., and Flores, F. (2019). Peligros del Volcán Guallatiri. Región de Arica y Parinacota. Escala 1:50.000. *Serv. Nac. Geol. y Minería, Cart. Geológica Chile. Ser. Geol. Ambient. 35*, 48.

Juvigne, E., Thouret, J. C., Mariño, J., Moscol, M., Legeley-Padovani, A., Loutsch, I., et al. (2002). Late pleistocene and holocene tephro-stratigraphy and chronology in southern Peru. *Resumes etendus, Inst. Rech. pour le Dev. Univ. Paul Sabatier*, 7.

Juvigné, E., Thouret, J., Loutsch, I., Lamadon, S., Frechen, M., Fontugne, M., et al. (2008). Retombées volcaniques dans des tourbières et lacs autour du massif des Nevados Ampato et Sabancaya (Pérou méridional, Andes Centrales). *Quaternaire* 19, 157–173. doi: 10.4000/quaternaire.3362.

Kaneoka, I., and Guevara, C. (1984). K-Ar age determinations of late Tertiary and Quaternary Andean volcanic rocks, Southern Peru. *Geochem. J.* 18, 233–239. doi: 10.2343/geochemj.18.233.

Karátson, D., Telbisz, T., and Wörner, G. (2012). Erosion rates and erosion patterns of Neogene to Quaternary stratovolcanoes in the Western Cordillera of the Central Andes: An SRTM DEM based analysis. *Geomorphology* 139–140, 122–135. doi: 10.1016/j.geomorph.2011.10.010.

Katsui, Y., and González, O. (1968). Geología del área neovolcánica de los Nevados de Payachata. *Univ. Chile, Dep. Geol. Publicación No. 29*, 61.

Kay, S. M., Coira, B., and Mpodozis, C. (2008). "Field trip guide: Neogene evolution of the central Andean Puna plateau and southern Central Volcanic Zone," in *GSA Field Guide 13: Field Trip Guides to the Backbone of the Americas in the Southern and Central Andes: Ridge Collision,* *Shallow Subduction, and Plateau Uplift* (Geological Society of America), 117–181. doi: 10.1130/2008.0013(05).

Kay, S. M., Mpodozis, C., and Gardeweg, M. (2013). Magma sources and tectonic setting of Central Andean andesites (25.5–28°S) related to crustal thickening, forearc subduction erosion and delamination. *Geol. Soc. London, Spec. Publ.* 385, 303–334. doi: 10.1144/SP385.11.

Kelfoun, K., and Druitt, T. H. (2005). Numerical modeling of the emplacement of Socompa rock avalanche, Chile. *J. Geophys. Res.* 110, B12202. doi: 10.1029/2005JB003758.

Kelfoun, K., Druitt, T., van Wyk de Vries, B., and Guilbaud, M.-N. (2008). Topographic reflection of the Socompa debris avalanche, Chile. *Bull. Volcanol.* 70, 1169–1187. doi: 10.1007/s00445-008-0201-6.

Klemetti, E. W., and Grunder, A. L. (2008). Volcanic evolution of Volcán Aucanquilcha: a long-lived dacite volcano in the Central Andes of northern Chile. *Bull. Volcanol.* 70, 633–650. doi: 10.1007/s00445-007-0158-x.

Kohlbach, I., and Lohnert, E. (1999). Geological map of Taapaca Volcano and adjacent areas (North Chile), 1:25 000. *Thesis (Inédito), Univ. zu Gottingen, Ger.*

Koukharsky, M., and Etcheverria, M. (1997). Geología del volcán Aracar. Sur de los Andes Centrales -24o19’00"S, 67°49’20"0- Argentina. *VIII Congr. Geológico Chil. Univ. Católica del Norte, Dep. Ciencias Geológicas* II, 1324–13.

Kukarina, E., West, M., Keyson, L. H., Koulakov, I., Tsibizov, L., and Smirnov, S. (2017). Focused magmatism beneath Uturuncu volcano, Bolivia: Insights from seismic tomography and deformation modeling. *Geosphere* 13, 1855–1866. doi: 10.1130/GES01403.1.

Kussmaul, S., Hörmann, P. K., Ploskonka, E., and Subieta, T. (1977). Volcanism and structure of southwestern Bolivia. *J. Volcanol. Geotherm. Res.* 2, 73–111. doi: 10.1016/0377-0273(77)90016-6.

Lahsen, A., and Munizaga, F. (1983). Geología de los cuadrángulos Putana, Licancabur, Cerros de Guayaques y Ayquina: Hoja Calama. *Serv. Nac. Geol. y Minería-Universidad Chile, Santiago*, 95.

Lamadon, S. (1999). Fluctuations glaciaires et téphrostratigraphie dans les montagnes intertropicales : une revue et application dans les Andes du Sud du Pérou (massifs des Nevados Ampato et

Coropuna). *Mémoire DEA, Univ. Blaise-Pascal, Clermont-Ferrand*, 180.

Lamberti, M. C., Chiodi, A., Agusto, M., Filipovich, R., Massenzio, A., Báez, W., et al. (2021). Carbon dioxide diffuse degassing as a tool for computing the thermal energy release at Cerro Blanco Geothermal System, Southern Puna (NW Argentina). *J. South Am. Earth Sci.* 105, 102833. doi: 10.1016/j.jsames.2020.102833.

Lara, L. ., Orozco, G., Amigo, A., and Silva, C. (2011). Peligros Volcánicos de Chile. Servicio Nacional de Geología y Minería, Carta Geológica de Chile, Serie Geología Ambiental. 0–24, 1 mapa escala 1:2.000.000.

Lavallée, Y., de Silva, S. L., Salas, G., and Byrnes, J. M. (2006). Explosive volcanism (VEI 6) without caldera formation: insight from Huaynaputina volcano, southern Peru. *Bull. Volcanol.* 68, 333–348. doi: 10.1007/s00445-005-0010-0.

Lavallée, Y., de Silva, S. L., Salas, G., and Byrnes, J. M. (2009). Structural control on volcanism at the Ubinas, Huaynaputina, and Ticsani Volcanic Group (UHTVG), southern Peru. *J. Volcanol. Geotherm. Res.* 186, 253–264. doi: 10.1016/j.jvolgeores.2009.07.003.

Legros, F. (2001). Tephra stratigraphy of Misti volcano, Peru. *J. South Am. Earth Sci.* 14, 15–29. doi: 10.1016/S0895-9811(00)00062-6.

Lelli, M. (2018). Socompa geothermal prospect. Report on waters geochemistry. *Cons. Naz. delle Ric. Ist. Geosci. e Georisorse. Serv. Geológico Min. Argentino, Buenos Aires*, 25.

Liu, F., Elliott, J., Ebmeier, S., Craig, T., Hooper, A., Novoa, C., et al. (2022). Unrest Detected at Socompa Volcano, Northern Chile, from Geodetic Observations. *AGU Fall Meet. Abstr.*, G46A-02. Available at: https://agu.confex.com/agu/fm22/meetingapp.cgi/Paper/1165165.

Liu, F., Elliott, J. R., Ebmeier, S. K., Craig, T. J., Hooper, A., Novoa Lizama, C., et al. (2023). First Onset of Unrest Captured at Socompa: A Recent Geodetic Survey at Central Andean Volcanoes in Northern Chile. *Geophys. Res. Lett.* 50. doi: 10.1029/2022GL102480.

Macedo, O., Taipe, E., Del Carpio, J., Ticona, J., Ramos, D., Puma, N., et al. (2016). Evaluación del Riesgo Volcánico en el Sur del Perú, situación actual de la vigilancia actual y requerimientos de monitoreo en el futuro. Arequipa.

Machacca, R., Del Carpio Calienes, J. A., Rivera Porras, M. A., Tavera Huarache, H. J., Macedo Franco, L. D., Concha Calle, J. A., et al. (2021). Monitoring of active volcanoes in Peru by the

Instituto Geofísico del Perú. *Volcanica* 4, 49–71. doi: 10.30909/vol.04.S1.4971.

MacQueen, P., Delgado, F., Reath, K., Pritchard, M. E., Bagnardi, M., Milillo, P., et al. (2020). Volcano-Tectonic Interactions at Sabancaya Volcano, Peru: Eruptions, Magmatic Inflation, Moderate Earthquakes, and Fault Creep. *J. Geophys. Res. Solid Earth* 125. doi: 10.1029/2019JB019281.

MacQueen, P., Gottsmann, J., Pritchard, M. E., Young, N., Ticona J, F., Ticona, E. (Tico), et al. (2021). Dissecting a Zombie: Joint Analysis of Density and Resistivity Models Reveals Shallow Structure and Possible Sulfide Deposition at Uturuncu Volcano, Bolivia. *Front. Earth Sci.* 9, 1–20. doi: 10.3389/feart.2021.725917.

Maher, S., and Kendall, J.-M. (2018). Crustal anisotropy and state of stress at Uturuncu Volcano, Bolivia, from shear-wave splitting measurements and magnitude–frequency distributions in seismicity. *Earth Planet. Sci. Lett.* 495, 38–49. doi: 10.1016/j.epsl.2018.04.060.

Maisonnave, B., and Page, S. (1997). Geología de las efusiones basales del volcán Aracar, Puna Salteña, República Argentina. *VIII Congr. Geológico Chil. Univ. Católica del Norte, Dep. Ciencias Geológicas* II, 1359–1363.

Mamani, M., Worner, G., and Sempere, T. (2010). Geochemical variations in igneous rocks of the Central Andean orocline (13 S to 18 S): Tracing crustal thickening and magma generation through time and space. *Geol. Soc. Am. Bull.* 122, 162–182. doi: 10.1130/B26538.1.

Manrique, N. (2013). Evolución Vulcanológica y Magmática del Edificio reciente del Complejo Volcánico Tutupaca (Tacna). 112.

Manrique, N., Samaniego, P., Médard, E., Schiavi, F., Mariño, J., and Liorzou, C. (2020). Pre-eruptive magmatic processes associated with the historical (218 ± 14 aBP) explosive eruption of Tutupaca volcano (southern Peru). *Bull. Volcanol.* 82, 6. doi: 10.1007/s00445-019-1335-4.

Mariño, J., Rivera, M., Cacy, L., and Cruz, V. (2006). Evaluación de seguridad física de áreas aledañas al volcán ubinas. *Ingemmet*. Available at: https://hdl.handle.net/20.500.12544/2367.

Mariño, J., Rivera, M., Cacya, L., Thouret, J., Macedo, L., Salas, G., et al. (2008). Mapa de Peligros del Volcán Misti.

Mariño, J., Samaniego, P., Manrique, N., Valderrama, P., and Macedo, L. (2019). Geología y Mapa de Peligros del Complejo Volcánico Tutupaca. *INGEMMET, Boletín Ser. C Geodinámica e Ing.*

Geológica N° 66, 168.

Mariño, J., Samaniego, P., Manrique, N., Valderrama, P., Roche, O., van Wyk de Vries, B., et al. (2021). The Tutupaca volcanic complex (Southern Peru): Eruptive chronology and successive destabilization of a dacitic dome complex. *J. South Am. Earth Sci.* 109, 103227. doi: 10.1016/j.jsames.2021.103227.

Mariño, J., Samaniego, P., Rivera, M., Bellot, N., Manrique, N., Macedo, L., et al. (2012). Mapa de peligros del complejo volcánico ampato-sabancaya. 1–5.

Mariño, J., and Thouret, J. (2003). Geología, historia eruptiva y evaluación de peligros del volcán Ticsani (sur del Perú). *Boletín la Soc. Geológica del Perú*, 27.

Mariño, J., Valdivia, D., Soncco, Y., Miranda, R., and Machacca, R. (2017). Lahares emplazados en el Valle de Ubinas en Febrero del 2016: Geología, Impacto, Modelamiento y Evaluación de Peligros. *INGEMMET, Inf. Técnico N° A6745*, 21.

Mariño, J., and Zavala, B. (2010). Cartografiado Geológico del Valle de los Volcanes de Andahua-Orcopampa. *XV Congr. Peru. Geol. Resúmenes Extendidos.* 9, 858–861.

Marinovic, N., and Lahsen, A. (1984). Hoja Calama: Región de Antofagasta, escala 1:250.000. *Serv. Nac. Geol. y Minería, Cart. Geol. Chile*.

Marocco, R., and Garcia, F. (1974). ESTUDIO GEOLOGICO DE LA REGION ENTRE CUZCO Y MACHU PICCHU. *Bull. Inst. Fr. Et. And.* III, 1–27.

Martínez, W., and Cervantes, J. (2003). Memoria descriptiva de la revisión y actualización del cuadrángulo de Pausa (31-p) Escala 1:100 000.

Masiokas, M. H., Rivera, A., Espizua, L. E., Villalba, R., Delgado, S., and Aravena, J. C. (2009). Glacier fluctuations in extratropical South America during the past 1000years. *Palaeogeogr. Palaeoclimatol. Palaeoecol.* 281, 242–268. doi: 10.1016/j.palaeo.2009.08.006.

Matthews, S. J., Gardeweg, M. C., and Sparks, R. S. J. (1997). The 1984 to 1996 cyclic activity of Lascar Volcano, northern Chile: cycles of dome growth, dome subsidence, degassing and explosive eruptions. *Bull. Volcanol.* 59, 72–82. doi: 10.1007/s004450050176.

Matthews, S. J., Jones, A. P., and Gardeweg, M. C. (1994). Lascar Volcano, Northern Chile; Evidence for Steady-State Disequilibrium. *J. Petrol.* 35, 401–432. doi: 10.1093/petrology/35.2.401.

Matthews, S. J., Sparks, R. S. J., and Gardeweg, M. C. (1999). The Piedras Grandes-Soncor Eruptions, Lascar Volcano, Chile; Evolution of a Zoned Magma Chamber in the Central Andean Upper Crust. *J. Petrol.* 40, 1891–1919. doi: 10.1093/petroj/40.12.1891.

Mattioli, M., Renzulli, A., Menna, M., and Holm, P. M. (2006). Rapid ascent and contamination of magmas through the thick crust of the CVZ (Andes, Ollagüe region): Evidence from a nearly aphyric high-K andesite with skeletal olivines. *J. Volcanol. Geotherm. Res.* 158, 87–105. doi: 10.1016/j.jvolgeores.2006.04.019.

McFarlin, H., Christensen, D., McNutt, S. R., Ward, K. M., Ryan, J., Zandt, G., et al. (2018). Receiver function analyses of Uturuncu volcano, Bolivia and vicinity. *Geosphere* 14, 50–64. doi: 10.1130/GES01560.1.

Mendivil, S. (1965). Geología de los cuadrángulos de Maure y Antajave (Hojas 35-X, 35-y). *INGEMMET, Boletín N°10*, 96.

Michelfelder, G. S., Feeley, T. C., and Wilder, A. D. (2014). The Volcanic Evolution of Cerro Uturuncu: A High-K, Composite Volcano in the Back-Arc of the Central Andes of SW Bolivia. *Int. J. Geosci.* 05, 1263–1281. doi: 10.4236/ijg.2014.511105.

Mon, R. (1987). Structural geology of two geothermal areas in the andes: Copahue and Tuzgle (Argentina)Géologie structurale de deux zones géothermiques dans les andes: Copahue et Tuzgle (Argentine). *Bull. Int. Assoc. Eng. Geol.* 35, 79–85.

Monge, R., and Cervantes, J. (2000). Memoria explicativa de la geología del cuadrángulo de Pachia (36-v) y Palca (36-x). 11.

Montecinos, F. (1970). Geología del yacimiento de azufre del volcán Tacora, Departamento de Arica. *Inst. Investig. Geológicas, Santiago* 25, 41.

Montecinos, R. (2018). Registro paleoambiental para el Holoceno tardío en un testigo de bofedal del Altiplano de la región de Arica y Parinacota, Chile (18°S; 4300 m.s.n.m). *Undergadute Thesis, Univ. Austral, Chile*.

Montero López, M. C., Hongn, F., Brod, J. A., Seggiaro, R., Marrett, R., and Sudo, M. (2010). Magmatismo ácido del mioceno superiorcuaternario en el área de cerro blancola hoyada, Puna austral. *Rev. la Asoc. Geol. Argentina* 67, 329–348.

Morales Rivera, A. M., Amelung, F., and Mothes, P. (2016). Volcano deformation survey over the

Northern and Central Andes with ALOS InSAR time series. *Geochemistry, Geophys. Geosystems* 17, 2869–2883. doi: 10.1002/2016GC006393.

Morand, A., Brandeis, G., and Tait, S. (2021). Application of a plate model to reproduce surface deformations observed at Uturuncu volcano, Bolivia. *J. Volcanol. Geotherm. Res.* 415. doi: 10.1016/j.jvolgeores.2021.107241.

Morche, W., and De la Cruz, N. (1994). Geología y petrografía de los volcanes pleistocénicos Yucamane y Tutupaca (Tacna). *Congr. Peru. Geol. Resúmenes extendidos. Soc. Geológica del Perú, Lima* 8, 209–213.

Morche, W., and Núñez, S. (1998). Estudio del Riesgo Geológico del Volcán Sara Sara. *Boletín N°21, Ser. C Geodinámica e Ing. Geológica. Inst. Geológico Min. y Met.*, 65.

Moussallam, Y., Peters, N., Masias, P., Apaza, F., Barnie, T., Ian Schipper, C., et al. (2017a). Magmatic gas percolation through the old lava dome of El Misti volcano. *Bull. Volcanol.* 79, 46. doi: 10.1007/s00445-017-1129-5.

Moussallam, Y., Tamburello, G., Peters, N., Apaza, F., Schipper, C. I., Curtis, A., et al. (2017b). Volcanic gas emissions and degassing dynamics at Ubinas and Sabancaya volcanoes; implications for the volatile budget of the central volcanic zone. *J. Volcanol. Geotherm. Res.* 343, 181–191. doi: 10.1016/j.jvolgeores.2017.06.027.

Mpodozis, C., Kay, S. M., Gardeweg, M., Proceedings, B. C., Argentine, X., Mpodozis, C., et al. (1996). Geología de la región de Ojos del Salado (Andes Centrales, 27° S): implicancias de la migración hacia el este del frente volcánico Cenozoico Superior. *Actas XIII Congr. Geológico Argentino, Buenos Aires*, 539–548.

Muir, D. D., Barfod, D. N., Blundy, J. D., Rust, A. C., Sparks, R. S. J., and Clarke, K. M. (2015). The temporal record of magmatism at Cerro Uturuncu, Bolivian Altiplano. *Geol. Soc. London, Spec. Publ.* 422, 57–83. doi: 10.1144/SP422.1.

Muir, D. D., Blundy, J. D., Hutchinson, M. C., and Rust, A. C. (2014). Petrological imaging of an active pluton beneath Cerro Uturuncu, Bolivia. *Contrib. to Mineral. Petrol.* 167, 980. doi: 10.1007/s00410-014-0980-z.

Mulcahy, P., Chen, C., Kay, S. M., Brown, L. D., Alvarado, P. M., Sandvol, E. A., et al. (2010). The Southern Puna seismic experiment: shape of the subducting Nazca Plate, areas of concentrated mantle and crustal earthquakes, and crustal focal mechanisms. *Am. Geophys. Union, Fall Meet. 2010, Abstr. id. T11A-2050*, 1.

Muñoz, N., and Charrier, R. (1996). Uplift of the western border of the Altiplano on a west-vergent thrust system, Northern Chile. *J. South Am. Earth Sci.* 9, 171–181. doi: 10.1016/0895-9811(96)00004-1.

Muñoz, N., and Sepulveda, P. (1992). Estructuras compresivas con vergencia al oeste en el borde oriental de la Depresion Central, Norte de Chile (19°15'S). *Nota Geológica* 19, 241–247. doi: 10.5027/andgeoV19n2-a07.

Naranjo, J. (1988). Coladas de azufre de los volcanes Lastarria y Bayo en el Norte de Chile: Reología, Génesis e importancia en geología planetaria. *Rev. Geol. Chile* 15, 3–12.

Naranjo, J. A. (1985). Sulphur flows at Lastarria volcano in the North Chilean Andes. *Nature* 313, 778–780. doi: 10.1038/313778a0.

Naranjo, J. A. (1992). Chemistry and petrological evolution of the Lastarria volcanic complex in the north Chilean Andes. *Geol. Mag.* 129, 723–740. doi: 10.1017/S0016756800008451.

Naranjo, J. A. (2010). Geología del Complejo Volcánico Lastarria, Región de Antofagasta. *Serv. Nac. Geol. y Minería, Cart. Geológica Chile, Ser. Geol. Básica*, 33 p., 1 mapa escala 1:25.000. Santiago.

Naranjo, J., and Cornejo, P. (1992). Hoja Salar de la Isla-Carta Geologica de Chile, escala 1: 250.000. *Serv. Nac. Geol. y Minería, Santiago Chile*.

Navas, S. (2019). Evolución geológica del Complejo volcánico Olca-Paruma (20°56'S – 68°30'W), Norte de Chile. *Mem. para optar al Título Geólogo. Undergrad. Thesis, Univ. Católica del Norte, Chile.*, 119.

Norini, G., Cogliati, S., Baez, W., Arnosio, M., Bustos, E., Viramonte, J., et al. (2014). The geological and structural evolution of the Cerro Tuzgle Quaternary stratovolcano in the back-arc region of the Central Andes, Argentina. *J. Volcanol. Geotherm. Res.* 285, 214–228. doi: 10.1016/j.jvolgeores.2014.08.023.

Núñez, S., and Valenzuela, G. (2001). Mapa Preliminar de Amenaza Volcánica Potencial del Volcán-Nevado Coropuna. *INGEMMET, Boletín N°25, Ser. C Geodinámica e Ing. Geológica*, 123.

O'Callaghan, L. J., and Francis, P. W. (1986). Volcanological and petrological evolution of San Pedro volcano, Provincia EI Loa, North Chile. *J. Geol. Soc. London.* 143, 275–286. doi: 10.1144/gsjgs.143.2.0275.

Olchauski, E. (1980). Geología de los cuadrángulos de Jaqui, Coracora, Chala y Chaparra, Hojas 31-ñ, 31-o, 32-ñ, 32-o. 69.

Olchauski, E., and Dávila, D. (1994). Geología de los cuadrángulos de Chuquibamba y Cotahuasi. Hojas: 32-q y 31-q. *INGEMMET, Boletín N°50, Ser. A Cart. Geológica Nac.*, 64.

ONEMI Antofagasta (2019). Plan de emergencia específico por variable de riesgo volcánico Región Antofagasta 2019. *Dir. Reg. protección Civ. y Emerg. Región Antofagasta*, 56. Available at: http://repositoriodigitalonemi.cl/web/bitstream/handle/20 12/1850/P-PEEVR-PO-ARD-04_II_04.11.2019.pdf?sequence=18&isAllowed=y.

ONEMI Arica y Parinacota (2018). Dirección Regional de protección civil y emergencia Región Arica y Parinacota. Plan de emergencia específico por variable de riesgo volcánico Región Arica y Parinacota 2018. in, 74. Available at: http://repositoriodigitalonemi.cl/web/bitstream/handle/2012/1896/P-PEEVRPO-ARD-04_XV_06.03.2018_2.pdf?sequence=9.

ONEMI Tarapacá (2017). Plan de emergencia específico por variable de riesgo volcánico Región Tarapacá 2017. *Dir. Reg. protección Civ. y Emerg. Región Tarapacá.*, 65. Available at: http://repositoriodigitalonemi.cl/web/bitstream/handle/20 12/1847/P-PEEVR-PO-ARD-04_I_16.05.2018.pdf?sequence=15.

Orozco, G., and Bertín, D. (2013). Mapa preliminar de peligros volcánicos Complejo volcánico Olca-Paruma, escala 1:75.000. *Serv. Nac. Geol. y Minería, Cart. Geológica Chile, Ser. Geol. Ambient. Programa Riesgo Volcánico*.

Otárola, A., Radford, S., and Sakamoto, S. (2002). Physical Parameters of the Chajnantor Science Preserve. *Alma Memo # 413*, 12.

OVI (2021). Observatorio Vulcanológico del INGEMMET. *Inst. Geol. Min. y Metal.* Available at: http://ovi.ingemmet.gob.pe/?page_id=26.

Pacheco, J., and Sykes, L. (1992). Seismic moment catalog of large shallow earthquakes, 1900 to 1989. *Bull Seism. Soc Am* 82, 1306–1349.

Palacios, D., Andrés, N., Úbeda, J., and Alcalá, J. (2009). Permafrost and Periglacial Activity

Distribution and Geothermal Anomalies in the Chachani and El Misti Volcanoes (Southern Peru). *Geophys. Res. Abstr.*, 2.

Pallares, C., Fabre, D., Thouret, J.-C., Bacconnet, C., Charca-Chura, J. A., Martelli, K., et al. (2015). Geological and geotechnical characteristics of recent lahar deposits from El Misti volcano in the city area of Arequipa, South Peru. *Geotech. Geol. Eng.* 33, 641–660. doi: 10.1007/s10706-015-9848-x.

Paquereau-Lebti, P., Fornari, M., Roperch, P., Thouret, J.-C., and Macedo, O. (2008). Paleomagnetism, magnetic fabric, and 40Ar/39Ar dating of Pliocene and Quaternary ignimbrites in the Arequipa area, southern Peru. *Bull. Volcanol.* 70, 977–997. doi: 10.1007/s00445-007-0181-y.

Paquereau, P., Thouret, J.-C., Wörner, G., and Fornari, M. (2006). Neogene and Quaternary ignimbrites in the area of Arequipa, Southern Peru: Stratigraphical and petrological correlations. *J. Volcanol. Geotherm. Res.* 154, 251–275. doi: 10.1016/j.jvolgeores.2006.02.014.

Paquereau, P., Thouret, J.-C., Wörner, G., Fornari, M., Macedo, O., and Roperch, P. (2005). Caractérisation des ignimbrites néogènes du bassin d'Arequipa, Pérou. *Comptes Rendus Geosci.* 337, 477–486. doi: 10.1016/j.crte.2004.12.004.

Pavez, A., Remy, D., Bonvalot, S., Diament, M., Gabalda, G., Froger, J.-L., et al. (2006). Insight into ground deformations at Lascar volcano (Chile) from SAR interferometry, photogrammetry and GPS data: Implications on volcano dynamics and future space monitoring. *Remote Sens. Environ.* 100, 307–320. doi: 10.1016/j.rse.2005.10.013.

Pavez, C., Comte, D., Gutiérrez, F., and Gaytán, D. (2019). Analysis of the magmatic – Hydrothermal volcanic field of Tacora Volcano, northern Chile using travel time tomography. *J. South Am. Earth Sci.* 94, 102247. doi: 10.1016/j.jsames.2019.102247.

Pearse, J., and Lundgren, P. (2013). Source model of deformation at Lazufre volcanic center, central Andes, constrained by InSAR time series. *Geophys. Res. Lett.* 40, 1059–1064. doi: 10.1002/grl.50276.

Pecho, V. (1983). Geología de los cuadrángulos de Pausa y Caraveli. Hojas: 31-p y 32-p. *Inst. Geológico Min. y Met. Boletín N°37, Ser. A. Cart. Geológica Nac.*, 68.

Perucca, L. P., and Moreiras, S. M. (2009). "Seismic and Volcanic Hazards in Argentina," in

Developments in Earth Surface Processes, 267–300. doi: 10.1016/S0928-2025(08)10014-1.

Petit-Breuilh, M. E. (2004). La historia eruptiva de los volcanes hispanoamericanos (Siglos XVI al XX). *Serv. Publicaciones del Exmo. Cabil. Insul. Lanzarote-Casa los volcanes*, 431.

Pieri, D., and Abrams, M. (2004). ASTER watches the world's volcanoes: a new paradigm for volcanological observations from orbit. *J. Volcanol. Geotherm. Res.* 135, 13–28. doi: 10.1016/j.jvolgeores.2003.12.018.

Pizarro, M., Aguilera, F., Tassi, F., and Saltori, O. (2012). Gas geochemistry of fumaroles from Irruputuncu volcano , northern Chile. 2, 483–485.

Pritchard, M. E. (2003). Recent crustal deformation in west-central South America. *Dr. Diss. Calif. Inst. Technol.* 2003.

Pritchard, M. E., de Silva, S. L., Michelfelder, G., Zandt, G., McNutt, S. R., Gottsmann, J., et al. (2018). Synthesis: PLUTONS: Investigating the relationship between pluton growth and volcanism in the Central Andes. *Geosphere* 14, 954–982. doi: 10.1130/GES01578.1.

Pritchard, M. E., Henderson, S. T., Jay, J. A., Soler, V., Krzesni, D. A., Button, N. E., et al. (2014). Reconnaissance earthquake studies at nine volcanic areas of the central Andes with coincident satellite thermal and InSAR observations. *J. Volcanol. Geotherm. Res.* 280, 90–103. doi: 10.1016/j.jvolgeores.2014.05.004.

Pritchard, M. E., and Simons, M. (2002). A satellite geodetic survey of large-scale deformation of volcanic centres in the central Andes. *Nature* 418, 167–171. doi: 10.1038/nature00872.

Pritchard, M., and Simons, M. (2004). An InSAR-based survey of volcanic deformation in the central Andes. *Geochemistry, Geophys. Geosystems* 5, 1–42. doi: 10.1029/2003GC000610.

Prival, J.-M., Thouret, J.-C., Japura, S., Gurioli, L., Bonadonna, C., Mariño, J., et al. (2020). New insights into eruption source parameters of the 1600 CE Huaynaputina Plinian eruption, Peru. *Bull. Volcanol.* 82, 7. doi: 10.1007/s00445-019-1340-7.

Raco, B. (2018). Socompa Geothermal Prospect. Report on Fluid Geochemistry (Soil CO2 degassing). *Cons. Naz. delle Ric. Ist. Geosci. e Georisorse. Serv. Geológico Min. Argentino, Buenos Aires*, 20.

Ramírez, C. (1988). Evidencias de glaciación en el macizo de los volcanes Púlar y Pajonales, Región de Antofagasta. *Congr. Geológico Chil. Santiago.* 5, 15.

Ramírez, C. ., and Gardeweg, M. (1982). Geología de la Hoja Toconao, Región de Antofagasta, escala 1:250.000. *Inst. Investig. Geológicas, Cart. Geológica Chile* 54, 123.

Ramírez, C. F., Gardeweg P., M., Davidson M., J., and Pino, H. (1991). Mapa geológico del área de los volcanes Socompa y Púlar, Escala 1:100.000 Región de Atacama [monografías]. *Serv. Nac. Geol. y Minería, Santiago*, 1 mapa pleg byn (Documentos de Trabajo : n.04).

Ramos, D. (2019). Evaluación de la Actividad de los Volcanes Misti y Coropuna. *INGEMMET, Inf. Técnico N°A69*, 27.

REAV Parinacota (2020). Reporte Especial de Actividad Volcánica, Región de Arica y Parinacota, Volcán Parinacota. *Serv. Nac. Geol. y Minería*, 2.

Reyes-Hardy, M.-P., Aguilera Barraza, F., Sepúlveda Birke, J. P., Esquivel Cáceres, A., and Inostroza Pizarro, M. (2021). GIS-based volcanic hazards, vulnerability and risks assessment of the Guallatiri Volcano, Arica y Parinacota Region, Chile. *J. South Am. Earth Sci.* 109, 103262. doi: 10.1016/j.jsames.2021.103262.

Reyes, M. P. (2019). Modelamiento de los peligros y riesgos asociados al sistema volcánico Guallatiri, Región de Arica y Parinacota, Chile. *Undergrad. Thesis, Univ. Católica del Norte, Chile.*, 249.

Reyes, N., Vidal, A., Ramirez, E., Arnason, K., Richter, B., Steingrimsson, B., et al. (2011). Geothermal exploration at Irruputuncu and Olca volcanoes: Pursuing a sustainable mining development in Chile. *Trans. - Geotherm. Resour. Counc.* 35 2, 983–986.

Richards, J. P., and Villeneuve, M. (2001). The Llullaillaco volcano, northwest Argentina: construction by Pleistocene volcanism and destruction by sector collapse. *J. Volcanol. Geotherm. Res.* 105, 77–105. doi: 10.1016/S0377-0273(00)00245-6.

Richards, J. P., and Villeneuve, M. (2002). Characteristics of late Cenozoic volcanism along the Archibarca lineament from Cerro Llullaillaco to Corrida de Cori, northwest Argentina. *J. Volcanol. Geotherm. Res.* 116, 161–200. doi: 10.1016/S0377-0273(01)00329-8.

Richter, N., Salzer, J. T., de Zeeuw-van Dalfsen, E., Perissin, D., and Walter, T. R. (2018). Constraints on the geomorphological evolution of the nested summit craters of Láscar volcano from high spatio-temporal resolution TerraSAR-X interferometry. *Bull. Volcanol.* 80, 21. doi:

10.1007/s00445-018-1195-3.

Risse, A., Trumbull, R. B., Coira, B., Kay, S. M., and Bogaard, P. van den (2008). 40Ar/39Ar geochronology of mafic volcanism in the back-arc region of the southern Puna plateau, Argentina. *J. South Am. Earth Sci.* 26, 1–15. doi: 10.1016/j.jsames.2008.03.002.

Rivera, F. (2019). Una Expedición al Aucanquilcha. Available at: https://altocielo.hypotheses.org/.

Rivera, M., Cueva, K., Le Pennec, J.-L., Vela, J., Samaniego, P., Manrique, N., et al. (2018a). Geología y Evaluación de Peligros del Volcán Sara Sara. *Foro Int. Los volcanes y su impacto*, 89–92.

Rivera, M., Cueva, K., Le Pennec, J.-L., Vela, J., Samaniego, P., Manrique, N., et al. (2020a). Geología y Evaluación de Peligros del volcán Sara Sara (Ayacucho). 154, 2 mapas.

Rivera, M., and Mariño, J. (2004). Volcán Yucamane (Sur del Perú): Geología, Petrología y Evaluación Preliminar de las Amenazas Volcánicas. *Boletín la Soc. Geológica del Perú* 98, 7–27.

Rivera, M., Mariño, J., Samaniego, P., Delgado, R., and Manrique, N. (2016). Geología y Evaluación de Peligros del Complejo Volcánico Ampato - Sabancaya (Arequipa). *INGEMMET, Boletín Ser. C Geodinámica e Ing. Geológica N° 61*, 133.

Rivera, M., Mariño, J., Thouret, J., and Cacya, L. (2008). Geología y Evaluación de Peligros del Volcán Ubinas. 87.

Rivera, M., Mariño, J., Thouret, J., and Samaniego, P. (2011). Mapa de Peligros del Volcán Ubinas, escala 1: 50,000.

Rivera, M., Martin, H., Le Pennec, J.-L., Thouret, J.-C., Gourgaud, A., and Gerbe, M.-C. (2017). Petro-geochemical constraints on the source and evolution of magmas at El Misti volcano (Peru). *Lithos* 268–271, 240–259. doi: 10.1016/j.lithos.2016.11.009.

Rivera, M., Samaniego, P., Vela, J., and Le Pennec, J.-L. (2018b). Geología y Evaluación de Peligros del Complejo Volcánico Yucamane - Calientes (Candarave - Tacna). *INGEMMET, Boletín Ser. C Geodinámica e Ing. Geológica N° 65*, 130.

Rivera, M., Samaniego, P., Vela, J., Le Pennec, J.-L., Guillou, H., Paquette, J.-L., et al. (2019). The eruptive chronology of the Yucamane-Calientes compound volcano: A potentially active edifice of the Central Andes (southern Peru). *8th Int. Symp. Andean Geodyn.*, 1.

Rivera, M., Samaniego, P., Vela, J., Le Pennec, J.-L., Guillou, H., Paquette, J.-L., et al. (2020b). The eruptive chronology of the Yucamane-Calientes compound volcano: A potentially active edifice of the Central Andes (southern Peru). *J. Volcanol. Geotherm. Res.* 393, 20. doi: 10.1016/j.jvolgeores.2020.106787.

Rivera, M., Thouret, J.-C., Mariño, J., Berolatti, R., and Fuentes, J. (2010). Characteristics and management of the 2006–2008 volcanic crisis at the Ubinas volcano (Peru). *J. Volcanol. Geotherm. Res.* 198, 19–34. doi: 10.1016/j.jvolgeores.2010.07.020.

Rivera, M., Thouret, J.-C., Samaniego, P., and Le Pennec, J.-L. (2014). The 2006–2009 activity of the Ubinas volcano (Peru): Petrology of the 2006 eruptive products and insights into genesis of andesite magmas, magma recharge and plumbing system. *J. Volcanol. Geotherm. Res.* 270, 122–141. doi: 10.1016/j.jvolgeores.2013.11.010.

Rivera, M., and Zavala, B. (2015). Volcanismo monogenético: paisajes y geoformas singurlares en el Valle de Volcanes de Andagua y Huambo. 43–47.

Robidoux, P., Rizzo, A. L., Aguilera, F., Aiuppa, A., Artale, M., Liuzzo, M., et al. (2020). Petrological and noble gas features of Lascar and Lastarria volcanoes (Chile): Inferences on plumbing systems and mantle characteristics. *Lithos* 370–371, 105615. doi: 10.1016/j.lithos.2020.105615.

Rodríguez, I., Roche, O., Moune, S., Aguilera, F., Campos, E., and Pizarro, M. (2015). Evolution of Irruputuncu volcano, Central Andes, northern Chile. *J. South Am. Earth Sci.* 63, 385–399. doi: 10.1016/j.jsames.2015.08.012.

Rojas, F. (2019). Testeo, resultados y metodología de la camara UV de bajo costo Picam UV, en los volcanes Olca, Ollagüe, San Pedro y Putana. *Tesina para optar al título Geólogo. Undergrad. Thesis, Univ. Católica del Norte, Chile.*, 143.

Roobol, M., Francis, P., Ridley, W., Rhodes, M., and Walker, G. (1976). Physio-chemical characteristics of the Andean volcanic chain between latitudes 21° and 22° south. *Proc Symp Andean Antarct. Volcanol. Probl. Rome IAVCEI*, 450–464.

Rubiolo, R., Martínez, L., and Pereyra, F. (2003). Hoja Geológica 2769-IV Fiambalá, Provincias de Catamarca y La Rioja. *Inst. Geol. y Recur. Miner. Serv. Geológico Min. Argentino, Buenos Aires*, 78.

Ruch, J., Anderssohn, J., Walter, T. R., and Motagh, M. (2008). Caldera-scale inflation of the Lazufre volcanic area, South America: Evidence from InSAR. *J. Volcanol. Geotherm. Res.* 174, 337–344. doi: 10.1016/j.jvolgeores.2008.03.009.

Ruch, J., Manconi, A., Zeni, G., Solaro, G., Pepe, A., Shirzaei, M., et al. (2009). Stress transfer in the Lazufre volcanic area, central Andes. *Geophys. Res. Lett.* 36, L22303. doi: 10.1029/2009GL041276.

Ruch, J., and Walter, T. R. (2010). Relationship between the InSAR-measured uplift, the structural framework, and the present-day stress field at Lazufre volcanic area, central Andes. *Tectonophysics* 492, 133–140. doi: 10.1016/j.tecto.2010.06.003.

Rudolph, W. E. (1955). Licancabur: Mountain of the Atacamenos. *Geogr. Rev.* 45, 151. doi: 10.2307/212227.

Ruprecht, P., and Wörner, G. (2007). Variable regimes in magma systems documented in plagioclase zoning patterns: El Misti stratovolcano and Andahua monogenetic cones. *J. Volcanol. Geotherm. Res.* 165, 142–162. doi: 10.1016/j.jvolgeores.2007.06.002.

Sáez, A., Valero-Garcés, B. L., Moreno, A., Bao, R., Pueyo, J. J., González-Sampériz, P., et al. (2007). Lacustrine sedimentation in active volcanic settings: the Late Quaternary depositional evolution of Lake Chungará (northern Chile). *Sedimentology* 54, 1191–1222. doi: 10.1111/j.1365-3091.2007.00878.x.

Sainato, C. M., and Pomposiello, M. C. (1997). Two-dimensional magnetotelluric and gravity models of the Tuzgle volcano zone (Jujuy province, Argentina). *J. South Am. Earth Sci.* 10, 247–261. doi: 10.1016/S0895-9811(97)00022-9.

Salas, M., Kast, R. F., Monteemos, F., and Salas, I. (1966). Geologia y recursos minerales del Departamento de Arica: Provincia de Tarapacá. *Inst. Investig. Geológicas* 21, 144.

Samaniego, P., Rivera, M., Manrique, N., Schiavi, F., Nauret, F., Liorzou, C., et al. (2020). Linking magmatic processes and magma chemistry during the post-glacial to recent explosive eruptions of Ubinas volcano (southern Peru). *J. Volcanol. Geotherm. Res.* 407, 107095. doi: 10.1016/j.jvolgeores.2020.107095.

Samaniego, P., Rivera, M., Mariño, J., Guillou, H., Liorzou, C., Zerathe, S., et al. (2016). The eruptive chronology of the Ampato–Sabancaya volcanic complex (Southern Peru). *J. Volcanol.*

Geotherm. Res. 323, 110–128. doi: 10.1016/j.jvolgeores.2016.04.038.

Samaniego, P., Valderrama, P., Mariño, J., van Wyk de Vries, B., Roche, O., Manrique, N., et al. (2015). The historical (218 ± 14 aBP) explosive eruption of Tutupaca volcano (Southern Peru). *Bull. Volcanol.* 77, 51. doi: 10.1007/s00445-015-0937-8.

Sánchez, R. (2017). Modelización de la amenaza del volcán Uturuncu utilizando métodos probabilísticos y SIG, Suroeste de Bolivia. *Memorias del II Congr. Nac. matemática*, 8. Available at: https://pubs.geoscienceworld.org/gsa/geosphere/article/14/3/954/529992/Synthesis-PLUTONS-Investigating-the-relationship.

Sandri, L., Thouret, J.-C., Constantinescu, R., Biass, S., and Tonini, R. (2014). Long-term multi-hazard assessment for El Misti volcano (Peru). *Bull. Volcanol.* 76, 771. doi: 10.1007/s00445-013-0771-9.

Sapper, K. (1917). Katalog der geschichtlichen Vulkanausbrüche. *Strassburg*, 284–295.

Schmitt, A., de Silva, S., Trumbull, R., and Emmermann, R. (2001). Magma evolution in the Purico ignimbrite complex, northern Chile: evidence for zoning of a dacitic magma by injection of rhyolitic melts following mafic recharge. *Contrib. to Mineral. Petrol.* 140, 680–700. doi: 10.1007/s004100000214.

Schoenbohm, L. M., and Carrapa, B. (2015). "Miocene–Pliocene shortening, extension, and mafic magmatism support small-scale lithospheric foundering in the central Andes, NW Argentina," in *Geodynamics of a Cordilleran Orogenic System: The Central Andes of Argentina and Northern Chile* (Geological Society of America), 167–180. doi: 10.1130/2015.1212(09).

Seggiaro, R., and Apaza, F. (2018). Geología del proyecto geotérmico Socompa. *Serv. Geológico Min. Argentino. Inst. Geol. y Recur. Miner. Buenos Aires*, 26.

Seggiaro, R., Becchio, R., Pereyra, F., and Martínez, L. (2007). Hoja Geológica 2569-IV, Antofalla, provincias de Catamarca y Salta. *Inst. Geol. y Recur. Miner. Serv. Geológico Min. Argentino, Buenos Aires.*, 62.

Seggiaro, R., Becchio, R., Ramallo, E., and Bercheñi, V. (2015). Hoja Geológica 2366-III, Susques (preliminar). *Inst. Geol. y Recur. Miner. Serv. Geológico Min. Argentino, Boletín 414, Buenos Aires*.

Seggiaro, R. E., and Hongn, F. (1999). Tectonic influence in Cenozoic vulcanism in North-Western Argentina. *Acta Geológica Hisp.* 34, 227–242.

Seggiaro, R., Hongn, F., Castillo, A., Pereyra, F., Villegas, D., and Martínez, L. (2006). Hoja Geológica 2769-II Paso San Francisco, Provincia de Catamarca, escala 1:250.000. *Inst. Geología y Recur. Miner. Serv. Geológico Min. Argentino, Buenos Aires. Boletín 294*, 62.

Sepúlveda, J. P. (2018). Evolución Geológica del Complejo Volcánico Guallatiri, Región de Arica y Parinacota, Norte de Chile. *Mem. para optar al Título Geólogo. Undergrad. Thesis, Univ. Católica del Norte, Chile.*, 99.

SERNAGEOMIN (2015). Ranking de peligrosidad de los volcanes activos de Chile. *Serv. Nac. Geol. y Minería, Chile.*

SERNAGEOMIN (2020a). Ranking de riesgo especifico de volcanoes activos de Chile 2019. 25. Available at: https://www.sernageomin.cl/wp-content/uploads/2020/02/Presentación_Ranking_Volcanes_Sernageomin_2020-web.pdf.

SERNAGEOMIN (2020b). Ranking de riesgo específico para volcanes activos de Chile 2019. *https//www.sernageomin.cl/wp-content/uploads/2020/07/2Ranking-2019_Tabla_Final.pdf (Última Visit. 03/08/2020).* Available at: https://www.sernageomin.cl/wp-content/uploads/2020/07/2Ranking-2019_Tabla_Final.pdf.

SERNAGEOMIN (2021). Servicio Nacional de Geología y Minería. *Red Nac. Vigil. volcánica. Volcanes Act. y Monit. por cada región del país, Chile.* Available at: https://www.sernageomin.cl/red-nacional-de-vigilancia-volcanica/.

Seynova, I. B., Chernomorets, S. S., Dokukin, M. D., Petrakov, D. A., Savernyuk, E. A., Lukashov, A. A., et al. (2017). Formation of water flow in lahars from active glacier-clad volcanoes. *Earth`s Cryosph.* 21, 118–128. doi: 10.21782/EC1560-7496-2017-6(103-111).

Simkin, T., and Siebert, L. (1994). Volcanoes of the World. *Second ed. Smithson. Institution, Geosci. Tucson*, 349.

Slawinska, J., and Robock, A. (2018). Impact of Volcanic Eruptions on Decadal to Centennial Fluctuations of Arctic Sea Ice Extent during the Last Millennium and on Initiation of the Little Ice Age. *J. Clim.* 31, 2145–2167. doi: 10.1175/JCLI-D-16-0498.1.

Soler, V., and Amigo (2012). Nota informativa sobre la actividad microsismica del volcan putana.

Andes centrales del norte de Chile. Periodo Sept 2009–Feb 2011. *Tech. Report, CSIC, Sernageomin.*

Sørensen, E. V., and Holm, P. M. (2008). Petrological inferences on the evolution of magmas erupted in the Andagua Valley, Peru (Central Volcanic Zone). *J. Volcanol. Geotherm. Res.* 177, 378–396. doi: 10.1016/j.jvolgeores.2008.05.021.

Sparks, R. S. J., Folkes, C. B., Humphreys, M. C. S., Barfod, D. N., Clavero, J., Sunagua, M. C., et al. (2008). Uturuncu volcano, Bolivia: Volcanic unrest due to mid-crustal magma intrusion. *Am. J. Sci.* 308, 727–769. doi: 10.2475/06.2008.01.

Sparks, R. S. J., Gardeweg, M. C., Calder, E. S., and Matthews, S. J. (1997). Erosion by pyroclastic flows on Lascar Volcano, Chile. *Bull. Volcanol.* 58, 557–565. doi: 10.1007/s004450050162.

Spica, Z., Legrand, D., Mendoza, A. I., Dahn, T., Walter, T., Heimann, S., et al. (2012). Analysis of surface waves extracted from seismic noise for the Lastarria volcanic zone, Chile. *Cities Volcanoes 7, Colima, México.*

Stebel, K., Amigo, A., Thomas, H., and Prata, A. J. (2015). First estimates of fumarolic SO 2 fluxes from Putana volcano, Chile, using an ultraviolet imaging camera. *J. Volcanol. Geotherm. Res.* 300, 112–120. doi: 10.1016/j.jvolgeores.2014.12.021.

Stern, C., Moreno, H., López-Escobar, L., Clavero, J., Lara, L., Naranjo, J., et al. (2007). Chilean Volcanoes. *Geol. Chile. Geol. Soc. London*, 147 – 179.

Sunagua, M. (2004). Amenaza volcánica en la región del volcán Uturuncu – Provincia Sud Lípez del Departamento de Potosí. *Univ. Autónoma Tomás Frías*.

Szakács, A. (1994). Redefining active volcanoes: a discussion. *Bull. Volcanol.* 56, 321–325. doi: 10.1007/BF00326458.

Tassi, F., Aguilera, F., Darrah, T., Vaselli, O., Capaccioni, B., Poreda, R. J., et al. (2010). Fluid geochemistry of hydrothermal systems in the Arica-Parinacota, Tarapacá and Antofagasta regions (northern Chile). *J. Volcanol. Geotherm. Res.* 192, 1–15. doi: 10.1016/j.jvolgeores.2010.02.006.

Tassi, F., Aguilera, F., Vaselli, O., Darrah, T., and Medina, E. (2011). Gas discharges from four remote volcanoes in northern Chile (Putana, Olca, Irruputuncu and Alitar): a geochemical survey. *Ann. Geophys.* 54, 121–136. doi: 10.4401/ag-5173.

Tassi, F., Aguilera, F., Vaselli, O., Medina, E., Tedesco, D., Delgado Huertas, A., et al. (2009). The magmatic- and hydrothermal-dominated fumarolic system at the Active Crater of Lascar volcano, northern Chile. *Bull. Volcanol.* 71, 171–183. doi: 10.1007/s00445-008-0216-z.

Tepley, F., De Silva, S., and Salas, G. (2013). Magma dynamics and petrological evolution leading to thevei 5 2000 BP Eruption of EL mistivolcano, southern Peru. *J. Petrol.* 54, 2033–2065. doi: 10.1093/petrology/egt040.

Thorpe, R. S. (1984). "The Tectonic Setting of Active Andean Volcanism," in *Andean Magmatism* (Boston, MA: Birkhäuser Boston), 4–8. doi: 10.1007/978-1-4684-7335-3_1.

Thouret, J.-C., Davila, J., and Eissen, J.-P. (1999). Largest explosive eruption in historical times in the Andes at Huaynaputina volcano, a.d. 1600, southern Peru. *Geology* 27, 435. doi: 10.1130/0091-7613(1999)027<0435:LEEIHT>2.3.CO;2.

Thouret, J.-C., Dávila, J., Rivera, M., Gourgaud, A., Eissen, J.-P., Pennec, J.-L. Le, et al. (1997). L'éruption explosive de 1600 au Huaynaputina (Pérou), la plus volumineuse de l'histoire dans les Andes centrales. *Comptes Rendus l'Académie des Sci. - Ser. IIA - Earth Planet. Sci.* 325, 931–938. doi: 10.1016/s1251-8050(97)82372-5.

Thouret, J.-C., Rivera, M., Wörner, G., Gerbe, M.-C., Finizola, A., Fornari, M., et al. (2005). Ubinas: the evolution of the historically most active volcano in southern Peru. *Bull. Volcanol.* 67, 557–589. doi: 10.1007/s00445-004-0396-0.

Thouret, J. C., Juvigne, E., Mariño, J., Moscol, M., Legeley-Padovani, A., Loutsch, I., et al. (2002). Late pleistocene and holocene tephro-stratigraphy and chronology in southern Peru. *Geodyn. Andin.*, 12.

Thouret, J., Finizola, A., Fornari, M., Suni, J., and Frechen, M. (2001). Geology of El Misti volcano near the city of Arequipa , Peru. *Geol. Soc. Am. Bull.* 113, 1593–1610. doi: 10.1130/0016-7606(2001)1132.0.CO;2.

Thouret, J., Gourgaud, A., and Pennec, L. (1996). Huaynaputina volcano, South Peru : site of the major explosive eruption in historical times in the Central Andes. *Third ISAG, Sr Malo (France), 17-1 91911 996 HUAYNAPUTINA*, 17–20.

Tibaldi, A., Bistacchi, A., Pasquarè, F. A., and Vezzoli, L. (2006). Extensional tectonics and volcano lateral collapses: insights from Ollagüe volcano (Chile-Bolivia) and analogue modelling. *Terra*

Nov. 18, 282–289. doi: 10.1111/j.1365-3121.2006.00691.x.

Tort, A., and Finizola, A. (2005). The buried caldera of Misti volcano, Peru, revealed by combining a self-potential survey with elliptic Fourier function analysis of topography. *J. Volcanol. Geotherm. Res.* 141, 283–297. doi: 10.1016/j.jvolgeores.2004.11.005.

Trumbull, R. ., Wittenbrink, R., Hahne, K., Emmermann, R., Büsch, W., Gerstenberger, H., et al. (1999). Evidence for Late Miocene to Recent contamination of arc andesites by crustal melts in the Chilean Andes (25–26°S) and its geodynamic implications. *J. South Am. Earth Sci.* 12, 135–155. doi: 10.1016/S0895-9811(99)00011-5.

Úbeda, J., Bonshoms, M., Iparraguirre, J., Sáez, L., de la Fuente, R., Janssen, L., et al. (2018). Prospecting Glacial Ages and Paleoclimatic Reconstructions Northeastward of Nevado Coropuna (16° S, 73° W, 6377 m), Arid Tropical Andes. *Geosciences* 8, 307. doi: 10.3390/geosciences8080307.

Úbeda, J., Palacios, D., and Vázquez-Selém, L. (2012). Glacial and volcanic evolution on Nevado Coropuna (Tropical Andes) based on cosmogenic 36Cl surface exposure dating. 14, 7343.

Úbeda, J., Yoshikawa, K., Pari, W., Palacios, D., Macias, P., and Apaza, F. (2015). Geophysical surveys on permafrost in Coropuna and Chachani volcanoes (southern Peru). in *Geophysical Research Abstracts*, 1.

Ureta, G., Németh, K., Aguilera, F., and Kósik, S. (2019). Scoria cones of the Quaternary Ollagüe Volcanic Field, Central Andean Volcanic Zone, northern Chile. *IAVCEI – 5th Int. Volcano Geol. Work.*, 4.

Urzúa, L., Powell, T., Cumming, W., and Dobson, P. (2002). Apacheta, a new geothermal prospect in Northern Chile. *Geotherm. Resour. Counc.*, 10.

Valderrama, P., Roche, O., Samaniego, P., van Wyk de Vries, B., Bernard, K., and Mariño, J. (2016). Dynamic implications of ridges on a debris avalanche deposit at Tutupaca volcano (southern Peru). *Bull. Volcanol.* 78, 14. doi: 10.1007/s00445-016-1011-x.

Valderrama, P., Roche, O., Samaniego, P., van Wyk des Vries, B., and Araujo, G. (2018). Granular fingering as a mechanism for ridge formation in debris avalanche deposits: Laboratory experiments and implications for Tutupaca volcano, Peru. *J. Volcanol. Geotherm. Res.* 349, 409–418. doi: 10.1016/j.jvolgeores.2017.12.004.

Valderrama, P., Samaniego, P., Mariño, J., Manrique, N., Van Wyk de Vires, B., and Fidel, L. (2015). Una gran erupción del VOlcán Tutupaca (Tacna) ocurrida hace aproximadamente 200 años AP: Implicaciones para la Evaluación de la Amenaza. 5–24.

Valderrama, P., Samaniego, P., Mariño, J., Van Wyk de Vries, B., Manrique, N., Roche, O., et al. (2014). Dos Colapsos Sectoriales Recientes Del Volcán Tutupaca : 3–6.

van Wyk de Vries, B., Self, S., Francis, P. ., and Keszthelyi, L. (2001). A gravitational spreading origin for the Socompa debris avalanche. *J. Volcanol. Geotherm. Res.* 105, 225–247. doi: 10.1016/S0377-0273(00)00252-3.

Vargas, V., Cruz, V., Antayhua, Y., and Rivera, M. (2012). Estudio Geotérmico del Campo. *INGEMMET, Boletín N° 47 Ser. C Geodinámica e Ing. Geológica*, 89.

Vela, J., Samaniego, P., and Rivera, M. (2014). Estudio tefro-estratigráfico preliminar del depósito de caída de la última erupción del volcán yucamane (tacna). *XVII Congr. Peru. Geol.*, 2–5.

Velarde, L., Tavera, H., Vargas, K., and Villegas, J. C. (2020). Análisis de la crisis sísmica ocurrida en julio de 2020 en el distrito de Tarata (Provincia de Tarata-Región Tacna). *IGP, Inf. Técnico N°003-2020/IGP CIENCIAS LA TIERRA SÓLIDA*, 23.

Vélez, M. ., Bustos, E., Euillades, L., Blanco, M., López, J. F. S., Barbero, I., et al. (2021). Ground deformation at the Cerro Blanco caldera: A case of subsidence at the Central Andes BackArc. *J. South Am. Earth Sci.* 106, 102941. doi: 10.1016/j.jsames.2020.102941.

Venturelli, G., Fragipane, M., Weibel, M., and Antiga, D. (1978). Trace element distribution in the cainozoic lavas of Nevado Coropuna and Andagua Valley, Central Andes of Southern Peru. *Bull. Volcanol.* 41, 213–228. doi: 10.1007/BF02597224.

Verosub, K. L., and Lippman, J. (2008). Global Impacts of the 1600 Eruption of Peru's Huaynaputina Volcano. *Eos, Trans. Am. Geophys. Union* 89, 141. doi: 10.1029/2008EO150001.

Vezzoli, L., Tibaldi, A., Renzulli, A., Menna, M., and Flude, S. (2008). Faulting-assisted lateral collapses and influence on shallow magma feeding system at Ollagüe volcano (Central Volcanic Zone, Chile-Bolivia Andes). *J. Volcanol. Geotherm. Res.* 171, 137–159. doi: 10.1016/j.jvolgeores.2007.11.015.

Viramonte, J. G., Arnosio, M., Becchio, R., Gropelli, G., Norini, G., Corazzatto, C., et al. (2005a). Cerro Blanco Volcanic Complex: the Youngest Caldera System in the Southern Central Andes.

A Multidisciplinary Earth Science Project. *Colloq. Lat. Am. Geosci. Potsdam*, 135. Available at: http://link.springer.com/10.1007/978-3-030-52010-6.

Viramonte, J. G., Becchio, R., Bolli, M. I., Petrinovic, I., and Tejada, R. S. A. (1995). Actividad eruptiva del volcan Lascar: Erupcion 18/24-Abril-1993. *Inst. Geonorte, Univ. Nac. Salta, Argentina*.

Viramonte, J. G., Galliski, M. A., Araña Saavedra, V., Aparicio, A., Garcia Cacho, L., and Martín Escorza, C. (1984). El finivolcanismo básico de la depresión de Arizaro, provincia de Salta. *IX Congr. Geológico Argentino Actas III*, 234–251.

Viramonte, J., Godoy, S., Arnosio, M., Becchio, R., and Poodts, M. (2005b). El campo geotermal de la caldera del cerro Blanco: utilización de imágenes aster. *Proc. Geol. Congr. Buenos Aires, Asoc. Geológica Argentina. La Plata, Argentina.* 2, 505–512.

Wadge, G., Francis, P. W., and Ramirez, C. F. (1995). The Socompa collapse and avalanche event. *J. Volcanol. Geotherm. Res.* 66, 309–336. doi: 10.1016/0377-0273(94)00083-S.

Walker, B. A., Klemetti, E. W., Grunder, A. L., Dilles, J. H., Tepley, F. J., and Giles, D. (2013). Crystal reaming during the assembly, maturation, and waning of an eleven-million-year crustal magma cycle: thermobarometry of the Aucanquilcha Volcanic Cluster. *Contrib. to Mineral. Petrol.* 165, 663–682. doi: 10.1007/s00410-012-0829-2.

Walker, B., Grunder, A., and Wooden, J. (2010). Organization and thermal maturation of long-lived arc systems: Evidence from zircons at the Aucanquilcha volcanic cluster, northern Chile. *Geology* 38, 1007–1010. doi: 10.1130/G31226.1.

Walter, T. R., and Motagh, M. (2009). Longevity of a large magma body beneath Uturuncu Volcano , Bolivia , as constrained by surface lineaments , stress models and InSAR. in *Geophysical Research Abstracts, Vol. 11, EGU2009-4111, 2009 EGU General Assembly 2009*.

Watts, R. . (2002). The emplacement of crystal-rich intermediate lavas. Ph.D. thesis (Unpublished). *Sch. Earth Sci. Univ. Bristol. United Kingdom*, 192.

Watts, R., Clavero, J., and Sparks, R. S. (2014). Origen y emplazamiento del Domo Tinto, volcán Guallatiri, Norte de Chile. *Andean Geol.* 41, 558–588. doi: 10.5027/andgeoV41n3-a04.

Weibel, M., Frangipane-Gysel, M., and Hunziker, J. (1978). Ein Beitrag zur Vulkanologie Süd-Perus. *Geol. Rundschau* 67, 243–252. doi: 10.1007/BF01803264.

Whelley, P. L., Jay, J., Calder, E. S., Pritchard, M. E., Cassidy, N. J., Alcaraz, S., et al. (2012). Post-depositional fracturing and subsidence of pumice flow deposits: Lascar Volcano, Chile. *Bull. Volcanol.* 74, 511–531. doi: 10.1007/s00445-011-0545-1.

Wörner, G., Hammerschmidt, K., Henjes-Kunst, F., Lezaun, J., and Wilke, H. (2000). Geochronology (40Ar/39Ar, K-Ar and He-exposure ages) of Cenozoic magmatic rocks from Northen Chile (18°-22°S): implications for magmatism and tectonic evolution of the Central Andes. *Rev. Geológica Chile*, 205–240.

Wörner, G., Harmon, R. S., Davidson, J., Moorbath, S., Turner, D. L., McMillan, N., et al. (1988). The Nevados de Payachata volcanic region (18°S/69°W, N. Chile). *Bull. Volcanol.* 50, 287–303. doi: 10.1007/BF01073587.

Zapettini, E., and Blasco, G. (1998). Hoja geológica 2569-II Socompa. Provincia de Salta, República Argentina. *Inst. Geol. y Recur. Miner. SEGEMAR, Argentina, Boletín 260*.

Zappettini, E., and Blasco, G. (2001). Hoja Geológica 2569-II, Socompa, escala 1:250.000. Provincia de Salta. *Serv. Geológico Min. Argentino, Programa Nac. Cart. Geológicas la República Argentina, Boletín N° 260*, 68.